Universidade de Aveiro Departamento de Biologia
Ano 2018

Maria João Martinho de Freitas

Abordagem à regulação da mobilidade do espermatozoide através da caracterização e modulação da via de sinalização GSK3/PPP1R2/PPP1

Addressing sperm motility regulation through characterization and modulation of the GSK3/PPP1R2/PPP1 signaling pathway

Universidade de Aveiro Departamento de Biologia
Ano 2018

Maria João Martinho de Freitas

Abordagem à regulação da mobilidade do espermatozoide através da caracterização e modulação da via de sinalização GSK3/PPP1R2/PPP1

Addressing sperm motility regulation through characterization and modulation of the GSK3/PPP1R2/PPP1 signaling pathway

Tese apresentada à Universidade de Aveiro para cumprimento dos requisitos necessários à obtenção do grau de Doutor em Biologia, realizada sob a orientação científica da Doutora Margarida de Sâncio da Cruz Fardilha, Professora Professora Auxiliar do Departamento de Ciências Médicas da Universidade de Aveiro e do Doutor Srinivasan Vijayaraghavan, Professor Professor Auxiliar do Departamento de Ciências Biológicas da Kent State University.

Este trabalho é financiado por Fundos FEDER através do Programa Operacional Fatores de Competitividade-COMPETE e por Fundos Nacionais através da FCT-Fundação para a Ciência e a Tecnologia no âmbito dos projetos «PTDC/DTP-PIC/0460/2012»; «PTDB/BBB-BQB/3804/2014»; «NIH R15 HD068971-01»; da bolsa individual «SFRH/BD/84876/2012»; e do instituto de Biomedicina- iBiMED «UID/BIM/04501/2013».

o júri

presidente

Professor Doutor Amadeu Mortágua Velho Da Maia Soares
professor Catedrático do Departamento de Biologia da Universidade de Aveiro

Professor Doutor Stephen Publicover
professor Associado da Universidade de Birmingham

Professor Doutor Carlos Pedro Fontes Oliveira
professor afiliado do Instituto de Ciências Biomédicas Abel Salazar da Universidade do Porto

Professora Doutora Maria De Lourdes Gomes Pereira
professor associado com agregação do Departamento de Biologia da Universidade de Aveiro

Professora Doutora Margarida Fardilha
professor auxiliar do Departamento de Ciências Médicas da Universidade de Aveiro

agradecimentos

À minha orientadora, Margarida Fardilha, por me ter apoiado desde que comecei a ser “cientista”. Por todas as oportunidades que me ofereceu e por todas as vezes que o seu positivismo derrotou o meu negativismo.

To my co-advisor, Dr. Vijay for welcoming in his lab and for all the scientific discussions and support during my stay in Kent.

A todos os meus colegas do Laboratório de Transdução de Sinais. Em especial à Joana e a Juliana (ou Jus), que apesar de todos os disparates que fiz e disse ao longo dos anos insistiram em encherem-me de amizade, companheirismo e comida.

To my colleagues in Kent State University, specially to Cameron and Nidaa.

À Vanessa, porque não interessa há quanto tempo não nos falamos, é sempre como se tivesse sido ontem.

Ao Roberto, simplesmente porque me faz feliz.

À minha família. Aos meus pais, porque sempre me disseram que podia ser o que eu quisesse. Sou a pessoa que sou hoje devido à vossa educação e carinho, muito obrigada.

palavras-chave

Espermatozoide, mobilidade do espermaotozoide, fosfoproteina fosfatase 1, fosfoproteina fosfatase 1 regulador 2, glicogénio sintase cinase 3; interações protein-proteina

resumo

A aquisição e manutenção da mobilidade do espermatozoide é fundamental para a fertilização do oócito e consequentemente conceção. Durante décadas, as vias de sinalização necessárias à aquisição de mobilidade por parte do espermatozoide foram alvo de intensos estudos. Contudo, este processo ainda não é inteiramente conhecido. Ademais, as limitadas opções disponíveis para contraceção masculina (preservativo, vasectomia e coito interrompido) refletem a necessidade de desenvolver um contracetivo masculino baseado na modulação da mobilidade do espermatozoide. A via de sinalização GSK3/PPP1R2/PPP1 está envolvida na aquisição de mobilidade do espermatozoide ao longo do transito do epidídimo. O objetivo principal deste trabalho é enriquecer o conhecimento dos eventos celulares necessários na mobilidade do espermatozoide através da caracterização e modulação da via de sinalização GSK3/PPP1R2/PPP1 em espermatozoides humanos. Desenhámos, sintetizámos e caracterizámos um bioportide que quebra interações proteicas baseado em tecnologia de cell penetrating peptides. Estudos in vitro revelaram que o bioportide de ruptura interfere com a interação PPP1R2/PPP1CC2 e é capaz de restabelecer a atividade da PPP1CC2. Também demonstramos que o bioportide reduz significativamente a mobilidade do espermatozoide. Com o objetivo de identificar interacções proteína-proteína adequadas à intervenção farmacológica, focámos a nossa atenção na proteína GSK3, um modulador da interação PPP1R2/PPP1CC2 em espermatozoides. Descrevemos pela primeira vez o interactoma da GSK3 no testículo e espermatozoide humanos e reportamos um papel específico da isoforma GSK3α na mobilidade do espermatozoide. Uma análise in silico revelou interatores da GSK3α e GSK3β que estão envolvidos na mobilidade do espermatozoide e potencialmente poderão ser alvos de intervenção farmacológica para um novo contraceptivo masculino. Em conclusão, demonstramos que é possível provocar a quebra de interações proteína-proteína e modular a mobilidade do espermatozoide usando de bioportides. Também identificamos potenciais novas interações proteicas envolvidas na mobilidade do espermatozoide. Finalmente, mostramos que é possível idealizar um novo tipo de contracepção masculina baseado na inibição da mobilidade do espermatozoide.

keywords

Sperm cell, sperm motility, phosphoprotein phosphatase 1, phosphoprotein phosphatase 1 regulatory subunit 2, glycogen synthase kinase 3, protein-protein interactions

abstract

Sperm motility acquisition and maintenance is a fundamental process for oocyte fertilization and consequently conception. The signaling events underling sperm motility acquisition have been studied for decades. However, many questions are still unanswered. Also, the limited options currently available for male contraception (condom, vasectomy and withdrawal) reflect the necessity of a new group of male contraceptives based on sperm motility modulation. GSK3/PPP1R2/PPP1 signaling pathway is involved in sperm motility acquisition during epididymis transit. The main goal for this work was to deepen the knowledge on the signaling events involved in human sperm motility by focusing on the characterization and modulation of the signaling pathway GSK3/PPP1R2/PPP1. We first designed, synthetized and characterized a disruptive bioportide based on cell penetrating peptide technology. In vitro studies revealed that the disruptive bioportide interferes with PPP1R2/PPP1CC2 interaction and restores PPP1CC2 activity. We also demonstrated that when exposed to the disruptive bioportide, sperm motility is significantly reduced. Aiming to identify sperm protein-protein interactions suitable for pharmacological intervention, we turn our attention to GSK3, a modulator of PPP1R2/PPP1CC2 interactions in sperm. We provide for the first time GSK3 human testis and sperm interactomes. We reported an isoforms specific role for GSK3α in human sperm motility and an in silico analysis revealed GSK3α and GSK3β interactions involved in sperm motility and potential targets for pharmacological intervention. In conclusion, we demonstrated that it is possible to target protein-protein interactions and modulate sperm complexes involved in motility using bioportides. Moreover, we identified new potential protein interactions involved in sperm motility and showed that the development of new type of male contraceptive based on inhibiting sperm motility is now achievable.

Table of Contents

Table of Figures

Table of Tables

Table of Supplementary Figures

Table of Supplementary Tables

Abbreviations

Abs	Absorbance
AD	Activating domain
AKAP11	A kinase anchor protein 11
AKAPs	A kinase anchor proteins
AKT	RAC-alpha serine/threonine-protein kinase
ARHGAP6	Rho GTPase-activating protein 6
ATP	adenosine triphosphate
BP	Bioportide
Ca^{2+}	Calcium
cAMP	Cyclic adenosine monophosphate
CatSper	Cation channel of sperm
co-IP	co-Immunoprecipitation
CPPs	Cell penetrating peptides
DAG	Diacylglycerol
DBD	DNA binding domain
DNA	Deoxyribonucleic acid
ESTs	Expressed sequence tag
GSK3	Glycogen synthase kinase 3
GSK3α	Glycogen synthase kinase 3 isoform alpha
GSK3β	Glycogen synthase kinase 3 isoform beta
H^{+}	Hydrogen
HCO3	Bicarbonate
HP	Homing peptides
KI	Knock in
KO	Knock out
LDHC	Lactate dehydrogenase C
LRP6	Low-density lipoprotein receptor-related protein 6
MAPKs	Mitogen-activated protein kinase
Mn^{2+}	Manganese
mRNA	messenger Ribonucleic acid
MS	Mass spectrometry

Na	Sodium
p17	17kDa protein
PBS	Phosphate buffer solution
PDPK1	3-phosphoinositide-dependent protein kinase 1
PFA	Paraformaldehyde
PGK2	Phosphoglycerate kinase 2
PIK3C	Phosphatidylinositol 3-kinase
PPIN	Protein-protein interactions network
PPIs	Protein-protein interactions
PPME1	Protein Phosphatase Methylesterase 1
PPP1	Phosphoprotein phosphatase 1
PPP1CC2	Phosphoprotein phosphatase 1 catalytic subunit C2
PPP1R11	Phosphoprotein phosphatase 1 regulatory subunit 11
PPP1R2	Phosphoprotein phosphatase 1 regulatory subunit 2
PPP1R2P3	PPP1R2 pseudogene 3
PPP1R7	Phosphoprotein phosphatase 1 regulatory subunit 7
PPP2CA	Phosphoprotein phosphatase 2 catalytic subunit A
PPP3CC	Phosphoprotein phosphatase 3 catalytic subunit C
PRKA	cAMP-dependent protein kinase catalytic subunit alpha
PRKC	Protein kinase C
PRSS37	Probable inactive serine protease 37
PSA	Prostate specific antigen
RAF-1	RAF proto-oncogene serine/threonine-protein kinase
RNA	Ribonucleic acid
RNA-seq	RNA sequencing
sAC	Soluble adenylyl cyclase
Ser	Serine residues
SERCAs	Sarco/endoplasmic reticulum Ca2+-ATPase
SFK	Src family kinase
Thr	Threonine residues
Tyr	Tyrosine residues
VOCCs	L-type voltage-operated Ca2+ channels
WHO	World health organization

YTH	Yeast two-hybrid
Zn^{2+}	Zinc

A. Introduction and Aims

A1. Male reproductive System

The male reproductive system has the purpose of producing, maturate and deliver the male gametes to the female reproductive tract. Anatomically, the male reproductive system is composed of two testes, a system of genital ducts (*tubuli recti*; efferent ducts; epididymis, deferent ducts; ejaculatory ducts and urethra), accessory glands (seminal vesicle, prostate and bulbourethral glands) and the penis. Functionally, spermatozoa or sperm must be produced (spermatogenesis) in the testis, matured in the epididymis and delivered to the female reproductive system by the penis. Moreover, the production of sexual hormones, specifically testosterone, occurs in the testis. In the next section, the morphological and functional characteristics of the *Homo sapiens* male reproductive system will be briefly described [1]. In Figure A1.1 an overview of the male reproductive system is presented.

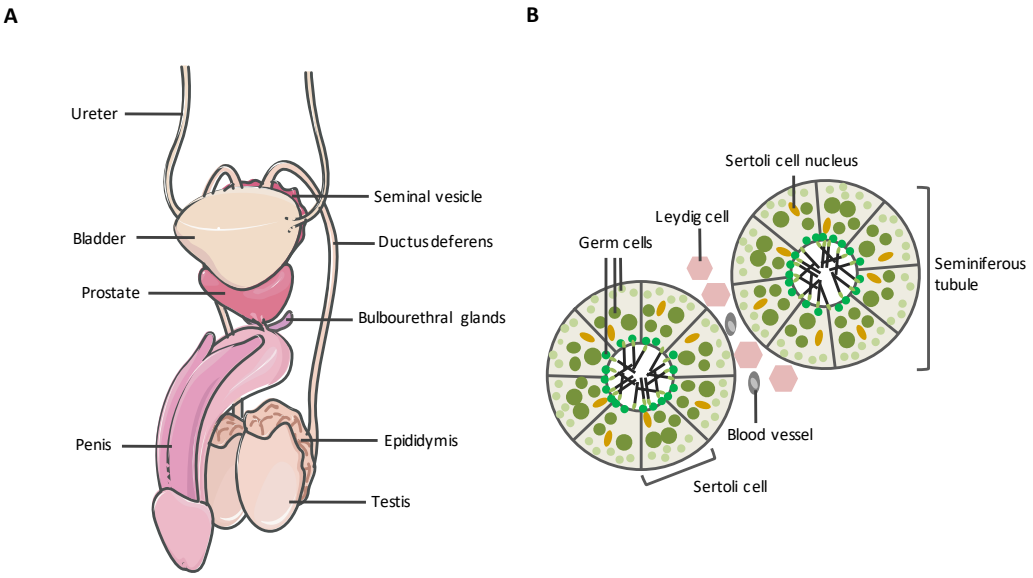

Figure A1.1. Overview of the male reproductive system. A. Components of the male reproductive system. The bladder and the ureter are not part of the male reproductive system**. B**. Schematic cross-section of a testicular tubule, showing germ cells inserted in Sertoli cells. In the interstitium there are Leydig cells and blood vessels. Figures were produced using Servier Medical Art.

A1.1. Testis – Where everything begins

Human testes are ovoid shape organs, localized outside the abdominal cavity and accommodated within the scrotum. This localization maintains the testes at an average temperature of 32ºC, optimal for its function. Within each lobule, there are 1 to 3 seminiferous tubules, the functional unit of the testis, and Leydig cells, which are responsible for the production of testosterone [2,3].

A1. Male Reproductive System

The seminiferous tubules are composed of germ cells line and Sertoli cells. Figure A1.1, describes the morphological structure of the seminiferous tubule. Germ cells will originate mature sperm through spermatogenesis. In *Homo sapiens* more than 200 million sperm are produced every day. Spermatogenesis can be divided in two distinct phases: (i) proliferative and meiotic phase; and (ii) haploid phase. The proliferative phase ensures the continuum of sperm production through a constant renewal of spermatogonia (the least mature germ cells). Consequently, spermatogonia can either undergo mitosis and duplicate itself or enter meiosis. By mitosis, spermatogonia yields primary spermatocytes and the latter, divides meiotically into two secondary spermatocytes. Finally, secondary spermatocytes divide into spermatids. Meiosis will reduce the chromosomal information into half. The haploid phase is characterized by the acquisition of crucial morphological structures necessary for fertilizing potential. It is divided in two sub-phases: spermiogenesis and spermiation. Spermiogenesis is defined as the process of transforming a round haploid spermatid into a highly specialized spermatozoon. At the organelle level, the Golgi complex will originate the acrosome [4]; the spermatid cytosol is merged into sperm head skeleton and, sperm axoneme is formed by outer dense fibers and fibrous sheath [5–9]. To accomplish such metamorphosis, transcription, translational and prost-translational modification increase drastically. Yet, by the end of spermiogenesis, transcription is ceased due to replacement of histones for protamines in sperm DNA, which results in highly packed DNA [10]. From this point on, sperm must rely on existing proteins to control its function. Spermiation refers to the detachment of fully differentiated sperm from the seminiferous epithelium and the journey through the lumen of the seminiferous tubules [11]. Also, during spermiation, the remnants of germ cells cytoplasm are rejected.

Sertoli cells provide structural support and nourishment of germ cells; perform phagocytosis of degenerating germ cells; allow spermiation of fully mature sperm, control germ cell proliferation and differentiation by paracrine secretion of regulatory proteins and create a unique microenvironment for the germ cell line (blood-testis barrier) [12–14]. Morphologically, Sertoli cells are pyrimid-like cells that involve partially the germ cell line. Around 18% of the seminiferous tubule is composed of Sertoli cells and the number of Sertoli cells positively correlates with sperm output. Adjacent Sertoli cells form tights junctions, creating a unique environment, isolating germ cells from the rest of the body. This is particularly important to isolate germ cells form the immune system [13].

The last type of cells present in testis are the Leydig cells. These cells lay between seminiferous tubules and contact directly with blood vessels. Beginning in puberty, Leydig cells increase the production of testosterone, in response to luteinizing hormone [15]. This stimulates the beginning

of spermatogenesis, through Sertoli cell signaling. Through the entire adulthood, spermatogenesis is controlled by constant feedback with the nervous system (hypothalamus and pituitary) [16].

A1.2. Epididymis – where everything starts to function

By the end of spermatogenesis, sperm is morphological complete but functionally immature. To be able to fertilize an oocyte, sperm must journey through the epididymis [17]. Epididymis is a highly-convoluted duct that connects the efferent ducts to the deferent ducts. It is localized in the posterior surface of the testis and in primates can have a length range from 1-7 meters [18]. Estimates of the time necessary for sperm to migrate through human epididymis are inconsistent. Rowley et al suggested a range of 1 to 21 days and Amann and Howards between 3-4 days [19,20].

The epididymis has five main roles: (i) transport of testicular sperm out of the testis; (ii) create a suitable environment for sperm maturation; (iii) promote progressive spermatozoa motility; (iv) prepare sperm for fertilization; (v) and sperm storage. Sperm goes through morphological and functional maturation in the epididymis.

Since testicular sperm are transcriptionally silent cells, the maturation of sperm through the epididymis depends on post-translational modification of pre-existing proteins and protein exchanges between the epididymal lumen and the sperm. Phosphorylation, glycosylation and proteolysis of sperm proteins are among the most common post-translational modification. Most proteins that suffer this process are linked to interaction between sperm and oocyte (*zona pellucida* and oocyte membrane) and acrosome reaction [21–23]. The role of phosphorylation on sperm maturation, particularly motility acquisition, is discussed further on section A2.

Epididymosomes, small extracellular vesicles secreted by the epididymis´s epithelial cells are the major players in the interchange of proteins between sperm and epididymal lumen. It was suggested by Cornwall that epididymosomes allow the safe delivery of proteins to sperm, escaping the proteolytic activity in the epididymal fluid [17]. Within the proteins delivered by epididymosomes, proteins involved in sperm motility, immunological protection and inhibition of capacitation are the more abundant [23].

A1.3. The spermatozoa – the final result

Sperm can be divided in two main structures: head and flagellum. These structures are surrounded by a unique plasma membrane. In the next section, we will focus on the morphological features of sperm head, connecting piece and plasma membrane composition (Figure A1.2). An extensive description of sperm flagellum can be consulted in section A2.

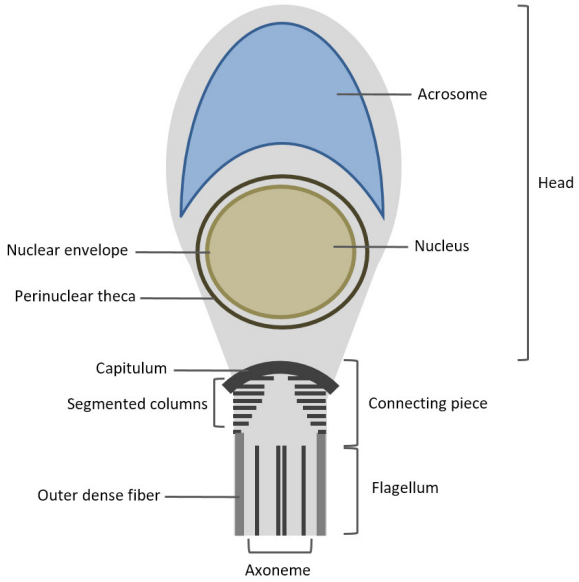

Figure A1.2. Schematic representation of the human sperm head and connecting piece. Human sperm head contains anteriorly the acrosome and posteriorly the nucleus. The nucleus is surrounded by the nuclear envelope and the perinuclear theca. The connecting piece is composed by the capitulum and the segmented columns and connects the head to the flagellum.

The human sperm head is spatula-shaped and its main components are the nucleus and the acrosome. These two structures are surrounded by a small amount of cytoplasm and cytoskeleton structures [24]. The acrosome lies anteriorly to the nucleus, and the cytoplasm lies in the narrow space between both structures and the plasma membrane. Within the nucleus, the DNA is highly compacted and its volume is considerably less than in somatic cells [24]. These results from: protamines highly compacted DNA and sperm only having half the genetic information of somatic cells. Still, approximately 4% of DNA is bound to histones and has been proved that the expression of such DNA is essential for early embryo development [25]. Surrounding the nucleus is the nuclear envelope. The unique feature of sperm nuclear envelope is that, contrary to somatic cells, it does not present nuclear pore complex [26]. Furthermore, the sperm nucleus is protected by a rigid structure formed by bonding of structural proteins, the perinuclear theca [5]. These features result in an optimal shaped nucleus for mobility and better protection of the genetic information. The acrosome covers half to two thirds of the sperm head. This organelle is derived from the Golgi

complex and presents an inner acrosomal membrane adjacent to the nucleus and an outer acrosomal membrane adjacent to the plasma membrane. The acrosome houses several proteases, hidroglycolases and esterases, some which are sperm-specific (e.g acrosin), that upon specific *zona pellucida* signaling are released by exocytosis (acrosome reaction). These proteases will create a path for sperm penetration into the *zona pellucida* [27]. After acrosome reaction, the equatorial region of these organelle is exposed and is involved in the initial interaction between sperm and oocyte membrane [28].

Immediately behind the sperm head is the connecting piece. This structure functions as an anchor between the head and the tail. Consequently, it must be somewhat flexible. The connecting piece is formed by two main structures: the capitulum and the segmented columns. The capitulum inserts into the head and distally interacts with the segmented columns. Distally, the segment columns fuse with the other dense fibers of the flagellum [29,30].

In general, the sperm plasma membrane contains 70% phospholipids, 25% neutral lipids and 5% glycolipids [31]. The most abundant phospholipid of the plasma membrane is sphingomyelin. This lipid confers rigidity to bilayer membranes. Regarding neutral lipids, human sperm membrane contains very high amounts of cholesterol. Cholesterol is a plasma membrane stabilizer with the particularity of maintaining membrane fluidity [32]. Consequently, cholesterol is a key lipid for sperm permeability and motility. In human sperm plasma membrane, the only glycolipid is seminolipid [33], which is present only in mammalian sperm and Schwann cells [34]. It is believed that this molecule participates in maintenance of lipid diffusion barriers (see bellow) [33]. After epididymis transit, plasma membrane presents high cholesterol/phospholipid ratio. This results in plasma membrane stabilization which is beneficial to the journey in the female reproductive system.

Mammalian sperm plasma membrane is divided into five macrodomains: acrosome; postacrosome, equatorial segment; midpiece and principal piece. Each domain appears to have a unique composition and organization which reflects different properties and functions [35,36]. For example, the acrosomal macrodomain is highly fusogenic compared with the post acrosomal macrodomain. One hypothesis for this is that the acrosomal macrodomain is rich in phospholipids that form “cone shape holes” into the membrane, resulting in an unstable membrane [33]. Another question that arises is how these macrodomains are confined to a specific part of the sperm**.** Lipid diffusing barriers have been described in sperm, specifically in the posterior ring and annulus. The

posterior ring segregates the content of sperm plasma membrane of the head and tail and the annulus between the midpiece and principal piece [36].

A1.4. Accessory glands

After epididymal transit, sperm are pushed to the deferent ducts, ejaculatory ducts and finally urethra, upon stimulation. During this journey, the accessory glands (Figure A1.1) secret several fluids that will form the seminal plasma. Please note that the epididymal fluid and sperm cells represent around 3-5% of all semen volume [37]. Altogether, sperm and seminal plasma form the semen.

Secretion from the seminal vesicle is responsible for around 50% of the seminal plasma content and is alkaline and very rich in fructose. Fructose will be consumed by sperm cells producing energy and the alkaline environment will balance the acidic female reproductive tract fluids. This will result in stimulation of sperm motility. Fructose quantification is widely used as a marker for seminal vesicle function. However, some question have arisen regarding the fidelity of such marker. Since fructose is consumed by sperm, fructose concentration also depends on the rate of fructose consumption sperm and not exclusively on seminal vesicle function. Several roles for seminal vesicle secretion have been described. Promotion of sperm motility; increase stability of sperm DNA and suppression the immune system activity in the female reproductive system are some [38].

The next contribution to the seminal plasma are the secretions from the prostate which represent around 20-30% [37]. Prostatic fluid is rich in zinc (Zn^{2+}), citric acid and prostate specific antigen (PSA). Moreover, it presents a slightly acidic pH [39]. It appears that Zn^{2+} stabilizes spermatic DNA and prevents DNA fragmentation, specifically by stabilizing chromatin [40] It further presents anti-microbial activity [39,41]. Citric acid maintains an acidic environment and since it is 100x more secreted by the prostate than by other accessory glands, it may be used as a prostate activity function biomarker. Finally, the PSA promotes liquefaction of semen and consequently stimulates sperm motility [39,42]. Similarly, to the epididymis, the prostate also secretes small vesicles, the prosteosomes, which may fuse with the sperm cell. Theses vesicles are rich in proteins and will transfer such proteins to sperm, by membrane fusing.

The last accessory glands are the bulbourethral glands which, upon sexual stimulation, secrete, to the urethra, an alkaline mucus-like fluid rich in glycoproteins. This fluid neutralizes the acidity of

pre-existing urine residues and provides lubrication for the penis during intercourse [43]. The bulbourethral contribution to the seminal plasma is very small (around 1%)[37].

Finally, the last step to accomplish fertilization is releasing the semen into the female reproductive system by ejaculation. Ejaculation is defined by the expulsion of the semen through the penis. Upon stimulation, the sympathetic nervous system activates the contraction of muscle in the epididymis, seminal vesicle, prostate and deferent ducts. Consequently, the semen is released to the urethra. The accumulation of semen in the urethra stimulates the contraction of muscles within the penis (bulbospongiosus and ischiocavernosus muscles) resulting in the release of semen [44].

A1.5. Male Fertility: infertility and contraceptives

Infertility is defined as the incapability of conceive after 12 months of unprotected intercourse [45]. In a recent study, Agarwal estimated that 15% couple's worldwide are infertile, from which 50% have a male contribution and 20-30% are exclusively due to male factors [46]. Furthermore, idiopathic male infertility predominates as the major cause of infertility (50% of all male infertility cases) [47]. The fact that key mechanisms responsible for several sperm processes, such motility, are still not fully understood, may be the key to understand idiopathic cases of male infertility. Understanding sperm physiology is a step towards unveil and more important diagnose and treat idiopathic male infertility.

On the other hand, male contraceptives have not evolved as much as female contraceptives in the last decades. They fall in three main categories: vasectomy, male condom and withdrawal. In 2015, all together, male contraceptives represented 21% of contraceptive practice worldwide [48]. Vasectomy, is the blockage of the vas deferens and consequently passage of sperm. It is an invasive procedure that until recently was irreversible and has a very high effectiveness (97%-98%). Male condom is a physical barrier that prevents sperm cells to meet the oocyte. Most men refer discomfort using a condom. However, it is the only contraceptive that prevents sexual transmitted diseases and has an effectiveness of 85%. Finally, withdrawal, the pulling out of the penis from the vagina prior to ejaculation, is the least effective contraceptive (73%) [49].

Considering that the period of male contraceptive usage is increasing (earlier sexual initiation and latter fatherhood) and the choices available for men are limited, we believe that a new male contraceptive is necessary. Targeting the signaling pathways involved in sperm motility acquisition may be the future of male contraceptives. Using this approach, spermatogenesis is not disturbed,

ensuring that it is reversible, but keeps sperm from encountering the oocyte. Therefore, understanding the mechanism involved in sperm motility acquisition is key.

A2. Signaling mechanisms in mammalian sperm motility[a]

Human spermatozoon is one of the most differentiated cell types and must leave the male body where is produced and achieve its goal in the female reproductive system [50]. In order to fertilize an egg, the sperm is formed in the testes, in a process called spermatogenesis. At the end of spermatogenesis, sperm are morphologically complete but functionally immature and incapable of fertilizing an egg. To be functional, sperm cells must undergo: (i) maturation in the epididymis; (ii) capacitation and (iii) acrosome reaction in the female reproductive system [51]. These events are co-dependent, since acrosome reaction does not occur if capacitation is impaired and capacitation depends on functional maturation of sperm in the epididymis. Motility acquisition is essential for human sperm function and ultimately male fertility. In 2011, Paoli defined sperm motility as a propagation of transverse waves along the flagellum in a proximal- distal direction producing an impulse that pushes the spermatozoon through the female genital tract [52].

Severe asthenozoospermia is one of the causes of male infertility which arises from the inability of the sperm cell to reach the oocyte [53]. Primary or activated motility is acquired throughout the journey in the epididymis. Although the exact mechanism behind motility acquisition is still far from being fully understood, specific signaling events are described in the literature as essential for this process [51,54]. Low-amplitude symmetrical tail movements characterize sperm activated motility and drive sperm in a straight line in a non-viscous media (seminal plasma) [55]. However, in fallopian tubes, sperm must acquire a specific type of motility, hyperactivated motility, which is characterized by high amplitude and asymmetric flagellar bends. Only this type of flagellar movement allows sperm to overcome dense mucus, detach from the oviductal epithelium and penetrate the egg's protective vestments [56]. Curiously, in the viscous media hyperactivated sperm swim in a circular or figure-8 pattern [55,57]. Alterations in pH, specific molecules, and ion concentration changes are a few of the crucial events for stimulation of hyperactivated motility [58,59]. However, the cellular mechanism and signaling pathways responsible for this type of motility are not fully described.

To be motile, human sperm need a morphologically complete flagellum; be able to produce energy

[a] Published review paper: **Freitas MJ**, Vijayaraghavan S, Fardilha M (2017) Signaling mechanisms in mammalian sperm motility. Biology of reproduction 96 (1):2-12. doi:10.1095/biolreprod.116.144337

to power flagellar movement; and functional signaling pathways (to transduce external signals into internal signals). This review will discuss these three topics, but will mainly focus on the signaling pathways involved in human sperm motility regulation. For an in-depth review on sperm bioenergetics please see du Plessis et al. [60]

A2.1. Sperm flagellum - structure and function

The human sperm are composed of two main structures: head and flagellum (Figure A2.1). The head comprises the nucleus and the acrosome. The nucleus houses the genetic information to be delivered to the oocyte. Upon acrosome reaction, the acrosome integrity is disrupted and its content is released digesting the oocyte's *zona pelucida* [61]. The flagellum contains the motile apparatus necessary for sperm motility [55,62] and is divided into four ultrastructures: connecting piece; midpiece; principal piece and end piece [55]. The connecting piece attaches the flagellum to the sperm head; the midpiece contains the sperm mitochondria; the principal piece and the end piece generate the flagellar waveform pattern motility [55,62,63]. The main structure of the flagellum is the axoneme, which is the sperm motility motor. This structure is well conserved throughout evolution, present in flagella from protozoans to humans [50,62]. The axoneme originates in the connecting piece and terminates in the end piece. Typically, the axoneme is composed of nine microtubules doublets and a central pair, designated a 9+2 structure. The nine microtubules doublets connect to each other by nexin links and connect to the central pair by projections, the radial spokes. The latter are responsible for positioning and spacing the microtubules doublets in a perfect circle around the central pair microtubule. Projecting from the microtubules doublets are the inner and outer axonemal dynein arms (classified according to their position in relation to the doublet microtubule). These proteins are key for motility, by promoting sliding of a microtubule doublet in relation to the adjacent. The flagellar beating pattern begins with a dynein from one doublet transiently interacting with the following doublet. In the presence of ATP, axonemal dynein "walks" towards the base of the flagellum, forcing the adjacent microtubule doublet to slide down. Since microtubules are attached to the connecting piece, this movement encounters resistance, leading to the bending of the flagellum. At the end, the dynein detaches from the adjacent microtubule. To obtain a flagellum waveform movement and consequently motility, this process has to occur on one side of the axoneme and be inactive on the opposite site. Hence, the flagellar beat appears to be based on an "on-and-off" switch of the axonemal dynein arms, in specific points in the axoneme [50,55,62,63].

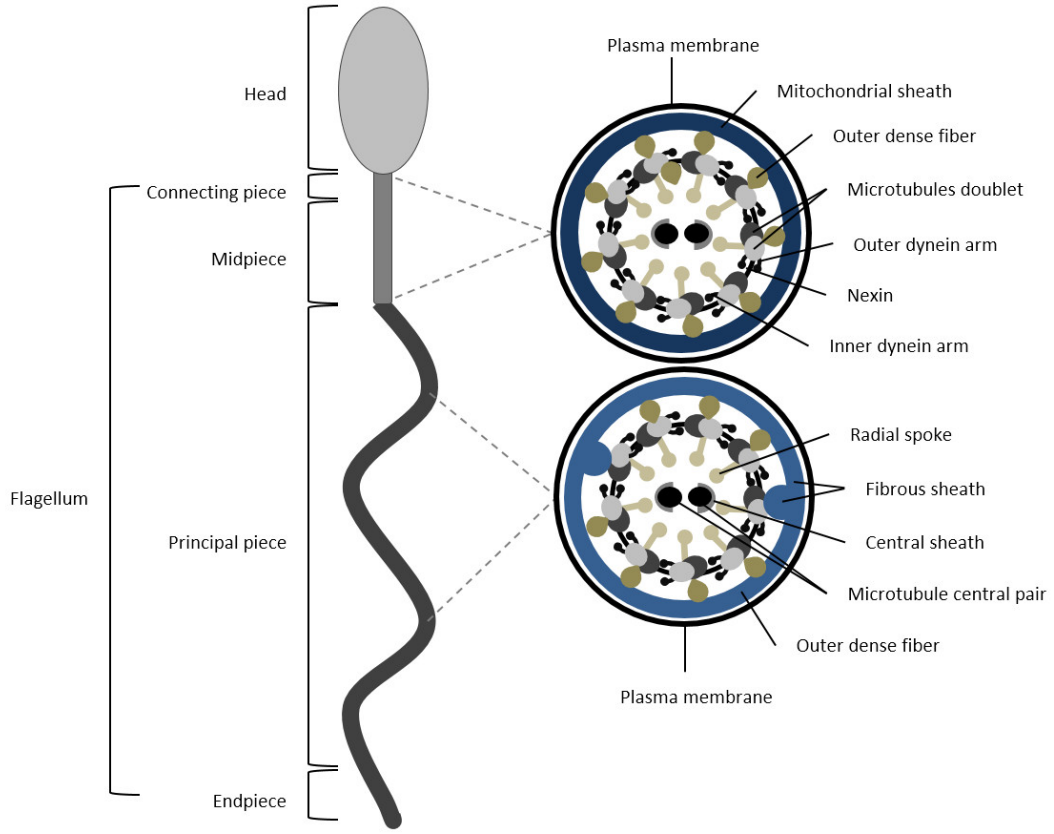

Figure A2.1. Schematic representation of human spermatozoon and flagellum structure. Human sperm is divided into two parts: head and flagellum. The flagellum is further divided into four structures: connecting piece; midpiece; principal piece and endpiece. A cross-section shows that the flagellum structure differs between midpiece and principal piece. In midpiece, plasma membrane and mitochondrial sheath surround the outer dense fibers. Within outer dense fibers, is the axoneme, composed of the microtubule doublets associated with the dyneins arms (inner and outer), radial spoke and microtubule central pair. Nexin connects adjacent microtubule doublet. In the principal piece, plasma membrane and fibrous sheath surround the outer dense fibers. In two opposing microtubule doublets, the outer dense fibers are replaced by to longitudinal columns of fibrous sheath.

In mammalian sperm, between the axoneme and the plasma membrane there are several accessory structures, such as the mitochondrial sheath, outer dense fibers and fibrous sheath [50,55]. In the midpiece, the axoneme is surrounded by outer dense fibers and the mitochondrial sheath, while in the principal piece the axoneme is surrounded by outer dense fibers and fibrous sheath. The end piece has no accessory structures between the axoneme and the plasma membrane [62]. The mitochondrial sheath is composed of individual mitochondria coiled helically around the axoneme. In humans, the midpiece length is about a dozen mitochondrial turns [64]. The outer dense fibers have a petal-like shape, are directly above the axoneme microtubules doublets and diminish in diameter from base to tip of the principal piece [65]. The outer dense fibers appear to be responsible for maintaining the passive elastic structure and recoil of the flagellum and to protect the axoneme against shearing forces [66]. In the principal piece, the fibrous sheath confers

flexibility, shape and plane to the flagellar beat [67]. It also supports and ensures compartmentalization of signaling proteins that regulate motility, capacitation, and hyperactivation. In the principal piece, two opposing outer dense fibers are replaced by fibrous sheath projections [65] (Figure A2.1).

The regulation and propagation of this “on-and-off” signal and the conversion into flagellar bending appears to reside in the control of the ATPase activity of axonemal dynein arms. Although this process is not fully understood, alterations in pH, ATP availability, calcium concentration and phosphorylation of key proteins appears to modulate axonemal dynein arms activity and consequently sperm motility. The process of ATP production and the signal pathways that control axonemal dynein activity will be discussed in the next topics [68].

A2.2. Energy for motility - Oxidative phosphorylation *vs* glycolysis

One of the key requirements for sperm motility is energy availability. ATP is the fuel used by axonemal dynein ATPases within the flagellum [69], and active protein modifications, such as phosphorylation, also depend on ATP. Thus, it is not surprising that sperm requires exceptionally high amounts of ATP when compared to somatic cells [70]. Consequently, a constant and adequate supply of ATP is crucial [69]. In spite of the efforts [69,71,72], a long-standing debate exists on the metabolic pathway responsible for sperm motility bioenergetics: oxidative phosphorylation in mitochondria, glycolysis in the flagellum and head, or both.

In mammalian sperm, oxidative phosphorylation occurs in mitochondria, which are exclusively located in the midpiece. A mature mammalian spermatozoon contains approximately 72-80 mitochondria [73] and in theory can produce more than 30 ATP molecules per glucose molecule [74]. Since midpiece is localized at the anterior end of the flagellum the transport of ATP to the all length of the flagellum must be efficient. Ford et al believe that the model of flux transfer chains proposed by Dzeja and Terzic in 2003, is able to transport the ATP produced in mitochondria through the entire flagellum [72,75]. It was indeed shown that an increase in human sperm motility requires a parallel increase in mitochondrial activity [52,71,76]. Also, the use of specific inhibitors for the mitochondrial electron transport chain and ATP synthase decreases drastically human sperm motility [74]. Moreover, high mitochondrial activity levels increase the success of *in vitro* fertilization rate [69]. These studies suggest that human sperm motility correlates with

mitochondrial functional status. Further, mitochondrial activity is negatively correlated with morphological alterations in the midpiece, which appears to reinforce the role of mitochondrial ATP production in sperm motility [71].

In spite of the reports supporting the role of mitochondria in sperm motility, its contribution to flagellar beat can be questioned. Since mitochondria are localized in the midpiece, it has been argued if ATP diffusion and carrier systems are able to supply ATP throughout the entire length of the flagellum (about 50µm in humans) [72,74]. Also, some authors argued that if ATP produced in the mitochondria fuels motility, the levels of reactive oxygen species produced during the electron transport chain would be harmful to DNA integrity [77]. However, both enzymatic (e.g. superoxide dismutase and glutathione peroxidases) and non-enzymatic antioxidants (e.g. glutathione and ascorbic acid) present in human sperm and seminal plasma appear to control the levels of ROS activity [77–79].

A growing hypothesis for the source of ATP (or at least part of the ATP) in sperm is the glycolytic pathway. Glycolysis is the process by which glucose is converted into pyruvate. During this process, energy is released in the form of ATP and NADH, with a rate of 2 ATP molecules per glucose. When human sperm are deprived of glucose (the starting unit of glycolysis) or when glycolysis is blocked, ATP content and protein tyrosine phosphorylation decreases. Consequently, sperm exhibits decreased motility [74,80–83]. Mukai and Okuno proved that even when mitochondria function is conserved, mouse sperm motility decreases when glycolysis is impaired. Moreover, a sperm-specific lactate dehydrogenase (LDHC) accounts for 80-100% of the LDHC activity in human sperm and is anchored to the fibrous sheath along the length of the flagellum, representing a local ATP production closer to the site of ATP consumption [83]. Also, Odet et al showed that a disruption in mouse sperm-specific *Ldhc* resulted in impaired fertility due to immotile sperm [84]. Furthermore, sperm-specific LDHC presents a low K_m for pyruvate and a high K_m for lactate, suggesting a higher affinity of LDHC for pyruvate and consequently a preference for the glycolytic energy pathway. It is noteworthy to mention that although most mammals rely, at least partially, on glycolysis for motility, the bull seems to be an exception. Oxidative phosphorylation in bull sperm appears to be the only source of ATP [85].

A third possibility for ATP availability in human sperm is a cooperation and dependence between oxidative phosphorylation in mitochondria and glycolysis in the flagellum. This hypothesis is supported by the different energetic subtracts of the reproductive tract fluids [60,70]. It appears

that mammalian sperm switch between metabolic pathways depending on oxygen availability and glucose, pyruvate, lactate, sorbitol, glycerol, and fructose concentration in the fluid [74,81,86–89]. For example, in the human female reproductive tract, glucose, pyruvate and lactate are found in the range of 0.5-3.2mM, 0.1-0.2-mM and 4.9-10.5mM, respectively. Sperm must adapt its bioenergetic metabolism according to the metabolites available from the epididymis until the fallopian tubes [90].

A2.3. Signaling pathways in sperm motility

Sperm leaving the testes are immotile and acquire motility throughout the epididymis journey. Sperm is virtually devoid of transcription and translation due to highly condensed DNA and lack of endoplasmatic reticulum [91]. Since gene expression cannot be accounted for functional alterations in sperm, activation or inhibition of specific signaling pathways and protein post-translational modifications must be involved. The interaction between sperm and the environment created by the epididymis and the female reproductive tract are essential to trigger sperm motility.

Several signaling pathways have been described as having a role in mammalian sperm motility. In the next section, the most relevant signaling pathways and messengers involved in sperm motility acquisition in the epididymis and hyperactivated motility in the female reproductive tract will be described.

A2.3.1. Sperm motility in the male reproductive system – A journey through the epididymis

After spermatogenesis, sperm is morphologically complete but functionally immature. When entering the epididymis, a long convoluted tubule that connects the testis to the vas deferens, human sperm is incapable of fertilizing an oocyte. The epididymis is roughly divided into three regions: caput, corpus, and cauda. The caput is adjacent to the testis and the caudal portion adjacent to the vas deferens [12]. Only during the journey through the epididymis the sperm acquire fertilization ability. Epididymal maturation involves the interaction of sperm with proteins that are synthesized and secreted into the epididymis in a region-dependent manner [17]. Most of studies concerning epididymis function are carried out in rodent models, due to the limited availability of human epididymal tissues at reproductive ages, the impossibility of mimicking the epididymis environment *in vitro* and the difficulty to manipulate the human epididymis experimentally. The exact mechanism behind sperm motility acquisition in the epididymis is still

unknown [55].

One of the first described signaling events responsible for sperm motility acquisition within the epididymis is the control of Phosphoprotein Phosphatase 1 (PPP1, also known as PP1) activity in sperm (Figure A2.2). PPP1CC2 (also known as PP1γ2), a testis-enriched sperm-specific PPP1 isoform is distributed throughout the flagellum, midpiece and posterior region of the head [92] suggesting a role in motility and acrosome reaction [93,94]. In 1996 Smith et al described, for the first time, the association between PPP1 activity and sperm motility. In caput sperm PPP1 activity is high and sperm is immotile. Conversely, in caudal sperm PPP1 is inactive and sperm are motile [95,96]. In the following years, several studies attempted to unveil the signaling pathways responsible for PPP1 activity modulation in sperm, through the epididymis journey. PPP1 regulatory subunit 2, PPP1R2 (also known as Inhibitor-2) is a PPP1 inhibitor [97]. In sperm, PPP1R2 localizes throughout the principal piece, midpiece and posterior and equatorial regions of the head. Former studies described PPP1R2 activity in human sperm and that some of the sperm PPP1 population is bound to PPP1R2 and therefore inactive [98]. When phosphorylated at threonine 73, human PPP1R2 is unable to bind to PPP1, rendering its activity [99]. Glycogen synthase kinase 3 (GSK3) is the kinase responsible for PPP1R2 phosphorylation. Interestingly, GSK3 activity has been extensible correlated with sperm motility regulation both in cauda and caput (bovine, mouse and macaque models) [100–102]. GSK3 is 6 times more active in caput than in caudal sperm and its activity is correlated negatively with sperm motility [100,102]. Moreover, GSK3 appears to have an isoform-specific function on sperm motility. When GSK3alpha is knockout there is a decrease in sperm motility and metabolism, while GSK3beta conditional knockout is fertile [103].

Recently, Koch et al showed that the Wnt signaling can be partially responsible for GSK3 activity regulation in epididymal sperm. In corpus and caudal epididymis, Wnt signaling proteins are released in epididymosomes from epididymal principal cells. In the epididymis lumen Wnt proteins bind to Low-density lipoprotein receptor-related protein 6 receptor (LRP6), activating it. In turn, LRP6 induces GSK3 inhibition, which leads to decreased PPP1R2 phosphorylation [104]. Synergistically, GSK3 activity can be modulated by Phosphoprotein phosphatase 2A (PPP2 also known as PP2A). Dudiki et al demonstrated that in caput sperm demethylated and phosphorylated PPP2 isoform alpha (PPP2CA) is active. Consequently, it dephosphorylates GSK3 in serine residues rendering active. Subsequently, PPP1R2 threonine 73 is phosphorylated and the inhibitor becomes inactive, resulting in active PPP1 and immotile sperm. On, caput sperm, methylation of PPP2CA increases due to a decrease in Protein phosphatase methylesterase 1 (PPME1) activity. In these

conditions, PPP2CA becomes inactive resulting in increased GSK3 serine phosphorylation and thus, its inactivation. Subsequently, PPP1R2 is active and inhibits PPP1, leading to motile sperm [105] (Figure A2.2).

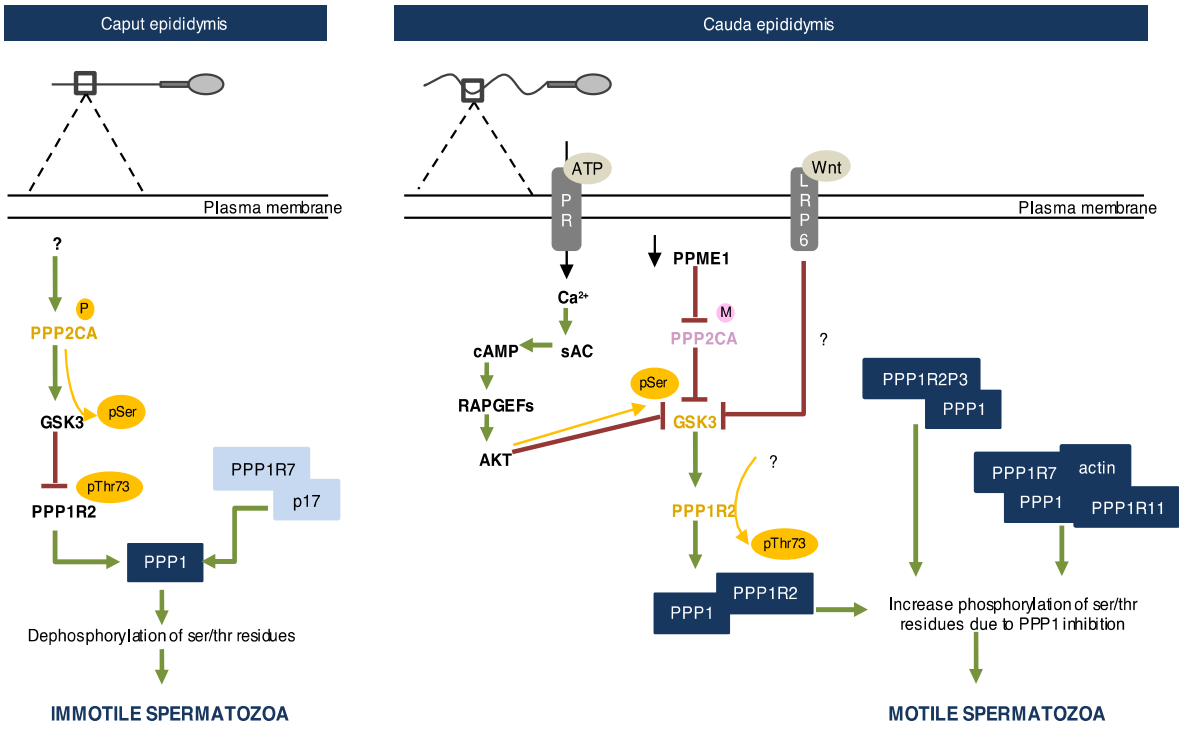

Figure A2.2. Schematic representation of the signaling events required for sperm motility acquisition in the epididymis. In caput epididymis, PPP2CA is phosphorylated and consequently active, which in turn dephosphorylates GSK3 at serine residues, rendering it active. GSK3 phosphorylates PPP1R2 at thr73 which inhibits the interaction between PPP1R2 and PPP1 resulting in active PPP1. PPP1R7 is bound to p17, which leads to free and active PPP1. Active PPP1 results in dephosphorylation of key residues and consequently immotile sperm. In cauda epididymis, PPME1 activity decreases increasing PPP2CA methylation, resulting in inhibition of PPP2CA. Consequently, GSK3 serine phosphorylation increases leading to GSK3 inhibition. Also, Wnt binds to LRP6 receptor which promotes GSK3 inhibition by an unknown mechanism. Moreover, ATP binds to purinergic receptors (PR), resulting in calcium influx. Calcium activates sAC, which produces cAMP activating Rap guanine nucleotide exchange factor **(**RAPGEFs). The latter activates AKT that phosphorylates GSK3 at serine residues inactivating it[106]. GSK3 is inhibited, which leads to decrease Thr73 PPP1R2 phosphorylation (the phosphatase responsible is unknown). Consequently, PPP1R2 binds PPP1. Also, PPP1 is bound to PPPP1R2P3 and in a complex with PPP1R7, actin and PPP1R11. Thus, PPP1 activity is inhibited and ser/thr phosphorylation of key residues increases leading to motile sperm. P: Phosphorylation; M: Methylation. Green arrows: activation. Red arrows: inhibition. Yellow arrows: phosphorylation. In yellow: phosphorylated proteins. In pink: methylated proteins.

Moreover, in 2013, Korrodi-Gregório et al identified a new PPP1R2 isoform in human sperm, PPP1R2P3 (also known as inhibitor 2-like) [98]. This isoform has the unique feature of threonine 73 being replaced by proline avoiding GSK3 phosphorylation. Korrodi-Gregório et al hypothesized that PPP1R2P3 is only present in caudal motile sperm, representing a constitutively inhibitor of PPP1, and therefore responsible for the process of sperm motility acquisition along the epididymis journey [98] (Figure A2.2).

Besides PPP1R2, PPP1 regulatory subunit 7 (PPP1R7) and PPP1 regulatory subunit 11 (PPP1R11), other two PPP1 inhibitors are present in sperm, suggesting a synergetic mechanism for PPP1 activity control [107]. PPP1R11 (also known as I3) is a human homolog of the mouse Tctex5, a protein associated with male infertility due to impaired sperm motility. On mouse sperm, PPP1R11 is localized in the head and principal piece of the flagellum, the same subcellular localization of PPP1 [108]. In rat liver cells, PPP1R7 (also known as sds22) inhibits PPP1, and in rat testis, it associates with PPP1CC2. In caput, bovine sperm PPP1R7 and PPP1CC2 do not interact. Instead, PPP1R7 is associated with a 17kDa protein (p17) [109], resulting in active PPP1. Conversely, in mouse caudal sperm, PPP1R7, PPP1R11, actin and PPP1 form a complex catalytically inactive [107] (Figure A2.2). Although PPP1 plays a crucial role in keeping motility at check in caput sperm, its substrates are still unknown. Besides PPP1, a sperm-specific isoform of calcineurin (PPP3CC) appears to be involved in epididymal maturation. Upon ablation of PPP3 and regulatory subunit PPP3R2, male mice are infertile due to impaired hyperactivation and penetration of *zona pelucida*. Phenotypically, sperm without PPP3CC presents an inflexible midpiece. When sperm is hyperactivated, the bending capacity of the midpiece increases, however, PPP3CC null sperm are incapable of exhibiting this increase. Interestingly, inhibition of PPP3CC with specific inhibitors, results in a quick phenotype (5 days) alteration from normal to inflexible midpieces. After one week of halting drug administration, the sperm are completely recovered and fertility is restored [110].

Since for sperm motility dephosphorylation must be shut down, it is not surprising that phosphorylation must increase. It is well known that the soluble adenylyl cyclase/Cyclic adenosine monophosphate/cAMP-dependent protein kinase (sAC/cAMP/PRKA; cAC/cAMP/PKA) signaling pathway affects positively sperm motility. Although the sAC/cAMP/PRKA signaling is mostly associated with hyperactivated motility [58], its involvement in sperm motility acquisition is unquestionable (see below) [111,112]. In 2013, Vadnais et al, proposed a cross talk between the GSK3/PPP1R2/PPP1 and sAC/cAMP/PRKA pathways during motility acquisition in the epididymis [106] (Figure A2.2). In Figure A.2. the main signaling pathways involved in motility acquisition in the epididymis are represented.

A2.3.2. Sperm motility in the female reproductive system

During unprotected intercourse, millions of sperm are deposited in the female reproductive tract, more specifically in the vagina. From there on sperm must swim until they reach the oocyte in the fallopian tube. Although sperm is already motile when ejaculated, hyperactivated motility must be acquired to overcome all the filters and traps imposed by the female reproductive tract.

Interestingly, it is the unique female enviroment that triggers the signaling pathways essential for sperm hyperactivated motility [113]. In the past years, many efforts have been made to unravel the role of key messengers and signaling pathways involved in hyperactivated motility.

Firsts messengers - Calcium, bicarbonate, and progesterone

In sperm, calcium (Ca^{2+}) plays a central role in events preceding fertilization, specifically, motility, chemotaxis and acrosome reaction. The relevance of Ca^{2+} on eukaryotic cell physiology is reflected in the several Ca^{2+}-depended enzymes, intracellular Ca^{2+} stores and Ca^{2+} channels [114] . Human sperm is no exception. The most described role of Ca^{2+} in human sperm motility is the activation of the soluble adenylyl cyclase (sAC). Moreover, inhibition of Ca^{2+} signaling is associated with male subfertility [115]

In human sperm, mean basal Ca^{2+} is kept around 100nM-200nM, while in the extracellular medium varies between 1-2mM [116]. This gradient concentration is accomplished by a Ca^{2+}-ATPase pump, which promotes Ca^{2+} efflux with ATP consumption [117,118]. A low resting Ca^{2+} concentration is what keeps human sperm in a basal motility state in the caudal portion of the epididymis and vas deferens. However, in the female reproductive tract, Ca^{2+} concentration must increase to induce hyperactivated motility. The female reproductive system controls the increase in Ca^{2+} concentration in the sperm through clues in specific places, and menstrual cycle phase [119].

The influx of Ca^{2+} into human sperm is promoted by several mechanisms: increase in membrane permeability [120]; depolarization [121]; inhibition of the Ca^{2+}-ATPase pump; activation of voltage-dependent calcium channel (VOCCs). Yet the main known mechanism for Ca^{2+} influx into sperm is the CatSper (cation channel of sperm), identified in 2001 by Ren et al [122]. This channel, located at the principal piece of the flagellum, is the only constitutively active Ca^{2+} conductance present in human sperm, responds weakly to voltage alterations and is pH-sensitive [122,123]. Moreover, null mice for *CatSper1* are infertile [122]. Human CatSper activation is triggered mainly by extracellular progesterone (see below), prostaglandins [124] and an alkaline environment (created by increasing HCO_3^- concentrations) [125]. Curiously, mouse CatSper is activated by neither progesterone nor prostaglandins. This suggests a species-specific Ca^{2+} influx process, possibly to avoid cross-species fertilization [124]. Although it is not located to the sperm's head, CatSper appears also to be involved in the acrosome reaction by increasing Ca^{2+} concentration [126]. Further, Brenker et al concluded that a range of small odorant molecules present in the female reproductive tract activates CatSper, resulting in chemotaxis of the sperm towards the oocyte [127].

Although the process of Ca^{2+} influx is essential for sperm motility, it is established that the human sperm has Ca^{2+} stores. The most promising candidates for Ca^{2+} stores in human sperm are the acrosome, the nuclear membrane and the cytoplasmic droplet [128]. Interestingly, it appears that in the sperm flagellum there are no Ca^{2+} stores, suggesting that the stores are important on processes such as acrosome reaction, rather than in motility. Moreover, the presence in human sperm of sarcoplasmic/endoplasmic reticulum calcium ATPases (SERCAs), channels that transport Ca^{2+} from the intracellular medium to Ca^{2+} stores in somatic cells, further reinforces the presence and functional importance of Ca^{2+} stores [128,129].

Progesterone is probably the most potent activator of capacitation of human sperm [130]. It is produced by the *cumulus oophorus* cells that surround the oocyte. At nanomolar concentration range, progesterone induces Ca^{2+} influx and promotes extensive phosphorylation through the activation of several kinases, such as PRKA [131], Protein kinase C (PRKC), Mitogen-activated protein kinases (MAPKs) and Phosphatidylinositol 4,5-bisphosphate 3-kinase (PIK3C, PI3K) [132,133]. Phenotypically, progesterone increases the number of motile sperm, induces hyperactivated motility and acrosome reaction, and appears to be involved in sperm chemotaxis towards the oocyte [133–138].

In somatic cells, progesterone acts through classic nuclear progesterone receptor and regulates gene expression. Conversely, sperm is transcriptionally silent and the effect of progesterone on sperm physiology is far too quick to be explained by gene expression [139]. In 2011, Strünker et al and Lishko and et al concluded that progesterone activates the CatSper channel [124,125]. As sperm leave the epididymis and mixes with the prostatic seminal vesicle fluid, the bicarbonate (HCO_3^-) content increases [140]. Reaching the female reproductive system, sperm encounters an acidic environment, which should reduce motility. Yet, the basic pH of the seminal plasma neutralizes the acidic pH and allows sperm motility [141] and the semen is deposited closely to the uterus cervix so that sperm can quickly move out of the vagina [56,142]. Within the uterus, the rich HCO_3^- alkaline environment is essential for sperm hyperactivated motility [143]. Curiously, throughout the menstrual cycle, HCO_3^- concentrations vary from 35nM at the follicular phase to at least 90nM at ovulation, potentiating fecundation [142]. Sperm-specific Na^+/ HCO_3^- co-transporters mediate the influx of HCO_3^- and, as a result, there is an increase on sperm pH and depolarization [144]. Though, to achieve complete depolarization, there must be a Na^+ and K^+ influx, Na^+ is transported by the Na^+/ HCO_3^- co-transporters and K^+ influx is mediated by Calcium-activated potassium channels and the ion transporter Na,K-ATPase. Calcium-activated potassium channels are regulated by

intracellular alkalinization and cAMP, which hints a HCO_3^- indirect regulation of K^+ [141]. Within the sperm, HCO_3^- activates factors that exchange phospholipids within the bilayer plasma membrane. Consequently, cholesterol is vulnerable to albumin, which is the most abundant protein on the female reproductive system, and the main cholesterol acceptor. Albumin can decrease up to 40% of the sperm cholesterol content and this leads to an increase on membrane fluidity [145,146]. Depolarization, intracellular alkalinization and increased membrane fluidity promote influx of Ca^{2+}.

The Na,K-ATPase pump is a membrane protein found in all eukaryotes [147]. By using the energy released from ATP hydrolysis the Na, K-ATPase pump promotes the efflux of three molecules of Na^+ and influx of two molecules of K^+ [148]. Two subunits compose the Na,K-ATPase protein, the alpha and beta subunits. In several species, including human, the alpha4 sbunit presents the most restricted expression. It is present in sperm principal piece only in mature sperm of males in sexual maturity. Besides the Na,K-ATPase alpha4 subunit, only subunit alpha1 is present in sperm [147]. Knockout studies revealed that the Na,K-ATPase alpha4 subunit is crucial for sperm physiology, since alpha4 subunit KO is completely sterile. Knockout sperm presents reduced primary and hyperactivated motility, bent flagellum, increased intracellular Na^+ and cell plasma membrane depolarization [149]). Mcdermott et al reinforce the role of Na,K-ATPase alpha4 subunit on human male fertility by showing that an overexpression of this protein in mouse testis results in an increased total motility (among other parameters of sperm movement) [150]. Although the exact mechanism underlying the role of Na,K-ATPase in sperm physiology is not fully characterized, Na,K-ATPase alpha4 isoform appears to regulate intracellular H^+. Since is unlikely that the Na,K-ATPase transports H^+, its ability to regulate intracellular H^+ arises from its effect on the activity of a Na^+/H^+ exchanger (NHE). NHE uses the Na^+ gradient established by the Na,K-ATPase to extrude H^+ in exchange for the influx of Na^+ [151] and, consequently there is an increase in the intracellular pH [151] (Figure A2.3). In bovine sperm, Jimenez et al demonstrate that Na,K-ATPase activity is up-regulated during capacitation. Also, when Na,K-ATPase activity is impaired, the intracellular decrease in Na^+ and plasma membrane depolarization that typically accompany sperm capacitation are inhibited [152]. Ouabain, a cardiac glycoside produced in adrenal glands, is a Na,K-ATPase inhibitor which may have a physiological role in fertilization.[153–155].

Signaling pathways in hyperactivated motility

It appears that all the processes that occur in the female reproductive system increase the Ca^{2+} and HCO_3^- concentrations in the sperm. This raises the question: within the sperm, what signaling

pathways Ca^{2+} and HCO_3^- modulate in order to promote hyperactivated motility?

The most well-known pathway that controls hyperactivity and is highly dependent on Ca^{2+} and HCO_3^- concentrations is the sAC/cAMP/PRKA pathway. The sAC is specific to sperm, does not interact with Guanosine-5'-triphosphate and for its activation, it needs to bind to HCO_3^- and Ca^{2+} [144]. Upon activation, sAC converts adenosine monophosphate into 3´.5´- Cyclic adenosine monophosphate (cAMP). The increase of cAMP activates PRKA, a serine/threonine kinase that is dependent on cAMP [54,156]. The fact that when sAC or Calpha2 sperm-specific PRKA subunit are knockout, sperm does not acquire motility reinforcing the necessity of such signaling pathway in sperm motility [157,158]. PRKA appears to target and activate tyrosine kinases since inhibition of PRKA is correlated with a decrease in tyrosine phosphorylation [159].

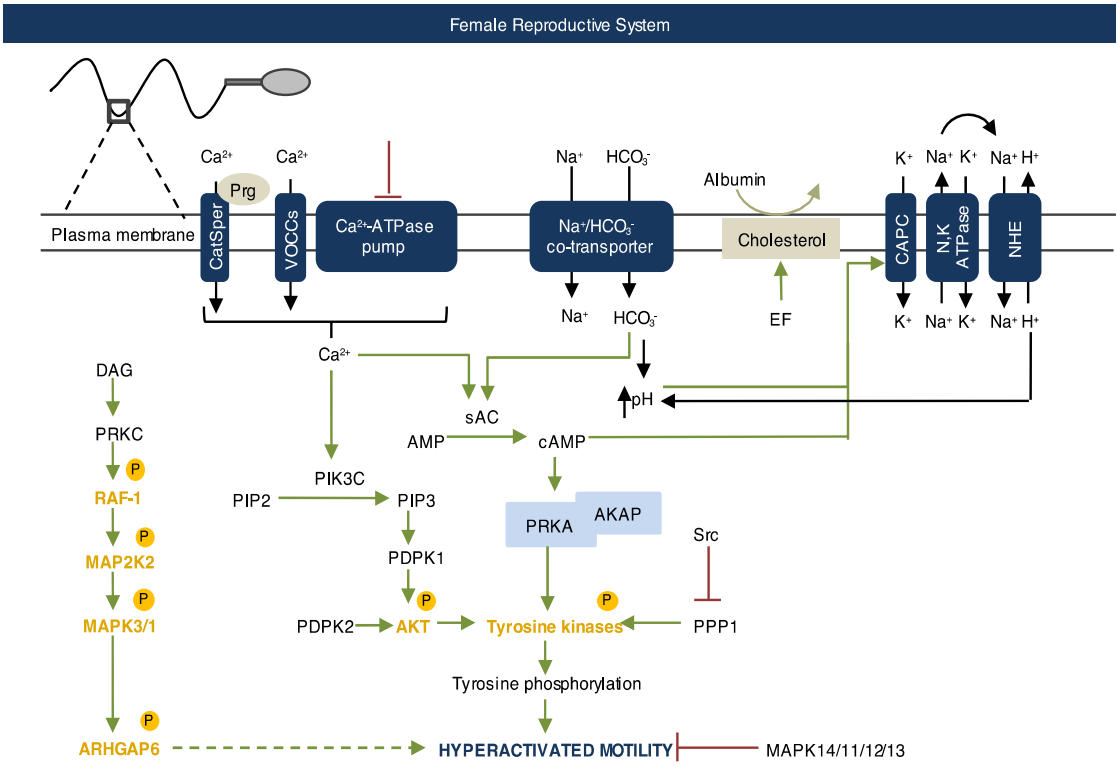

Figure A2.3. Schematic representation of the signaling events required for sperm hyperactivated motility in the female reproductive system. Several mechanisms are responsible for intracelullar Ca^{2+} increase in sperm. Progesterone binding to CatSper; activate VOCCs and inhibition of Ca^{2+}-ATPase pump promote Ca^{2+} influx. In sperm, HCO_3^- and Na^+ increase due to activation of Na^+/HCO_3^- co-transporter. Potassium enters through a calcium-activated potassium channels (CAPC) and Na,K-ATPase. The Na+ gradient created by the Na,K-ATPase, activates the Na^+/H^+ exchanger that promotes the influx of Na^+ and de efflux of H^+. HCO_3^- activates exchange factors (EF) that promote cholesterol externalization, becoming vulnerable to albumin. HCO_3^- and Ca^{2+} activate sAC, which converts AMP to cAMP and activates PRKA. PRKA activates tyrosine kinases, by phosphorylation. Also, Ca^{2+} activates PIK3C, which forms PIP3, that in turn activates PDPK1 and PDPK1 and PDPK2 activate AKT by phosphorylation. AKT activates tyrosine kinases by phosphorylation. At the same time, DAG activates PRKC which phosphorylates RAF-1; RAF-1 activates MAP2K2 and MAP2K2 activates MAPK3/1. Again, MAPK3/1 activates tyrosine kinases by phosphorylation. MAPK3/1 phosphorylates ARHGAP6 which may be involved in

hyperactivated motility. MAPK14/11/12/13 inhibits hyperactivated motility. Src inhibits PPP1, which allows an increase of tyrosine kinases phosphorylation. Tyrosines kinases phosphorylate key proteins inducing hyperactivated motility. P: Phosphorylation; Prg: Progesterone. Green arrows: activation. Red arrows: inhibition. Dashed arrow: predicted function. In yellow: phosphorylated proteins.

PRKA activity control and its subcellular localization are crucial for compartmentalization of its effect. In sperm, PRKA is typically tethered to A-kinase anchor proteins (AKAPs), which in turn targets PRKA to specific subcellular sites and provides a mechanism for defining its substrates [131]. Besides anchoring PRKA, it has been showed that AKAPs can also scaffold phosphatases and other kinases from macromolecular complexes essential for signaling cascades within the sperm [131]. In flagellum sperm, AKAPs have a prominent role and AKAP4 is the main component of the fibrous sheath. Moreover, when AKAP4 is knockout sperm numbers are normal but sperm is incapable of progressive motility and proteins usually associated with the fibrous sheath, such as PRKA, are absent or significantly reduced [117].

Besides increasing PRKA activity, Battistone et. al proved that serine/threonine phosphatases must be inactivated to allow the increase in serine/threonine phosphorylation. Members of the Src family kinase (SFK) inactivate members of the serine/threonine phosphatases family possible by tyrosine phosphorylation. In human sperm, PPP1CC2 is the most promising candidate since it exhibits predicted tyrosine phosphorylation sites and only high okadaic acid concentrations overcome the SKI606 effect (an SFK inhibitor) [160]. Nevertheless, the involvement of other serine/threonine phosphatases, such PPP2CA or PPP4C cannot be ruled out [160].

Although sAC/cAMP/PRKA plays a central role in hyperactivated motility, it is not the only signaling pathway involved in this process. The involvement of the PIK3C-AKT pathway in sperm hyperactivated motility was described by Sagare-Patil et al. Progesterone promotes the influx of Ca^{2+} through the CatSper channel. Within the sperm, Ca^{2+} activates PIK3C (unknown mechanism) converting PIP2 into PIP3. The latter binds and activates 3-phosphoinositide-dependent protein kinase 1 (PDPK1), which phosphorylates RAC-alpha serine/threonine-protein kinase (AKT or PKB) in threonine 308. Consequently, AKT serine 473 becomes exposed and vulnerable to phosphorylation by PDPK2. Both phosphorylations render an active AKT, that phosphorylates serine residues on key proteins in sperm motility [133].

The Mitogen-activated protein kinase (MAPK) signaling is also involved in human sperm hyperactivated motility, although its role is controversial. In 2005, a study in human sperm stated that tryptase, a product of mast cells in the female reproductive system, activates MAPK3/1 (also known as ERK1/2), which in turn inhibits motility [161]. However, in 2008, Almog et al

demonstrated the existence of the MAPK cascade elements, more specifically, MAPK3/1, SOS, RAF-1, MAP2K1 and MAPK14/11/12/13 (also know as p38 proteins) in the tail of mature ejaculated human sperm and revealed a positive correlation between MAPK3/1 and motility. Upon activation by diacylglycerol (DAG), Protein kinase C (PRKC, PKC) becomes active and phosphorylates RAF-1, which in turn phosphorylates and activates MAP2K1. MAP2K1 activates MAPK3/1 by phosphorylation. One of the identified substrates of MAPK3/1 was Rho GTPase-activating protein 6 (ARHGAP6). This protein may control the active slide of microtubules in sperm flagellum since it has already been described as being involved in cell motility and actin remodeling [162]. On the other hand, active MAPK14/11/12/13 inhibits sperm motility [163]. Again in 2015, Silva et al also showed a negative correlation between MAPK14/11/12/13 activation and human sperm motility [164]. In Figure A2.3 the signaling pathways involved in sperm hyperactivated motility in the female reproductive system are represented.

A2.3.3. Correlation between sperm motility and tyrosine phosphorylation

In 1989, Leyton and Saling described for the first time the presence of tyrosine phosphorylation in mammalian sperm (mouse) [165]. Twenty-six years later, the importance of tyrosine phosphorylation in capacitation and motility is unquestionable. The increase of proteins tyrosine phosphorylated in the human sperm is a hallmark of capacitation and has been positively associated with acquired and hyperactivated motility [159,166,167]. Most of the signaling pathways involved in human motility, including the ones described previously, culminate in activation of tyrosine kinases. The identity of most tyrosine kinases is unknown, still, the tyrosine kinases Scr [168], FGFR1 [169] and ABL1 [170] are already associated with tyrosine phosphorylation in mammalian sperm.

Several studies proved that dozens of proteins undergo tyrosine phosphorylation during capacitation in the sperm, mainly proteins localized in the flagellum [102,171–174]. In fact, human AKAP4 (see above), was one of the first proteins to be identified as a substrate for tyrosine phosphorylation[175]. Fibrous sheath protein of 95 kDa [176]; CABYR [177] and HSP90 [178] are other targets of tyrosine kinases [144]. Also, it has been hypothesized that dyneins are tyrosine phosphorylated and that this post translation modification controls the sliding of microtubules and therefore motility. The challenge for the next years is to identify new tyrosine phosphorylation targets and their relationship with sperm motility [159].

A2.4. Concluding remarks

This review attempts to summarize the current knowledge on the signaling pathways involved in sperm motility regulation. Since the first observation of the sperm by Anton van Leeuwenhoek´s in 1677, the knowledge concerning the sperm cell grew exponentially. The sperm structure, energy metabolism, epididymal maturation, and capacitation are indispensable for fertilization. Nevertheless, the road to unraveling the molecular players involved in the regulation of this processes is still long. Specifically, the molecular basis of sperm motility is not fully understood. Nowadays, we believe that the major setback to fully comprehend the molecular basis of human sperm motility is a technical one. Animal models and *in vitro* experiments are the only options to study epididymal maturation and capacitation. Understanding the mechanism responsible for human sperm motility is of great value. Sperm motility is the perfect target for male contraception since it does not disturb spermatogenesis and hormone production. Also, decreased sperm motility is increasing in developed countries, resulting in an escalation in male infertility rates. Understanding the signaling pathways behind sperm motility can help pinpoint the cause of male infertility and contribute to the development of new therapies.

A3. Interactomics and Bioinformatics: making sense of a big mess

Proteins are the “working force” of cells, having roles that go from structural support, enzymatic activity, production of other proteins, extracellular signals reception, etc. Protein-protein interactions (PPIs) control all biological processes within a cell and sperm cells are not an exception. After spermiogenesis, human sperm cells are virtually transcriptionally silent. This implies that sperm cannot rely on production of new proteins to respond to environment changes and orchestrate cellular processes. For that reason, two questions arise: what proteins are present in the human sperm and what interactions they stablish? Two scientific fields try to answer these questions, Proteomics and Interactomics. Proteome is the entire set of proteins being expressed in a given cell at a given time. Interactomics is the entire set of interactions occurring in a given cell at a given time [179]. Note that interactions can occur between every molecule within a cell, for example protein-protein; protein-DNA, Protein-RNA, DNA-RNA, etc. In the next section, we will focus on PPIs and those will be referred as the interactome, for simplification.

How big is the sperm proteome? In 2009, Baker estimated that the human sperm proteome would comprise around 2000-2500 proteins [180]. Several attempts have been made to decipher human sperm proteome. These studies not only aimed to establish the normospermic human proteome [181–185], but also depicted the proteomes of different stages of sperm maturation (e.g. ejaculated and capacitated) [186–189]; specific fertility/infertility conditions (asthenozoospermic; normal but IVF failure) [190–197]; specific subcellular compartments of spermatozoa (head or flagellum) [198,199]; post-translational protein modifications (phosphoproteome, nitrosylations, glycosilation) [186,200,201] and associated pathologies (diabetes, obesity, epididymitis) [202–204]. As far as our knowledge goes, more than 50 studies unveil a small portion of the human sperm proteome. The disparities between normospermic and asthenozoospermic samples have been extensively analyzed. This reflects the merging need to understand sperm motility mechanisms. Regarding human testis proteome, much has already been revealed. In 2015, the Human Protein Atlas project released the human tissues proteome, which included the testis-specific proteome. Eighty-two percent of all human transcripts analyzed are expressed in testis and around 11% present an elevated/restricted expression in testis. As expected, the elevated/restricted proteins are mainly involved in spermatogenesis [205]. Previously, Guo and colleagues and Djureinovic and colleagues characterized the human testis proteome [206,207].

By contrast, there are few interactomic studies on both testis and sperm, but none aimed to unveil the complete interactome of testis and sperm. Still, specific protein interactomes have been characterized in human testis. In 2011, Fardilha et al identified the interactome of PPP1CC1 and PPP1CC2 in human testis [92]. Among others, the testis interactome of APP, TCTEX1D4 and BRAP2 have been identified and characterized [208–210]. In human sperm, interactomes appear to be restricted to sperm-egg interactions [211]. Still, several PPIs have been identified in both testis and human sperm, but not resorting to an "Omic" approach.

Taking this into account, revealing the interactome of already known proteins involved in sperm motility will deepen our knowledge on motility mechanisms and may contribute to the identification of potential targets for a new male contraceptive.

A3.1. All or nothing: high-throughput techniques for protein-protein interactions identification

The term "Interactome" was first created by Sanchez in 1999 and intended to describe all binary PPIs in an organism [212]. Since the human genome was sequenced in 2001 [213], revealing the proteome and interactome of *Homo Sapiens* has been set as the next goal. However, it has been estimated that the human interactome contains a range of 130,000–650,000 binary interactions, far too complex to currently map [214,215].

Interactomes can be identified using two approaches: *in silico* through prediction algorithms or experimentally via high-throughput techniques [216]. *In silico* techniques will not be discussed further. The biggest attraction of high-throughput techniques is that in a single experiment hundreds of PPIs can be identified. There are several high-throughput techniques available that allow PPIs identification. However, we consider that two stand out: Yeast two-hybrid (YTH) and Co-immunoprecipitation followed by Mass spectrometry (co-IP/MS). In the next section, both techniques will be briefly described as well as their advantages and disadvantages.

A3.1.1. Yeast two-hybrid

Yeast two-hybrid was the father of all high-throughput techniques for PPIs identification. In 1989, Fields and Song, idealized the YTH system by taking advantage of two properties of eukaryotic transcription factors: (i) gene transcription only occurs in the presence of the DNA binding domain

(DBD) and the activation domain (AD) of a transcription factor; (ii) the two domains only need to be in close proximity and no covalent bond is necessary. In the original YTH, one protein of interest (bait) was fused into the DBD of GAL4 transcription factor and another protein to the AD (prey). If both proteins interact, the GAL4 transcription factor was resembled and the LacZ reporter gene was transcribed. This resulted in yeast colonies turning-blue in the presence of the substrate X-gal [217]. Quickly the YTH gained popularity mainly because it offered significant advantages compared to biochemical methods of PPIs identification (for example *in vivo* vs *in vitro*) [215]. Figure A3.1 is a schematic representation of the YTH principle.

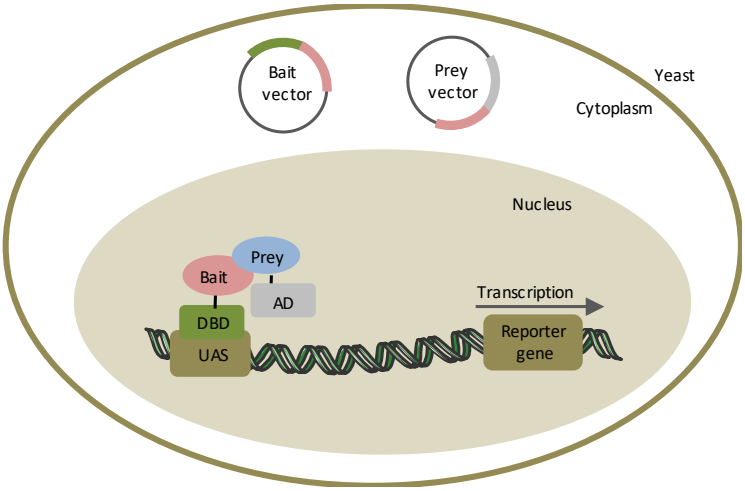

Figure A3.1. Schematic representation of YTH principle. The cDNA of a protein of interest (bait) is cloned into a vector with the DNA binding domain (DBD) of a transcription factor. A cDNA library or a cDNA of a protein (bait) is cloned into a vector with an activating domain (AD) of a transcription factor. Both vectors are transformed into yeast. Within the yeast, two hybrid proteins are produced and if bait and prey protein interact the DBD and AD come into close proximity in the nucleus and transcription of reporter genes is activated.

In its almost 30 years of existence, YTH has evolved, modified and improved. One of the biggest modification of this method is the possibility of high-throughput screening. The usage of cDNA libraries as preys, allows the identification of complete interactomes of a specific protein in one single experiment [218,219]. To further improve the method, several modifications were introduced to increase the number of interactions identified; decrease the rate of false positives; perform the screen in mammalian cells; identify protein-DNA and protein-RNA interactions and in different subcellular compartments [220,221].

The contribution of YTH to unveil interactomes is indisputable. In fact, the YTH became one of the most popular tools in molecular biology and thousands of PPIs have been identified with this method. Several interactomes have been characterized by YTH, ranging from complete organisms

to disease-specific interactomes [222–224]. The significant contribution of YTH to PPIs databases reflects the utmost importance of this technique. Around 50% of the interactions reported in PubMed resulted from YTH screenings and from 1990 to 2007 the number of high confidence binary interaction described by YTH increased exponentially [223,225]. We believe that even 30 years later, the YTH is probably the most commonly used technique for the detection of PPIs [215,226]. In 2005, two separated YTH experiments tried to characterize the human interactome. Rual et al identified around 2800 interactions (300 new) and Stelzl et al identified 3186 interactions (mostly new ones) [227,228]. Although both interactomes were obtained using the YTH, the experimental procedures were distinct. This may explain the low percentage overlap between both interactomes datasets (16% of common proteins and from those only 15% of the interactions were common) [229].

A3.1.2. Co-immunoprecipitation and Mass spectrometry

Co-immunoprecipitation was first coupled with Western blot allowing small-scale PPI identification. Yet, coupling co-IP with mass spectrometry (co-IP/MS), transformed this technique in a high-throughput approach for detection and identification of PPIs [230,231]. As the name suggests, co-IP isolates PPIs from cells or tissues by using an antibody that specifically recognizes a protein. Since it is typically performed in non-denaturing conditions, the antibody will not only “pull-down” its antigen but all proteins bond to it [232–234]. The biggest advantages of co-IP are that physiological conditions are kept (protein concentration, protein tridimensional structure, post-translational modifications, etc) and it is very specific and compatible with several downstream applications. Mass spectrometry is capable of identifying thousands of proteins in a single experiment. Thus, it seems wise to use mass spectrometry as the technique to identify PPIs after a co-IP in a high throughput manner (Figure A3.2 shows a schematic representation of co-IP/MS). Still, co-IP does not prove a direct interaction, since, protein complexes are often identified by co-immunoprecipitation.

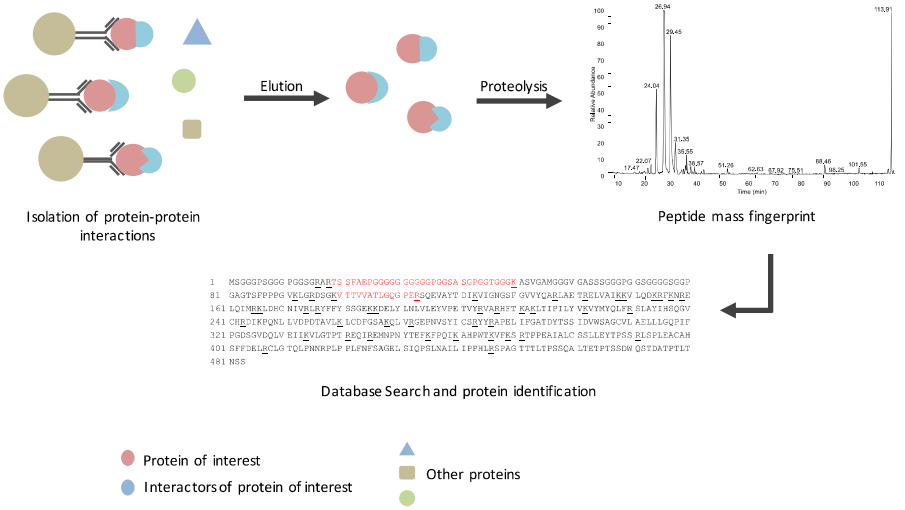

Figure A3.2. Schematic representation of a co-immunoprecipitation followed by mass spectrometry. Protein-protein interactions are isolated by using antibody specific to a protein of interest and eluted for Mass spectrometry analysis. For mass spectrometry, isolated proteins are cleaved and analyzed according to their mass to charge ratio. The peptide mass fingerprint is compared with repositories of mass fingerprints in publicly available databases. Finally, interactors of a protein of interest are identified.

Mass spectrometry measures the mass-to-charge ration of ions, originated by breaking a complex mixture of proteins. The major advantages of mass spectrometry it is sensitivity; quantity of information obtained and its ability to identify the peptide sequence of the interactors. Still, the high cost, challenging optimization, not only of the mass spectrometry itself, but also for the combination of this technique with for example co-immunoprecipitation, and the complex analysis of the results can be discouraging to the researchers [235]. In sperm, co-immunoprecipitation is particularly significant, since it is one of the only techniques that allows interactome identification. Any technique for PPI identification that relies on expression of exogenous DNA (e.g. tag based pull-down) or construction of a sperm cDNA library (e.g. yeast two-hybrid) cannot be employed to unveil the sperm interactome.

A key aspect that must be considered when choosing and analyzing results from high-throughput PPIs techniques is the type of interactions detected. PPIs can be classified as transient or stable, according to the temporal range of interaction. Transient PPIs have a higher probability of complex dissociation while stable PPIs have a higher temporal stability. Note that, a transient interaction can have high values of affinity and consequently be a strong interaction that last short period of time [236,237]. Focusing on YTH and Co-IP/MS, the PPIs identified are from distinct nature. YTH is able to detect transient and stable interactions due to the genetic reporter gene approach (amplifies the signal). Consequently, YTH must be used when, for example, signaling interactions are the goal of the study [233,238]. Co-IP/MS often detects stable and strong interactions. These result in the enrichment of PPIs from protein complexes such, the proteasome and cytoskeleton structures, or

strong interactions, such PPIs from anchoring proteins. The use of strong detergent in the lysis buffer and the multiple washing steps is the main reason for the loss of transient and weak interactions [216].

A3.2. And now what? *In silico* analysis of interactomes

High-throughput techniques for PPIs detection are the best option for interatomes identification. Yet, the fact that these techniques provide a great amount of information can be overwhelming. What are the key binary interactions in testis and sperm? Have these interactions already been described elsewhere? What is the biological meaning of such interaction? The challenge is to extract meaningful information from an immense amount of data and ultimately provide answer to one biological question. *In silico* analysis of interactome data can help answer such questions and decipher the biological relevance of the identified interactome.

Typically, bioinformatics analysis is based on extracting information from databases, enrichment and information visualization tools. In the next section, we provide a rough guide on how to perform an *in silico* analysis of interactomics data. To a more detailed guide please consult [242].

A3.2.1. Protein-protein interactions databases

To complement data obtained by experimental approaches, PPIs from public accessible databases can be retrieved. Currently, there are more than 200 PPIs publicly accessible databases [243]. Thus, it can be very difficult to choose the best option to retrieved PPIs data. Databases can range from PPIs, gene expression patterns, protein subcellular localization, among many others. There are two main types of databases: primary or secondary. Primary databases are repositories of experimental results submitted directly into the database. These data can be curated by database-associated researchers to ensure accuracy of the information. Secondary databases collect information from primary, other secondary databases and scientific literature and manually or computationally analyze this data to create new knowledge [239]

First, it is crucial to understand the origin of PPIs data in each database. PPIs can either be experimentally proved by small-scale or high-throughput techniques or predicted by extrapolation based on genomic context, structural information, network topology, text mining or machine learning algorithms. Although predict PPIs information can be suitable for an initial approach on a

specific protein interaction, high confident experimentally PPIs data must be used in an *in silico* analysis approach. To achieve high confident PPIs, each database classifies PPIs using quantitative or qualitative scores and different levels of curation. Typically, scores take into account the type of interaction, the number and quality of the experimental techniques used, the number of times the PPI is described in the literature and if the interaction is described in several non-human organisms [244]. Curation relates to constant update and confirmation of PPIs by a great human effort. Specifically, curators review publications and extract PPIs information. The type of information is vast, from identity of the interactions partners; experimental technology used; organism where PPIs was detected, among others [245]. Each PPIs database has a different curation policy (deep or shallow), which results in low overlap between repositories. Consequently, a choice must be made between recovering only PPIs information (shallow) or recovering as much detail about PPIs as possible (deep) [179,246].

In 2012, the International Molecular Exchange (IMEx) consortium established common curation rules and a central registry to manage article incorporation into databases [247]. Several PPIs databases were encouraged to incorporate the IMEx curation rules and became members of the IMEx consortium. The consortium aims to coordinate curation to avoid redundant work, increase curation coverage by pre-establishing scientific publication to each database and synchronize curation to ensure data consistency across all IMEx databases. Table A3.1 lists the publicly available PPIs databases that present human PPI data (data obtained on 18 July 2017).

Besides the quality and origin of the PPIs data in each database, the way PPIs information is reported must be considered. Due to the individual data report formats of each database, merging and comparing information could be challenging. In 2004, several databases united efforts and created the PSI-MI XML format which has been supplemented by a tabular format (PSI-MITAB). Currently, these table puts together 15 types of information from each binary and uses a controlled vocabulary (standardization of terms). These allows an easiest way to interchange, download, combine, visualize and analyze data in a single format from multiple resources [247,248].

A3.2.2. Adding biological meaning to protein-protein interactions

High-throughput PPIs identification techniques pushed the interactomic area forward. However, PPI biological context is partial lost when using high-throughput techniques. To circumvent this problem, biological information can be added to PPIs. Biological enrichment tools are defined as bioinformatics methods that take advantage of biological knowledge accumulated in databases and

apply these knowledge into raw data. [240]. Enriching PPIs with information such as tissue expression, gene ontology, cell signaling involvement and association with mammalian phenotypes, will allow to pinpoint biological important interactions in the overwhelming number of PPIs identified. In the next section, we will describe how to add biological context to PPIs.

Table A3.1. Protein-protein interactions databases. Publicly PPIs available that present human PPIs information. Name, type of database, curation level, latest update, reference and some features are described. Data retrieved on 18 July 2017.

Database	Type of database	Curation level	Features	Last Update	Reference
IntAct	Primary (self-curation) and secondary (data curated by other platforms) Only experimental data	IMEx (manually curated)	Around 750 000 interactions Scoring system relies on type of interaction and interaction detection method Binary interactions (protein-protein and protein-other molecules) data for several organisms besides *Homo Sapiens*	February 2016	[245,249]
DIP	Primary	IMEx (manually and computer approaches curated)	More than 81.000 binary interactions for 10 different organisms It is possible to search PPIs by interactions motifs or protein domains.	February 2017	[250]
HPIDB	Primary (self-curation) and secondary (curation of 12 external databases)	IMEx (manually curated)	Host-pathogen PPIs More than 55.000 interactions between 55 host (animal and plant) and 523 pathogen species (virus, bacteria, fungi, etc)	March 2017	[251,252]
MINT	Primary	IMEx (manually curated)	Around 125.000 binary interactions (PPIs and proteins-other molecules) in more than 600 organisms or *in vitro* assays. Association with human disease is stablished	Currently being update by IntAct	[245,253,254]
MatrixDB	Primary (experimental only)	IMEX (manually curated)	Binary interactions established by extracellular matrix proteins, proteoglycans and polysaccharides More than 15.000 molecular interactions (IMEx extended). However, the core of MatrixDB is composed by 789 interactions	2015	[245,255]

A3. Interactomics and Bioinformatics: making sense of a big mess

I2D	Secondary (experimental and predicted)	IMEx	PPIs for five model organisms and *Homo Sapiens* More than 1 million PPIs	October 2015	[256,257]
InnateDB	Primary (experimental) and secondary	IMEX (manually)	Genes and proteins interactions and signaling pathways involved in the immune system of humans, mice and bovine to microbial infection. 18,780 described interactions.	Junes 2017	[258]
UniProt	Secondary	IMEx	Data drives from multiple databases	Updated monthly	[259]
HIPPIE	Secondary	Manually curated	More than 300 000 experimental PPIs retrieved form 7 primary databases Scoring system is based on the nr of studies reporting an interaction; the nr and quality of the experimental techniques used to detect the interactions and the nr of non-human organism in which the interaction is reported	July 2017	[260,261]
PSICQUIC View	Web Service	-	Search web service that allows retrieval of PPIs and protein-molecules interactions from 36 primary and secondary databases. Access to more than 151 million binary interactions Results are reported in a controlled vocabulary in a specific format (PSI-MITAB).	-	[262]

A3.2.3. Gene Expression databases: Where are proteins being expressed?

PPIs are constantly changing to adapt to the biological context. Furthermore, interactomes are unique to cell types, tissues, development stage, etc. Consequently, adding expression data to PPIs offers a better understanding of binary interactions in a tissue-specific context. Mapping proteins in a given tissue is typically based on measuring its mRNA levels. High-throughput techniques for mRNA quantification includes RNA sequencing and expressed sequence tags (ESTs). ESTs are short sequence reads generated from 5´and 3´ends of tissue cDNA library (immobilized in a microarray). Since these sequences are fluorescently tagged, it is possible to measure the amount of cDNA. So, the higher abundance of a gene, the higher abundance of the EST derived from its transcripts and consequently the higher the signal [263,264]. RNA sequencing (RNA-seq) is an update of ESTs technique. Instead of generating short sequences of RNA only from 5´and 3´end, RNA-seq generates random cDNA fragments. This is particularly useful, to distinguish between isoforms [265].There are several options of tissue gene expression databases and repositories available. The main freely available databases are listed in Table A3.2.

Table A3.2. Tissue gene expression databases and repositories. Name, gene expression technique, latest update reference and some features are described. Data retrieved on 18 of July 2017.

Database	Gene expression detection technique	Features	Last Update	Reference
Human Protein Atlas (HPA)	RNA-seq and Cap Analysis of Gene Expression (CAGE)	Human protein-coding genes, expression and localization of the corresponding proteins based on both mRNA and protein data. Coverage of 100% mRNA data and 87% of protein data of the predictive human genes Presents several tissue-specific and cancer proteomes.	January 2017	[205,266]
BioGPS	Affymetrix chips (microarray) and imported data.	Expression data for *Homo Sapiens, Mus musculus, Rattus novergicus; Sus scrofa* and others Expression data for cancer tissues Based on submission of expression datasets by the users	May 2017	[267,268]

PaGenBase	Affymetrix chips (microarray), next generation sequencing (NGS) and curated data-mining	Expression of specific, selective and housekeeping genes of tissues of *Homo Sapiens* and 10 model organisms Tissue/cell, time/development /differentiation specific data	May 2013	[269]
Expression Atlas	RNA-seq and Affymetrix chips (microarray).	Data results from more than manually curated 3.000 independent studies. One third of the data is mRNA expression for Homo Sapiens. Other species, like chicken, pig and 17 plant species are also represented.	May 2017	[270]
UniGene	ESTs	For *Homo Sapiens*, there are more than 130.000 mRNA expression data Data for more than 100 other organisms (plants, fungi, bacteria, virus, etc.) Tissue/pathology/development specific data.	Updated monthly	[271]
Human Protein Reference Database (HPRD)		Data restricted to normal human tissues	April 2010	[272]

Since different methodologies for gene expression quantification are used by different databases, merging and comparing data can be challenging. If the goal is to retrieve data from two or more databases, normalization of the expression must be performed. Besides retrieving gene expression data, pin-pointing proteins that are specific or enriched into a particular tissue can be of importance. Some databases either provide a subset of tissue-specific proteins (such as HPA) or classify proteins as tissue-specific. However, there is no uniformed rules to classify a protein as tissue-specific. For example, HPA databases considers tissue-specific proteins as requiring an expression in one tissue at least five-fold higher than all other tissues [205]. On the other hand, UniGene considers a restricted expression when at least 75% of the detected gene expression is clustered in a single tissue [271].

A3.2.4. Gene phenotype and disease associated databases

In medicine, phenotype refers to relevant abnormalities (symptoms, behavioral anomalies, etc) that have an impact on quality of life. Typically, genetic abnormalities of multiple genes result in protein deregulation at cellular level and consequently a malfunction of the tissue, resulting in a phenotype. By analyzing the phenotype produced, we can infer the protein role within a cell [273].

Studying gene-phenotype association is based on two approaches: human gene-disease association and animal model gene-phenotype association. Although the ultimate goal is to unravel human gene-disease association, human sample shortage and ethical issues make it challenging. Using animals to create gene-phenotype model, more specifically mice, help complement the human based knowledge. In Table A3.3, most human gene-disease association databases and animal model gene-phenotype databases are listed. Most databases allow a phenotype based search (e.g male infertility) or a gene based search (e.g. PGK2) and data can be retrieved in a singular tabular format. Again, the lack of uniformed rules to classify phenotypes is the biggest challenge when unifying and comparing data between distinct databases.

Table A3.3. Gene-disease association and animal model gene-phenotype databases. Name, lasts update, reference and type of data presented are described. Data retrieved on 18 of July 2017

Database	Type of data	Last Update	Reference
Mouse Genome Informatics (MGI)	Freely available gene-phenotype data derived from *knock out* mice	June 2107	[274]
Online Mendelian Inheritance in Man (OMIM)	Human gene-disease and gene-phenotype on all known mendelian disorders and over 15.000 genes.	Update daily	[275]
Phenopedia/Genopedia	Human gene-disease and gene-phenotype data derived from manually curated data-mining. Disease (phenopedia) and genes (genopedia) query is possible.	July 2017	[276]
DisGeNet	Human gene/variants-diseases data curated from repositories; genome wide	May 2017	[277,278]

	associated studies catalogs, animal models and scientific literature.		
DISEASES	Gene-disease data obtained from automatic text mining, manually curated literature, cancer mutation data and genome wide associated studies catalogs	No information	[279]

A3.2.5. Enrichment analysis tools

So far, the databases presented provide information for individual proteins. However, can we analyze PPIs as a group of proteins? Enrichment analysis tools systematically analyze large protein lists and assemble a summary of the most enriched and pertinent biological processes [240]. The degree of enrichment is only significant when calculated by comparing the PPIs list against a specific background. Depending on the purpose of the study, the background is either the complete human genome; tissue-specific background; a control condition etc. Currently, more than 60 enrichment tools are available [240]. Most of these tools perform Gene Ontology annotations (enrichment of molecular function, biological process and cellular component). The Gene Ontology (GO) project is a major bioinformatics initiative to develop a computational representation of our evolving knowledge of how genes encode biological functions at the molecular, cellular and tissue system levels. The project has developed formal ontologies that represent over 40,000 biological concepts, and are constantly being revised to reflect new discoveries. To date, these concepts have been used to "annotate" gene functions based on experiments reported in over 100,000 peer-reviewed scientific papers.

Nevertheless, there are enrichment tools for signaling pathway, protein feature (e.g. domains, secondary structures) and gene expression profiles, among others. Database for Annotation, Visualization and Integrated Discovery, best known as DAVID, is a secondary enrichment tool. It collects information from multiple annotations sources (e.g. GO, KEGG pathway) and presents a broader enrichment analysis (DAVID was updated in 2016 [280]).

The main reason for such diversity in enrichment analysis tools relates to the statistical methods employed to determined enrichment. Consequently, even when analyzing the same set of PPIs,

results vary among tools (for a more comprehensive knowledge about enrichment statistical methods please consult [281]) [282]. Other differences, reported between tools are: organism supported; user friendly interface and results presentation.

A3.2.6. Visualization tools: building protein-protein networks

Information visualization tools transform crude data into structured and visually representations to simplify the analysis and interpretation of biological data, tipicaly networks [241]. The latter are a visual representation of how two or more entities influence each other. The first report of network based solution dates to 1735, when Euler used graph theory to solve the seven bridges question [283]. In PPIs networks (PPIN), proteins are typically represented as nodes and interactions as edges connecting the proteins. More than visually representing PPIs and interactomes, PPIN topology (space arrangement of edges and nodes) can uncover crucial biological information [284]. Topological properties include connectivity degree, which is the number of interactions for each protein and node, betweenness centrality, which is the number of shortest paths that go through a protein among all shortest paths between all possible pairs of nodes [285]. Edge properties include types of relationships (inhibition; phosphorylation, etc) and edge betweenness centrality, which is the number of shortest paths that go through an edge among all possible shortest paths between all the pairs of proteins [286]. Analysis of such properties allows to identify, among other, hub proteins, bottleneck proteins and clustering sub-networks [287].

Cytoscape is the most widely used tool to create and analyze PPINs. Its popularity is reflected in the almost 1 million downloads and more than 300 plug-ins, accessible through the Cytoscape app store or directly on the software (information from 16 July of 2017) [288]. Also, numerous biological databases and repositories (e.g PSIQUIC VIEW; DisGeNet; String; Reactome) can be directly accessed using Cytoscape and enabling integration of PPIs; gene expression; gene phenotype and disease association; enrichment and many others. Nevertheless, all these data can be imported by the user as attributes given to each protein/node. After building a network, the user can visually represent biological information by using nodes an edges characteristics, such color, shape, name, etc; choose the best layout to stress a topological feature, among many other features (consult [289]). Although a bit rough, Cytoscape can analyze the PPIN topological features and find clusters (groups of highly connected nodes). Clusters are of particular important, since is expected that highly connected proteins share the same biological role [290]. Nevertheless, there are several apps that can perform an intense topological analysis [291].

A3.3. Concluding remarks

In silico analysis of interactomes is key to pinpoint crucial interactions and it is a starting point to narrow vast lists to a promising set of interactions. However, keep in mind that in bioinformatics approaches have its setbacks. Conclusion cannot be drawn without further experimental evidence; the rate of false positives reported in databases are still an issue and the fact that proteins exhaustive studied are overrepresented in databases, while other proteins are underrepresented.

A4. Available techniques for sperm internalization of exogenous material

Sperm is a unique cell which besides being the only haploid cell in the male body and fulfil its goal in the female reproductive system, it does not have the necessary machinery to produce new proteins, new lipids and other molecules, and its plasma membrane constitution is one of a kind [31]. Sperm plasma membrane is stable and metabolically inert [31]. Consequently, working with this type of cell can be challenging. Also, contrary to other type of cells, in which upon a few genetic alterations, can be grown and cultured *in vitro* (cell culture), full mature sperm cannot. In 2011, Sato et all reported producing spermatids and sperm using primitive spermatogonia from neonatal mouse testis. However, the process is long and intricate [292]. Moreover, human sperm samples are typically obtained in fertility clinics, resulting in a bias towards samples with fertility issues. Even more difficult is to obtain human epididymal sperm, which results in most motility acquisition studies to be performed in animal models.

Studying signaling mechanisms in somatic cells, is based on overexpression or deletion of a protein and evaluation of the phenotype produced. This is accomplished by either, transfection of foreign DNA into cultured cells or producing *knock out* (KO) or *knock in* (KI) mice. Testis-specific KO or KI has been successfully accomplished for several proteins [293,294]. This allows the study of the role of such protein in testis and spermatozoa. Yet, transgenic mice are an expensive, laborious and time-consuming technique. Regarding overexpression (transfection of gene copy) or deletion (siRNA) of proteins using foreign DNA, in sperm these techniques are useless, since sperm does not transcribe and translate DNA into proteins [10]. Another approach to studying signaling proteins is the use of inhibitor or activation drugs/molecules. However, some of these drugs cannot penetrate sperm plasma membrane [295,296].

Considering all the sperm peculiarities, working with this type of cell can be frustrating. Yet, in the past decades, several alternative methodologies have been developed and applied on studying signaling proteins, interactions and pathways in sperm. Most studies aimed to incorporate exogenous DNA material into spermatozoa for oocyte deliver (sperm-mediated gene transfer) [297]. Little effort has been put towards incorporating other molecules, such as proteins, into human sperm. In the next section, we will describe and discuss some methodologies to study sperm pathophysiology.

A4.1. Streptolysin-O

One of the first approaches to translocate impermeable molecules into mammalian cells involved using non-ionic detergents such as Triton-X (normally in immunocytochemistry studies) [298]. Although these reagents successfully expose the intracellular environment, since lipids and membrane proteins are removed, signaling pathways that depend on extracellular factors to be triggered are impaired. To circumvent these problem, in 1996, Dominguez used a bacterial toxin, streptolysin-O, to form large pores (26nm) that allowed entry of large molecules into mouse spermatozoa [299]. The use of streptolysin-O did not affect acrosomal reaction but only when pre-incubated with Ca^{2+}sperm motility was kept. Yet, the pattern of sperm motility changes when permeabilized with streptolysin-O. Since most plasma membrane is kept intact, signal transduction events initiated with cell surface components are kept intact. Nevertheless, since sperm cannot synthetize new lipids, disrupting the plasma membrane can cause sperm physiological alterations, for example motility and membrane dynamics [299,300]. Streptolysin-O has been used in human spermatozoa to transfer proteins [301], antibodies [302] and ions [303], among others.

A4.2. Lipossomes

Another strategy employed to transfer exogenous impermeant molecules into mammalian cells is the use pf liposomes. Liposomes are small vesicles that can occur naturally or are artificially produced from cholesterol and phospholipids. Due to the nature of these molecules (both hydrophobic and hydrophilic) they form spherical macromolecules, in which aqueous units ate enclosed and isolated from the outside. Depending on the lipid composition, liposomes differ considerable in surface charge, size, fluidity and rigidity [304]. Considering all properties, liposomes were developed as delivery system, by enclosing impermeant material into liposomes. They work by fusing with the plasma membrane and introduction of the enclosed material into the intracellular environment of mammalian cells [305]. Liposomes present low toxicity and high efficiency.

Specifically, in the male reproductive system, they occur naturally as epididymosomes and prostasomes (see section A1). Artificial liposomes already have been used in sperm, for protection after cryopreservation; incorporation of foreign material; trigger capacitation, acrosome reaction and gamete interaction by lipid membrane alteration [306,307]. Most of the material introduced into mammalian sperm was foreign DNA with the goal of being delivered to the oocyte [308,309].

Although the incorporation of DNA into the sperm is successful, no transgenic animals were obtained [310,311]. The first report of offspring obtained from liposome-transfected sperm are in silver sear bream [312]. Regarding, the usage of liposomes to modulate signaling events in sperm, the effect of inositol 1,5,5-triphosphate and bindin on sperm activation was assessed by deliver of both molecules into sperm [305,313].

A common laboratory reagent used for transfection of cultured cells, lipofectamine, is based on creating liposomes that incorporated foreign DNA and translocated into the cultured cells. Lipofectamine was already used in sperm (bovine) and did not improve either the transfection rate compared with detergent based permeabilization and in some cases sperm motility was affected after lipofectamine usage [314,315]. This may reflect the lack of compatibility between a general liposome composition (more suitable for somatic cells) and the uniqueness of sperm plasma membrane composition (see section A1). Moreover, this general liposome-delivery approach was mainly performed in poultry and cattle sperm to delivery exogenous DNA [314,315]

A4.3. Nanoparticles

Nanomaterials have been applied in several fields, from medical devices, food products, cosmetic and drug delivery systems [316]. Specifically, nanoparticles are advantageous to medical application since their surface to mass ratio is high and their ability to adsorb and carry several molecules, such proteins, drugs and DNA. Typically, nanoparticles present a dimension below 100nm, although in drug delivery larger particles may be needed to ensure sufficient amount of drug [317]. The nature of the nanoparticle can vary greatly, from metallic to magnetic nanoparticles [318]. From a biomedical point of view, the ability to customize nanoparticles is particularly advantageous. This allows large loading capacity, stability and specificity towards a selected cell population [319,320].

In sperm, most reports focus on using nanoparticle to deliver DNA into the spermatozoa or in the effects of nanoparticles used in medical applications on testis and sperm [319]. In 2008, Makhluf et al, successfully used nanoparticles to deliver anti-protein kinase C alpha antibody into bovine sperm cells [321]. In 2012, Feugang labeled sperm by fusing the protein *Renilla* luciferase with nanoparticles [322]. These reports proved that is possible to use nanoparticles as a delivery system for molecular research tools into sperm. However, a great concern is the fact that most nanoparticles tested for safety in spermatozoa are non-biodegradable which raises the question about reversibility and in a medical perspective their potential long-term effect [319].

A4.4. Cell penetrating peptides

Cell penetrating peptides (CPPs) are short peptide sequences (less than 40 aminoacids) that have the ability to rapid translocate into most mammalian cells [323]. The discovery of CPPs arouse from the observation that certain proteins could cross the plasma membrane. Tat transactivator of HIV virus type 1 could enter cells and target the nucleus. This observation resulted in Tat, and several structural variants of this protein, to originate the first CPP. Moreover, further studies identified the specific sequence of Tat necessary for translocation across the plasma membrane [324]. Since Tat, dozens of CPPs were either identified in proteins or designed and have been successfully used to transport proteins, peptides, oligonucleotides, plasmids and large particles, like liposomes, into cells [325–334].

Typically, CPPs are polybasic and/or amphipatic molecules and their cell-penetrating properties arise from positively charged aminoacids [335,336]. Besides, the importance of positively charged aminoacids, there is still much debate on how CPPs are uptake into cells. Several models for CPPs internalization, from energy-depended endocytosis mechanisms to direct plasma translocation (e.g. carpet and pore formation model) have been suggested and proved [337,338]. Moreover, distinct CPPs may have different uptake methods [336]. Also, within the cell, CPPs target specific intracellular organelles or compartments [339].

The CPPs were first developed to exclusively deliver bioactive cargo to cells, by covalent binding cargo and CPPs (message-address hypothesis). Consequently, they were required to be relatively inert. Yet, the report of adverse effects such as toxicity or inhibition of key signaling pathways, proved that CPPs with favorable bioactive properties could be a useful strategy in both research tools and diagnostic agents. So recently the term bioportide was introduced. Bioportides are peptides that can translocate the mammalian plasma membrane and at the same time have a biological role within the cell (bioactive) [340,341]. Bioportides designed to mimic proteins domains appear to be more efficient, as they are able to directly modulate cellular events, such as protein-protein interactions. One of the first examples of a bioportide is int-H1-S6A, F8A. This bioportide results from a variation of 14 aminoacid sequence of c-Myc extended with CPP penetratin and demonstrated anti-proliferative and apoptogenic properties towards cancer cell lines [342]. Since int-H1-S6A, F8A many others were developed, from bioportides with anti-apoptotic effects; cAMP modulation; promotion of blood vessel contraction; anti-adrenergic to stimulation of inflammatory mediators secretion [340,343–347].

The use of CPPs or bioportides in the male reproductive system is still a new field. Due to the reduced cytoplasm and lack of energy dependent endocytosis mechanism, sperm cells are a suitable model for the study of CPP or bioportide translocation and accretion [339]. The preference accumulation of several CPPs was evaluated in bovine sperm. Tat accumulates in the head; MitP in midpiece and C105Y is absent from interior head and acrosome. Also, since bovine sperm is incapable of clathrin-mediated endocytosis and micropinocytosis, neither CPP tested were internalized using these routes. The advantages of using CPPs and bioportide in sperm are clear: targeted delivery of bioactive cargos into subcellular compartments; any CPP effect in gene expression is irrelevant in sperm; CPP can be altered to the unique plasma membrane sperm composition and certain CPPs do not alter sperm physiology (viability and motility) [348]. Even more, since sperm rely on protein-protein interactions to mature in the epididymis and to adapt to new environments, the use of bioportides targeting such protein-proteins is a promising field.

A4.5. Concluding remarks

The singularity of the sperm cell make it also unique to work with. The distinct plasma membrane composition, the fact that it is a transcriptional silent cell and highly compartmentalization rises problems on using common molecular research tools. Over several decades, alternative methods to work with spermatozoa have been developed, from reagents to demembrane sperm cells to using cell penetrating peptides to target sperm proteins. Regardless, we believe that much is still to be overcome. The biggest obstacle is the lack of sperm samples, particularly testicular and epididymal sperm. Although animal models are of great value, transposing knowledge acquired in animal models to human physiology has its setbacks. A great example is the role of glucose in capacitation. In hamster [349] and macaque [350] sperm, glucose is essential for capacitation, while in bovine [351] and dog sperm [352] glucose inhibits capacitation.

Studying human sperm motility is of great value, since poorly motility samples account for 15% of male related infertile phenotypes.

A5. References

[1] Bernardo C, Amaro A. Aparelho reprodutor masculino-uma prespectiva anatómica e funcional. In: Fardilha M, Silva JV, Conde M (eds.), Reprodução Humana Masculina - Princípios fundamentais. 1st ed. Aveiro: ARC Publishing; 2015.

[2] Netter FH. Atlas of human anatomy. 4th ed. Philadelphia, PA: Saunders/Elsevier; 2006.

[3] VanPutte CL, Seeley RR. Seeley's anatomy & physiology. 10th ed. New York, NY: McGraw-Hill; 2014.

[4] Moreno RD, Ramalho-Santos J, Sutovsky P, Chan EK, Schatten G. Vesicular traffic and golgi apparatus dynamics during mammalian spermatogenesis: implications for acrosome architecture. Biol Reprod 2000; 63:89–98.

[5] Oko RJ. Developmental expression and possible role of perinuclear theca proteins in mammalian spermatozoa. Reprod Fertil Dev 1995; 7:777–97.

[6] Oko R. Occurrence and formation of cytoskeletal proteins in mammalian spermatozoa. Andrologia n.d.; 30:193–206.

[7] Kleene KC. Multiple controls over the efficiency of translation of the mRNAs encoding transition proteins, protamines, and the mitochondrial capsule selenoprotein in late spermatids in mice. Dev Biol 1993; 159:720–31.

[8] Eddy EM. Male germ cell gene expression. Recent Prog Horm Res 2002; 57:103–28.

[9] Dadoune J-P, Siffroi J-P, Alfonsi M-F. Transcription in haploid male germ cells. Int Rev Cytol 2004; 237:1–56.

[10] Meistrich ML, Mohapatra B, Shirley CR, Zhao M. Roles of transition nuclear proteins in spermiogenesis. Chromosoma 2003; 111:483–8.

[11] Guraya SS. The comparative cell biology of accessory somatic (or Sertoli) cells in the animal testis. Int Rev Cytol 1995; 160:163–220.

[12] Alves, M.; Rato, L.; Moreira, A.; Oliveira P. Célula se Sertoli: fisiologia, estrutura e função. In: Fardilha, Margarida; Vieira, J.V; Conde M (ed.), Reprodução Humana Masculina: Princípios fundamentais. 1st ed. Aveiro: ARC Publishing; 2015:45–55.

[13] Cheng CY, Wong EWP, Yan HHN, Mruk DD. Regulation of spermatogenesis in the microenvironment of the seminiferous epithelium: new insights and advances. Mol Cell Endocrinol 2010; 315:49–56.

[14] Johnson L, Thompson DL, Varner DD. Role of Sertoli cell number and function on regulation of spermatogenesis. Anim Reprod Sci 2008; 105:23–51.

[15] Ewing LL, Zirkin B. Leydig cell structure and steroidogenic function. Recent Prog Horm Res 1983; 39:599–635.

[16] Lipshultz LI, Howards SS, Niederberger CS. Infertility in the male. Cambridge University Press; 2009.

[17] Cornwall GA. New insights into epididymal biology and function. Hum Reprod Update 2008; 15:213–227.

[18] Dacheux J-L, Belleannée C, Guyonnet B, Labas V, Teixeira-Gomes A-P, Ecroyd H, et al. The

contribution of proteomics to understanding epididymal maturation of mammalian spermatozoa. Syst Biol Reprod Med 2012; 58:197–210.

[19] Rowley MJ, Teshima F, Heller CG. Duration of transit of spermatozoa through the human male ductular system. Fertil Steril 1970; 21:390–6.

[20] Amann RP, Howards SS. Daily spermatozoal production and epididymal spermatozoal reserves of the human male. J Urol 1980; 124:211–5.

[21] Tulsiani DR, NagDas SK, Skudlarek MD, Orgebin-Crist MC. Rat sperm plasma membrane mannosidase: localization and evidence for proteolytic processing during epididymal maturation. Dev Biol 1995; 167:584–95.

[22] Saxena DK, Oh-Oka T, Kadomatsu K, Muramatsu T, Toshimori K. Behaviour of a sperm surface transmembrane glycoprotein basigin during epididymal maturation and its role in fertilization in mice. Reproduction 2002; 123:435–44.

[23] Korrodi-Gregório L, Vijayaraghavan S. Maturação e transporte do espermatozoide no epididímo. In: Fardilha M, Silva JV, Conde M (eds.), Reprodução Humana Masculina - Princípios Fundamentais. ARC Publishing; 2015.

[24] Plant TM, Zeleznik AJ, Toshimori K, Eddy EM. Chapter 3 – The Spermatozoon. Knobil and Neill's Physiology of Reproduction. 2015:99–148.

[25] Hammoud SS, Nix DA, Zhang H, Purwar J, Carrell DT, Cairns BR. Distinctive chromatin in human sperm packages genes for embryo development. Nature 2009; 460:473–8.

[26] Sutovsky P, Manandhar G. Mammalian spermatogenesis and sperm structure: anatomical and compartmental analysis. In: De Jonge CJ, Barratt C (eds.), The Sperm Cell. Cambridge: Cambridge University Press; n.d.:1–30.

[27] Abou-Haila A, Tulsiani DRP. The Sperm Acrosome: Formation and Contents. In: Tulsiani DRP (ed.), Introduction to Mammalian Reproduction. Boston, MA: Springer US; 2003:21–39.

[28] Yoshinaga K, Toshimori K. Organization and modifications of sperm acrosomal molecules during spermatogenesis and epididymal maturation. Microsc Res Tech 2003; 61:39–45.

[29] Guraya SS. Neck. Biology of Spermatogenesis and Spermatozoa in Mammals. Berlin, Heidelberg: Springer Berlin Heidelberg; 1987:248–251.

[30] Eddy EM. The spermatozoon. In: Neil JD (ed.), Knobil and Neill's Physiology of Reproduction. New York: Elsevier; 2006:3–54.

[31] Flesch FM, Gadella BM. Dynamics of the mammalian sperm plasma membrane in the process of fertilization. Biochim Biophys Acta 2000; 1469:197–235.

[32] Leahy T, Gadella BM. New insights into the regulation of cholesterol efflux from the sperm membrane. Asian J Androl n.d.; 17:561–7.

[33] Martínez P, Morros A. Membrane lipid dynamics during human sperm capacitation. Front Biosci 1996; 1:d103-17.

[34] Vos JP, Lopes-Cardozo M, Gadella BM. Metabolic and functional aspects of sulfogalactolipids. Biochim Biophys Acta 1994; 1211:125–49.

[35] Holt W V. Membrane heterogeneity in the mammalian spermatozoon. Int Rev Cytol 1984; 87:159–94.

[36] Mackie AR, James PS, Ladha S, Jones R. Diffusion barriers in ram and boar sperm plasma

membranes: directionality of lipid diffusion across the posterior ring. Biol Reprod 2001; 64:113–9.

[37] Verze P, Cai T, Lorenzetti S. The role of the prostate in male fertility, health and disease. Nat Rev Urol 2016; 13:379–86.

[38] Gonzales GF. Function of seminal vesicles and their role on male fertility. Asian J Androl 2001; 3:251–8.

[39] Alshahrani S, McGill J, Agarwal A. Prostatitis and male infertility. J Reprod Immunol 2013; 100:30–6.

[40] Björndahl L, Kvist U. A model for the importance of zinc in the dynamics of human sperm chromatin stabilization after ejaculation in relation to sperm DNA vulnerability. Syst Biol Reprod Med 2011; 57:86–92.

[41] Fair WR, Couch J, Wehner N. Prostatic antibacterial factor. Identity and significance. Urology 1976; 7:169–77.

[42] Zaneveld LJ, Tauber PF. Contribution of prostatic fluid components to the ejaculate. Prog Clin Biol Res 1981; 75A:265–77.

[43] Chughtai B, Sawas A, O'Malley RL, Naik RR, Ali Khan S, Pentyala S. A neglected gland: a review of Cowper's gland. Int J Androl 2005; 28:74–7.

[44] Alwaal A, Breyer BN, Lue TF. Normal male sexual function: emphasis on orgasm and ejaculation. Fertil Steril 2015; 104:1051–60.

[45] Gnoth C, Godehardt E, Frank-Herrmann P, Friol K, Tigges J, Freundl G. Definition and prevalence of subfertility and infertility. Hum Reprod 2005; 20:1144–7.

[46] Agarwal A, Mulgund A, Hamada A, Chyatte MR. A unique view on male infertility around the globe. Reprod Biol Endocrinol 2015; 13:37.

[47] Roy A, Lin Y-N, Matzuk MM. Genetics of Idiopathic Male Infertility. The Genetics of Male Infertility. Totowa, NJ: Humana Press; 2007:99–111.

[48] United Nations. Trends in Contraceptive Use Worldwide 2015 2015.

[49] WHO. WHO | Family planning/Contraception. WHO 2017.

[50] Inaba K. Sperm flagella: comparative and phylogenetic perspectives of protein components. Mol Hum Reprod 2011; 17:524–538.

[51] Abou-haila A, Tulsiani DRP. Signal transduction pathways that regulate sperm capacitation and the acrosome reaction. Arch Biochem Biophys 2009; 485:72–81.

[52] Paoli D, Gallo M, Rizzo F, Baldi E, Francavilla S, Lenzi A, et al. Mitochondrial membrane potential profile and its correlation with increasing sperm motility. Fertil Steril 2011; 95:2315–9.

[53] Chemes HE, Alvarez Sedo C. Tales of the Tail and Sperm Head AchesChanging concepts on the prognostic significance of sperm pathologies affecting the head, neck and tail. Asian J Androl 2012; 14:14–23.

[54] Visconti PE, Westbrook VA, Chertihin O, Demarco I, Sleight S, Diekman AB. Novel signaling pathways involved in sperm acquisition of fertilizing capacity. J Reprod Immunol 2002; 53:133–50.

[55] Turner RM. Moving to the beat: a review of mammalian sperm motility regulation. Reprod

Fertil Dev 2006; 18:25–38.

[56] Suarez SSS, Pacey AA. Sperm transport in the female reproductive tract. Hum Reprod Update 2005; 12:23–37.

[57] Eddy EM. Knobil and Neill's Physiology of Reproduction. Knobil and Neill's Physiology of Reproduction, vol. 1. Elsevier; 2006:3–54.

[58] Suarez SS. Control of hyperactivation in sperm. Hum Reprod Update 2008; 14:647–657.

[59] Ho HC, Suarez SS. Hyperactivation of mammalian spermatozoa: function and regulation. Reproduction 2001; 122:519–26.

[60] du Plessis SS, Agarwal A, Mohanty G, van der Linde M. Oxidative phosphorylation versus glycolysis: what fuel do spermatozoa use? Asian J Androl 2015; 17:230–5.

[61] Florman HM, Ducibella T. Knobil and Neill's Physiology of Reproduction. vol. 1. Elsevier; 2006.

[62] Inaba K. Molecular Architecture of the Sperm Flagella: Molecules for Motility and Signaling. Zoolog Sci 2003; 20:1043–1056.

[63] Lindemann CB, Lesich KA. Flagellar and ciliary beating: the proven and the possible. J Cell Sci 2010; 123:519–528.

[64] Fawcett DW. The mammalian spermatozoon. Dev Biol 1975; 44:394–436.

[65] Pesch S, Bergmann M. Structure of mammalian spermatozoa in respect to viability, fertility and cryopreservation. Micron 2006; 37:597–612.

[66] Petersen C, Füzesi L, Hoyer-Fender S. Outer dense fibre proteins from human sperm tail: molecular cloning and expression analyses of two cDNA transcripts encoding proteins of approximately 70 kDa. Mol Hum Reprod 1999; 5:627–35.

[67] Eddy EM, Toshimori K, O'Brien DA. Fibrous sheath of mammalian spermatozoa. Microsc Res Tech 2003; 61:103–15.

[68] Darszon A, Nishigaki T, Beltran C, Trevino CL. Calcium Channels in the Development, Maturation, and Function of Spermatozoa. Physiol Rev 2011; 91:1305–1355.

[69] Piomboni P, Focarelli R, Stendardi A, Ferramosca A, Zara V. The role of mitochondria in energy production for human sperm motility. Int J Androl 2012; 35:109–124.

[70] Miki K. Energy metabolism and sperm function. Soc Reprod Fertil Suppl 2007; 65:309–25.

[71] Ferramosca A, Provenzano SP, Coppola L, Zara V. Mitochondrial Respiratory Efficiency is Positively Correlated With Human Sperm Motility. Urology 2012; 79:809–814.

[72] Ford WCL. Glycolysis and sperm motility: does a spoonful of sugar help the flagellum go round? Hum Reprod Update 2006; 12:269–274.

[73] Rajender S, Rahul P, Mahdi AA. Mitochondria, spermatogenesis and male infertility. Mitochondrion 2010; 10:419–28.

[74] Hereng TH, Elgstoen KBP, Cederkvist FH, Eide L, Jahnsen T, Skalhegg BS, et al. Exogenous pyruvate accelerates glycolysis and promotes capacitation in human spermatozoa. Hum Reprod 2011; 26:3249–3263.

[75] Dzeja PP, Terzic A. Phosphotransfer networks and cellular energetics. J Exp Biol 2003; 206:2039–47.

[76] Ruiz-Pesini E, Lapeña AC, Díez C, Alvarez E, Enríquez JA, López-Pérez MJ. Seminal quality correlates with mitochondrial functionality. Clin Chim Acta 2000; 300:97–105.

[77] Amaral A, Lourenco B, Marques M, Ramalho-Santos J. Mitochondria functionality and sperm quality. Reproduction 2013; 146:R163–R174.

[78] Aitken RJ, Gibb Z, Mitchell LA, Lambourne SR, Connaughton HS, De Iuliis GN. Sperm Motility Is Lost In Vitro as a Consequence of Mitochondrial Free Radical Production and the Generation of Electrophilic Aldehydes but Can Be Significantly Rescued by the Presence of Nucleophilic Thiols. Biol Reprod 2012; 87:110–110.

[79] Ramalho-Santos J, Varum S, Amaral S, Mota PC, Sousa AP, Amaral A. Mitochondrial functionality in reproduction: from gonads and gametes to embryos and embryonic stem cells. Hum Reprod Update 2009; 15:553–572.

[80] Mukai C, Okuno M. Glycolysis plays a major role for adenosine triphosphate supplementation in mouse sperm flagellar movement. Biol Reprod 2004; 71:540–7.

[81] Williams AC, Ford WC. The role of glucose in supporting motility and capacitation in human spermatozoa. J Androl 2011; 22:680–95.

[82] Barbonetti A, Vassallo MRC, Fortunato D, Francavilla S, Maccarrone M, Francavilla F. Energetic Metabolism and Human Sperm Motility: Impact of CB 1 Receptor Activation. Endocrinology 2010; 151:5882–5892.

[83] Miki K, Qu W, Goulding EH, Willis WD, Bunch DO, Strader LF, et al. Glyceraldehyde 3-phosphate dehydrogenase-S, a sperm-specific glycolytic enzyme, is required for sperm motility and male fertility. Proc Natl Acad Sci U S A 2004; 101:16501–6.

[84] Odet F, Duan C, Willis WD, Goulding EH, Kung A, Eddy EM, et al. Expression of the gene for mouse lactate dehydrogenase C (Ldhc) is required for male fertility. Biol Reprod 2008; 79:26–34.

[85] Galantino-Homer HL, Florman HM, Storey BT, Dobrinski I, Kopf GS. Bovine sperm capacitation: assessment of phosphodiesterase activity and intracellular alkalinization on capacitation-associated protein tyrosine phosphorylation. Mol Reprod Dev 2004; 67:487–500.

[86] Ruiz-Pesini E, Díez-Sánchez C, López-Pérez MJ, Enríquez JA. The role of the mitochondrion in sperm function: is there a place for oxidative phosphorylation or is this a purely glycolytic process? Curr Top Dev Biol 2007; 77:3—19.

[87] Cao W, Aghajanian HK, Haig-Ladewig LA, Gerton GL. Sorbitol can fuel mouse sperm motility and protein tyrosine phosphorylation via sorbitol dehydrogenase. Biol Reprod 2009; 80:124–33.

[88] Jones AR, Chantrill LA, Cokinakis A. Metabolism of glycerol by mature boar spermatozoa. J Reprod Fertil 1992; 94:129–34.

[89] Rigau T, Farré M, Ballester J, Mogas T, Peña A, Rodríguez-Gil JE. Effects of glucose and fructose on motility patterns of dog spermatozoa from fresh ejaculates. Theriogenology 2001; 56:801–15.

[90] Storey BT. Mammalian sperm metabolism: oxygen and sugar, friend and foe. Int J Dev Biol 2008; 52:427–37.

[91] Baldi E, Luconi M, Bonaccorsi L, Forti G. Signal transduction pathways in human spermatozoa. J Reprod Immunol 2002; 53:121–31.

[92] Fardilha M, Esteves SLCC, Korrodi-Gregório L, Vintém AP, Domingues SC, Rebelo S, et al. Identification of the human testis protein phosphatase 1 interactome. Biochem Pharmacol 2011; 82:1403–1415.

[93] Huang Z, Khatra B, Bollen M, Carr DW, Vijayaraghavan S. Sperm PP1gamma2 is regulated by a homologue of the yeast protein phosphatase binding protein sds22. Biol Reprod 2002; 67:1936–42.

[94] Ashizawa K, Wishart GJ, Katayama S, Takano D, Ranasinghe ARAH, Narumi K, et al. Regulation of acrosome reaction of fowl spermatozoa: evidence for the involvement of protein kinase C and protein phosphatase-type 1 and/or -type 2A. Reproduction 2006; 131:1017–24.

[95] Vijayaraghavan S, Stephens DT, Trautman K, Smith GD, Khatra B, da Cruz e Silva EF, et al. Sperm motility development in the epididymis is associated with decreased glycogen synthase kinase-3 and protein phosphatase 1 activity. Biol Reprod 1996; 54:709–18.

[96] Han Y, Haines CJ, Feng HL. Role(s) of the Serine/Threonine Protein Phosphatase 1 on Mammalian Sperm Motility. Syst Biol Reprod Med 2007; 53:169–177.

[97] Cohen P. Methods in Enzymology. Academic Press; 1991.

[98] Korrodi-Gregório L, Ferreira M, Vintém AP, Wu W, Muller T, Marcus K, et al. Identification and characterization of two distinct PPP1R2 isoforms in human spermatozoa. BMC Cell Biol 2013; 14:15.

[99] Wang QM, Park IK, Fiol CJ, Roach PJ, DePaoli-Roach AA. Isoform differences in substrate recognition by glycogen synthase kinases 3 alpha and 3 beta in the phosphorylation of phosphatase inhibitor 2. Biochemistry 1994; 33:143–7.

[100] Somanath PR, Jack SL, Vijayaraghavan S. Changes in sperm glycogen synthase kinase-3 serine phosphorylation and activity accompany motility initiation and stimulation. J Androl n.d.; 25:605–17.

[101] Vijayaraghavan S, Mohan J, Gray H, Khatra B, Carr DW. A role for phosphorylation of glycogen synthase kinase-3alpha in bovine sperm motility regulation. Biol Reprod 2000; 62:1647–54.

[102] Smith GD, Wolf DP, Trautman KC, Vijayaraghavan S. Motility potential of macaque epididymal sperm: the role of protein phosphatase and glycogen synthase kinase-3 activities. J Androl n.d.; 20:47–53.

[103] Bhattacharjee R, Goswami S, Dudiki T, Popkie AP, Phiel CJ, Kline D, et al. Targeted disruption of glycogen synthase kinase 3A (GSK3A) in mice affects sperm motility resulting in male infertility. Biol Reprod 2015; 92:65.

[104] Koch S, Acebron SP, Herbst J, Hatiboglu G, Niehrs C. Post-transcriptional Wnt Signaling Governs Epididymal Sperm Maturation. Cell 2015; 163:1225–1236.

[105] Dudiki T, Kadunganattil S, Ferrara JK, Kline DW, Vijayaraghavan S. Changes in Carboxy Methylation and Tyrosine Phosphorylation of Protein Phosphatase PP2A Are Associated with Epididymal Sperm Maturation and Motility. PLoS One 2015; 10:e0141961.

[106] Vadnais ML, Aghajanian HK, Lin A, Gerton GL. Signaling in Sperm: Toward a Molecular Understanding of the Acquisition of Sperm Motility in the Mouse Epididymis. Biol Reprod 2013; 89:127–127.

[107] Cheng L, Pilder S, Nairn AC, Ramdas S, Vijayaraghavan S. PP1gamma2 and PPP1R11 are parts

of a multimeric complex in developing testicular germ cells in which their steady state levels are reciprocally related. PLoS One 2009; 4:e4861.

[108] Pilder SH, Lu J, Han Y, Hui L, Samant SA, Olugbemiga OO, et al. The molecular basis of 'curlicue': a sperm motility abnormality linked to the sterility of t haplotype homozygous male mice. Soc Reprod Fertil Suppl 2007; 63:123–33.

[109] Mishra S, Somanath PR, Huang Z, Vijayaraghavan S. Binding and inactivation of the germ cell-specific protein phosphatase PP1gamma2 by sds22 during epididymal sperm maturation. Biol Reprod 2003; 69:1572–9.

[110] Miyata H, Satouh Y, Mashiko D, Muto M, Nozawa K, Shiba K, et al. Sperm calcineurin inhibition prevents mouse fertility with implications for male contraceptive. Science 2015; 350:442–5.

[111] Vijayaraghavan S, Critchlow LM, Hoskins DD. Evidence for a role for cellular alkalinization in the cyclic adenosine 3',5'-monophosphate-mediated initiation of motility in bovine caput spermatozoa. Biol Reprod 1985; 32:489–500.

[112] San Agustin JT, Witman GB. Role of cAMP in the reactivation of demembranated ram spermatozoa. Cell Motil Cytoskeleton 1994; 27:206–18.

[113] Westbrook VA (et al. . Introduction to Mammalian Reproduction. In: Tulsiani DRP (ed.). Boston, MA: Springer US; 2003.

[114] Publicover SJ, Giojalas LC, Teves ME, de Oliveira GSMM, Garcia AAM, Barratt CLR, et al. Ca2+ signalling in the control of motility and guidance in mammalian sperm. Front Biosci 2008; 13:5623–37.

[115] Espino J, Mediero M, Lozano GM, Bejarano I, Ortiz Á, García JF, et al. Reduced levels of intracellular calcium releasing in spermatozoa from asthenozoospermic patients. Reprod Biol Endocrinol 2009; 7:11.

[116] Wennemuth G. CaV2.2 and CaV2.3 (N- and R-type) Ca2+ Channels in Depolarization-evoked Entry of Ca2+ into Mouse Sperm. J Biol Chem 2000; 275:21210–21217.

[117] Miki K, Willis WD, Brown PR, Goulding EH, Fulcher KD, Eddy EM. Targeted disruption of the Akap4 gene causes defects in sperm flagellum and motility. Dev Biol 2002; 248:331–42.

[118] DasGupta S, Mills CL, Fraser LR. A possible role for Ca(2+)-ATPase in human sperm capacitation. J Reprod Fertil 1994; 102:107–16.

[119] Kirichok Y, Lishko P V. Rediscovering sperm ion channels with the patch-clamp technique. Mol Hum Reprod 2011; 17:478–499.

[120] Anu Bashamboo and Kenneth David McElreavey. Male Infertility. InTech; 2012.

[121] Patrat C, Serres C, Jouannet P. The acrosome reaction in human spermatozoa. Biol Cell 2000; 92:255–66.

[122] Ren D, Navarro B, Perez G, Jackson AC, Hsu S, Shi Q, et al. A sperm ion channel required for sperm motility and male fertility. Nature 2001; 413:603–9.

[123] Kirichok Y, Navarro B, Clapham DE. Whole-cell patch-clamp measurements of spermatozoa reveal an alkaline-activated Ca2+ channel. Nature 2006; 439:737–40.

[124] Lishko P V., Botchkina IL, Kirichok Y. Progesterone activates the principal Ca2+ channel of human sperm. Nature 2011; 471:387–391.

[125] Strünker T, Goodwin N, Brenker C, Kashikar ND, Weyand I, Seifert R, et al. The CatSper channel mediates progesterone-induced Ca2+ influx in human sperm. Nature 2011; 471:382–386.

[126] Olson SD, Suarez SS, Fauci LJ. A model of CatSper channel mediated calcium dynamics in mammalian spermatozoa. Bull Math Biol 2010; 72:1925–46.

[127] Brenker C, Goodwin N, Weyand I, Kashikar ND, Naruse M, Krähling M, et al. The CatSper channel: a polymodal chemosensor in human sperm. EMBO J 2012; 31:1654–65.

[128] Costello S, Michelangeli F, Nash K, Lefievre L, Morris J, Machado-Oliveira G, et al. Ca2+-stores in sperm: their identities and functions. Reproduction 2009; 138:425–37.

[129] Alasmari W, Costello S, Correia J, Oxenham SK, Morris J, Fernandes L, et al. Ca2+ signals generated by CatSper and Ca2+ stores regulate different behaviors in human sperm. J Biol Chem 2013; 288:6248–58.

[130] Publicover S, Harper C V, Barratt C. [Ca2+]i signalling in sperm--making the most of what you've got. Nat Cell Biol 2007; 9:235–42.

[131] Harrison DA, Carr DW, Meizel S. Involvement of protein kinase A and A kinase anchoring protein in the progesterone-initiated human sperm acrosome reaction. Biol Reprod 2000; 62:811–20.

[132] Sagare-Patil V, Galvankar M, Satiya M, Bhandari B, Gupta SK, Modi D. Differential concentration and time dependent effects of progesterone on kinase activity, hyperactivation and acrosome reaction in human spermatozoa. Int J Androl 2012; 35:633–44.

[133] Sagare-Patil V, Vernekar M, Galvankar M, Modi D. Progesterone utilizes the PI3K-AKT pathway in human spermatozoa to regulate motility and hyperactivation but not acrosome reaction. Mol Cell Endocrinol 2013; 374:82–91.

[134] Yoshida M, Yoshida K. Sperm chemotaxis and regulation of flagellar movement by Ca2+. Mol Hum Reprod 2011; 17:457–465.

[135] Uhler ML, Leung A, Chan SY, Wang C. Direct effects of progesterone and antiprogesterone on human sperm hyperactivated motility and acrosome reaction. Fertil Steril 1992; 58:1191–8.

[136] Roldan ER, Murase T, Shi QX. Exocytosis in spermatozoa in response to progesterone and zona pellucida. Science 1994; 266:1578–81.

[137] Revelli A, Massobrio M, Tesarik J. Nongenomic actions of steroid hormones in reproductive tissues. Endocr Rev 1998; 19:3–17.

[138] Teves ME, Guidobaldi HA, Uñates DR, Sanchez R, Miska W, Publicover SJ, et al. Molecular Mechanism for Human Sperm Chemotaxis Mediated by Progesterone. PLoS One 2009; 4:e8211.

[139] Reid AT, Redgrove K, Aitken RJ, Nixon B. Cellular mechanisms regulating sperm-zona pellucida interaction. Asian J Androl 2011; 13:88–96.

[140] Tresguerres M, Levin LR, Buck J. Intracellular cAMP signaling by soluble adenylyl cyclase. Kidney Int 2011; 79:1277–1288.

[141] Bailey JL. Factors regulating sperm capacitation. Syst Biol Reprod Med 2010; 56:334–48.

[142] Liu Y, Wang D-K, Chen L-M. The physiology of bicarbonate transporters in mammalian

reproduction. Biol Reprod 2012; 86:99.

[143] Muchekehu RW, Quinton PM. A new role for bicarbonate secretion in cervico-uterine mucus release. J Physiol 2010; 588:2329–2342.

[144] Visconti PE, Krapf D, de la Vega-Beltrán JL, Acevedo JJ, Darszon A. Ion channels, phosphorylation and mammalian sperm capacitation. Asian J Androl 2011; 13:395–405.

[145] Gadella BM, Harrison RA. The capacitating agent bicarbonate induces protein kinase A-dependent changes in phospholipid transbilayer behavior in the sperm plasma membrane. Development 2000; 127:2407–20.

[146] Witte TS, Schäfer-Somi S. Involvement of cholesterol, calcium and progesterone in the induction of capacitation and acrosome reaction of mammalian spermatozoa. Anim Reprod Sci 2007; 102:181–193.

[147] Hlivko JT, Chakraborty S, Hlivko TJ, Sengupta A, James PF. The human Na,K-ATPase alpha 4 isoform is a ouabain-sensitive alpha isoform that is expressed in sperm. Mol Reprod Dev 2006; 73:101–15.

[148] Blanco G. Na,K-ATPase subunit heterogeneity as a mechanism for tissue-specific ion regulation. Semin Nephrol 2005; 25:292–303.

[149] Jimenez T, McDermott JP, Sánchez G, Blanco G. Na,K-ATPase alpha4 isoform is essential for sperm fertility. Proc Natl Acad Sci U S A 2011; 108:644–9.

[150] McDermott J, Sánchez G, Nangia AK, Blanco G. Role of human Na,K-ATPase alpha 4 in sperm function, derived from studies in transgenic mice. Mol Reprod Dev 2015; 82:167–81.

[151] Woo AL, James PF, Lingrel JB. Roles of the Na,K-ATPase alpha4 isoform and the Na+/H+ exchanger in sperm motility. Mol Reprod Dev 2002; 62:348–56.

[152] Jimenez T, Sánchez G, Blanco G. Activity of the Na,K-ATPase α4 isoform is regulated during sperm capacitation to support sperm motility. J Androl n.d.; 33:1047–57.

[153] Thundathil JC, Anzar M, Buhr MM. Na+/K+ATPase as a signaling molecule during bovine sperm capacitation. Biol Reprod 2006; 75:308–17.

[154] Laredo J, Hamilton BP, Hamlyn JM. Ouabain is secreted by bovine adrenocortical cells. Endocrinology 1994; 135:794–7.

[155] Hamlyn JM, Blaustein MP, Bova S, DuCharme DW, Harris DW, Mandel F, et al. Identification and characterization of a ouabain-like compound from human plasma. Proc Natl Acad Sci U S A 1991; 88:6259–63.

[156] Signorelli J, Diaz ES, Morales P. Kinases, phosphatases and proteases during sperm capacitation. Cell Tissue Res 2012; 349:765–82.

[157] Esposito G, Jaiswal BS, Xie F, Krajnc-Franken MAM, Robben TJAA, Strik AM, et al. Mice deficient for soluble adenylyl cyclase are infertile because of a severe sperm-motility defect. Proc Natl Acad Sci U S A 2004; 101:2993–8.

[158] Nolan MA, Babcock DF, Wennemuth G, Brown W, Burton KA, McKnight GS. Sperm-specific protein kinase A catalytic subunit Calpha2 orchestrates cAMP signaling for male fertility. Proc Natl Acad Sci U S A 2004; 101:13483–8.

[159] Naz RK, Rajesh PB. Role of tyrosine phosphorylation in sperm capacitation / acrosome reaction. Reprod Biol Endocrinol 2004; 2:75.

[160] Battistone MA, Da Ros VG, Salicioni AM, Navarrete FA, Krapf D, Visconti PE, et al. Functional human sperm capacitation requires both bicarbonate-dependent PKA activation and down-regulation of Ser/Thr phosphatases by Src family kinases. Mol Hum Reprod 2013; 19:570–580.

[161] Almog T, Naor Z. The role of Mitogen activated protein kinase (MAPK) in sperm functions. Mol Cell Endocrinol 2010; 314:239–243.

[162] Prakash SK. Functional analysis of ARHGAP6, a novel GTPase-activating protein for RhoA. Hum Mol Genet 2000; 9:477–488.

[163] Almog T, Lazar S, Reiss N, Etkovitz N, Milch E, Rahamim N, et al. Identification of Extracellular Signal-regulated Kinase 1/2 and p38 MAPK as Regulators of Human Sperm Motility and Acrosome Reaction and as Predictors of Poor Spermatozoan Quality. J Biol Chem 2008; 283:14479–14489.

[164] Silva JV, Freitas MJ, Correia BR, Korrodi-Gregório L, Patrício A, Pelech S, et al. Profiling signaling proteins in human spermatozoa: biomarker identification for sperm quality evaluation. Fertil Steril 2015; 104:845–856.e8.

[165] Leyton L, Saling P. 95 kd sperm proteins bind ZP3 and serve as tyrosine kinase substrates in response to zona binding. Cell 1989; 57:1123–30.

[166] Nassar A, Mahony M, Morshedi M, Lin MH, Srisombut C, Oehninger S. Modulation of sperm tail protein tyrosine phosphorylation by pentoxifylline and its correlation with hyperactivated motility. Fertil Steril 1999; 71:919–23.

[167] Vijayaraghavan S, Trautman KD, Goueli SA, Carr DW. A tyrosine-phosphorylated 55-kilodalton motility-associated bovine sperm protein is regulated by cyclic adenosine 3',5'-monophosphates and calcium. Biol Reprod 1997; 56:1450–7.

[168] Mitchell LA, Nixon B, Baker MA, Aitken RJ. Investigation of the role of SRC in capacitation-associated tyrosine phosphorylation of human spermatozoa. Mol Hum Reprod 2008; 14:235–43.

[169] Cotton L, Gibbs GM, Sanchez-Partida LG, Morrison JR, de Kretser DM, O'Bryan MK. FGFR-1 [corrected] signaling is involved in spermiogenesis and sperm capacitation. J Cell Sci 2006; 119:75–84.

[170] Baker MA, Hetherington L, Curry B, Aitken RJ. Phosphorylation and consequent stimulation of the tyrosine kinase c-Abl by PKA in mouse spermatozoa; its implications during capacitation. Dev Biol 2009; 333:57–66.

[171] Urner F, Sakkas D. Protein phosphorylation in mammalian spermatozoa. Reproduction 2003; 125:17–26.

[172] Si Y, Okuno M. Role of tyrosine phosphorylation of flagellar proteins in hamster sperm hyperactivation. Biol Reprod 1999; 61:240–6.

[173] Shukla KK, Kwon W-S, Rahman MS, Park Y-J, You Y-A, Pang M-G. Nutlin-3a decreases male fertility via UQCRC2. PLoS One 2013; 8:e76959.

[174] Ijiri TW, Mahbub Hasan AKM, Sato K-I. Protein-tyrosine kinase signaling in the biological functions associated with sperm. J Signal Transduct 2012; 2012:181560.

[175] Carrera A, Moos J, Ning XP, Gerton GL, Tesarik J, Kopf GS, et al. Regulation of protein tyrosine phosphorylation in human sperm by a calcium/calmodulin-dependent mechanism: identification of A kinase anchor proteins as major substrates for tyrosine phosphorylation.

Dev Biol 1996; 180:284–96.

[176] Mandal A, Naaby-Hansen S, Wolkowicz MJ, Klotz K, Shetty J, Retief JD, et al. FSP95, a testis-specific 95-kilodalton fibrous sheath antigen that undergoes tyrosine phosphorylation in capacitated human spermatozoa. Biol Reprod 1999; 61:1184–97.

[177] Naaby-Hansen S, Mandal A, Wolkowicz MJ, Sen B, Westbrook VA, Shetty J, et al. CABYR, a novel calcium-binding tyrosine phosphorylation-regulated fibrous sheath protein involved in capacitation. Dev Biol 2002; 242:236–54.

[178] Ecroyd H, Jones RC, Aitken RJ. Tyrosine phosphorylation of HSP-90 during mammalian sperm capacitation. Biol Reprod 2003; 69:1801–7.

[179] Koh GCKW, Porras P, Aranda B, Hermjakob H, Orchard SE. Analyzing Protein–Protein Interaction Networks †. J Proteome Res 2012; 11:2014–2031.

[180] Baker MA, Aitken RJ. Proteomic insights into spermatozoa: critiques, comments and concerns. Expert Rev Proteomics 2009; 6:691–705.

[181] Wang G, Guo Y, Zhou T, Shi X, Yu J, Yang Y, et al. In-depth proteomic analysis of the human sperm reveals complex protein compositions. J Proteomics 2013; 79:114–22.

[182] Johnston DS, Wooters J, Kopf GS, Qiu Y, Roberts KP. Analysis of the human sperm proteome. Ann N Y Acad Sci 2005; 1061:190–202.

[183] Martínez-Heredia J, Estanyol JM, Ballescà JL, Oliva R. Proteomic identification of human sperm proteins. Proteomics 2006; 6:4356–69.

[184] Baker MA, Reeves G, Hetherington L, Müller J, Baur I, Aitken RJ. Identification of gene products present in Triton X-100 soluble and insoluble fractions of human spermatozoa lysates using LC-MS/MS analysis. Proteomics Clin Appl 2007; 1:524–32.

[185] de Mateo S, Martínez-Heredia J, Estanyol JM, Domínguez-Fandos D, Domíguez-Fandos D, Vidal-Taboada JM, et al. Marked correlations in protein expression identified by proteomic analysis of human spermatozoa. Proteomics 2007; 7:4264–77.

[186] Ficarro S, Chertihin O, Westbrook VA, White F, Jayes F, Kalab P, et al. Phosphoproteome analysis of capacitated human sperm. Evidence of tyrosine phosphorylation of a kinase-anchoring protein 3 and valosin-containing protein/p97 during capacitation. J Biol Chem 2003; 278:11579–89.

[187] Secciani F, Bianchi L, Ermini L, Cianti R, Armini A, La Sala GB, et al. Protein profile of capacitated versus ejaculated human sperm. J Proteome Res 2009; 8:3377–89.

[188] Bogle OA, Kumar K, Attardo-Parrinello C, Lewis SEM, Estanyol JM, Ballescà JL, et al. Identification of protein changes in human spermatozoa throughout the cryopreservation process. Andrology 2017; 5:10–22.

[189] Wang S, Wang W, Xu Y, Tang M, Fang J, Sun H, et al. Proteomic characteristics of human sperm cryopreservation. Proteomics 2014; 14:298–310.

[190] Zhao C, Huo R, Wang F-Q, Lin M, Zhou Z-M, Sha J-H. Identification of several proteins involved in regulation of sperm motility by proteomic analysis. Fertil Steril 2007; 87:436–8.

[191] Siva AB, Kameshwari DB, Singh V, Pavani K, Sundaram CS, Rangaraj N, et al. Proteomics-based study on asthenozoospermia: differential expression of proteasome alpha complex. Mol Hum Reprod 2010; 16:452–62.

[192] Xu W, Hu H, Wang Z, Chen X, Yang F, Zhu Z, et al. Proteomic characteristics of spermatozoa

in normozoospermic patients with infertility. J Proteomics 2012; 75:5426–36.

[193] Frapsauce C, Pionneau C, Bouley J, Delarouziere V, Berthaut I, Ravel C, et al. Proteomic identification of target proteins in normal but nonfertilizing sperm. Fertil Steril 2014; 102:372–80.

[194] Martínez-Heredia J, de Mateo S, Vidal-Taboada JM, Ballescà JL, Oliva R. Identification of proteomic differences in asthenozoospermic sperm samples. Hum Reprod 2008; 23:783–91.

[195] Amaral A, Paiva C, Attardo Parrinello C, Estanyol JM, Ballescà JL, Ramalho-Santos J, et al. Identification of proteins involved in human sperm motility using high-throughput differential proteomics. J Proteome Res 2014; 13:5670–84.

[196] Légaré C, Droit A, Fournier F, Bourassa S, Force A, Cloutier F, et al. Investigation of male infertility using quantitative comparative proteomics. J Proteome Res 2014; 13:5403–14.

[197] Shen S, Wang J, Liang J, He D. Comparative proteomic study between human normal motility sperm and idiopathic asthenozoospermia. World J Urol 2013; 31:1395–401.

[198] Amaral A, Castillo J, Estanyol JM, Ballescà JL, Ramalho-Santos J, Oliva R. Human sperm tail proteome suggests new endogenous metabolic pathways. Mol Cell Proteomics 2013; 12:330–42.

[199] Baker MA, Naumovski N, Hetherington L, Weinberg A, Velkov T, Aitken RJ. Head and flagella subcompartmental proteomic analysis of human spermatozoa. Proteomics 2013; 13:61–74.

[200] Lefièvre L, Chen Y, Conner SJ, Scott JL, Publicover SJ, Ford WCL, et al. Human spermatozoa contain multiple targets for protein S-nitrosylation: an alternative mechanism of the modulation of sperm function by nitric oxide? Proteomics 2007; 7:3066–84.

[201] Wang G, Wu Y, Zhou T, Guo Y, Zheng B, Wang J, et al. Mapping of the N-linked glycoproteome of human spermatozoa. J Proteome Res 2013; 12:5750–9.

[202] Kriegel TM, Heidenreich F, Kettner K, Pursche T, Hoflack B, Grunewald S, et al. Identification of diabetes- and obesity-associated proteomic changes in human spermatozoa by difference gel electrophoresis. Reprod Biomed Online 2009; 19:660–70.

[203] Paasch U, Heidenreich F, Pursche T, Kuhlisch E, Kettner K, Grunewald S, et al. Identification of increased amounts of eppin protein complex components in sperm cells of diabetic and obese individuals by difference gel electrophoresis. Mol Cell Proteomics 2011; 10:M110.007187.

[204] Pilatz A, Lochnit G, Karnati S, Paradowska-Dogan A, Lang T, Schultheiss D, et al. Acute epididymitis induces alterations in sperm protein composition. Fertil Steril 2014; 101:1609-17–5.

[205] Uhlén M, Fagerberg L, Hallström BM, Lindskog C, Oksvold P, Mardinoglu A, et al. Proteomics. Tissue-based map of the human proteome. Science 2015; 347:1260419.

[206] Djureinovic D, Fagerberg L, Hallström B, Danielsson A, Lindskog C, Uhlén M, et al. The human testis-specific proteome defined by transcriptomics and antibody-based profiling. Mol Hum Reprod 2014; 20:476–88.

[207] Guo X, Zhang P, Huo R, Zhou Z, Sha J. Analysis of the human testis proteome by mass spectrometry and bioinformatics. Proteomics Clin Appl 2008; 2:1651–7.

[208] Freitas MJ, Korrodi-Gregório L, Morais-Santos F, da Cruz e Silva E, Fardilha M, Cruz e Silva E da, et al. TCTEX1D4 Interactome in Human Testis: Unraveling the Function of Dynein Light

Chain in Spermatozoa. Omi A J Integr Biol 2014; 18:242–253.

[209] Silva JV, Yoon S, Domingues S, Guimarães S, Goltsev A V, da Cruz E Silva EF, et al. Amyloid precursor protein interaction network in human testis: sentinel proteins for male reproduction. BMC Bioinformatics 2015; 16:12.

[210] Fatima S, Wagstaff KM, Loveland KL, Jans DA. Interactome of the negative regulator of nuclear import BRCA1-binding protein 2. Sci Rep 2015; 5:9459.

[211] Naz RK, Dhandapani L. Identification of human sperm proteins that interact with human zona pellucida3 (ZP3) using yeast two-hybrid system. J Reprod Immunol 2010; 84:24–31.

[212] Sanchez C, Lachaize C, Janody F, Bellon B, Röder L, Euzenat J, et al. Grasping at molecular interactions and genetic networks in Drosophila melanogaster using FlyNets, an Internet database. Nucleic Acids Res 1999; 27:89–94.

[213] Venter JC, Adams MD, Myers EW, Li PW, Mural RJ, Sutton GG, et al. The sequence of the human genome. Science 2001; 291:1304–51.

[214] Stumpf MPH, Thorne T, de Silva E, Stewart R, An HJ, Lappe M, et al. Estimating the size of the human interactome. Proc Natl Acad Sci U S A 2008; 105:6959–64.

[215] Silva JV, Freitas MJ, Felgueiras J, Fardilha M. The power of the yeast two-hybrid system in the identification of novel drug targets: building and modulating PPP1 interactomes. Expert Rev Proteomics 2015; 12:147–58.

[216] Xing S, Wallmeroth N, Berendzen KW, Grefen C. Techniques for the Analysis of Protein-Protein Interactions in Vivo. Plant Physiol 2016; 171:727–58.

[217] Fields S, Song O. A novel genetic system to detect protein-protein interactions. Nature 1989; 340:245–6.

[218] Dhingra V, Gupta M, Andacht T, Fu ZF. New frontiers in proteomics research: a perspective. Int J Pharm 2005; 299:1–18.

[219] Auerbach D, Stagljar I. Yeast Two-Hybrid Protein-Protein Interaction Networks. In: Waksman G (ed.), Proteomics and Protein-Protein Interactions: Biology, Chemistry, Bioinformatics, and Drug Design. Boston, MA: Springer US; 2005:19–31.

[220] Stynen B, Tournu H, Tavernier J, Van Dijck P. Diversity in genetic in vivo methods for protein-protein interaction studies: from the yeast two-hybrid system to the mammalian split-luciferase system. Microbiol Mol Biol Rev 2012; 76:331–82.

[221] Moosavi B, Mousavi B, Yang W-C, Yang G-F. Yeast-based assays for detecting protein-protein/drug interactions and their inhibitors. Eur J Cell Biol 2017.

[222] Roberts GG, Parrish JR, Mangiola BA, Finley RL. High-throughput yeast two-hybrid screening. Methods Mol Biol 2012; 812:39–61.

[223] Rezwan M, Auerbach D. Yeast 'N'-hybrid systems for protein-protein and drug-protein interaction discovery. Methods 2012; 57:423–9.

[224] Hamdi A, Colas P. Yeast two-hybrid methods and their applications in drug discovery. Trends Pharmacol Sci 2012; 33:109–18.

[225] Koegl M, Uetz P. Improving yeast two-hybrid screening systems. Brief Funct Genomic Proteomic 2007; 6:302–12.

[226] Velasco-García R, Vargas-Martínez R. The study of protein-protein interactions in bacteria.

Can J Microbiol 2012; 58:1241–57.

[227] Stelzl U, Worm U, Lalowski M, Haenig C, Brembeck FH, Goehler H, et al. A human protein-protein interaction network: a resource for annotating the proteome. Cell 2005; 122:957–68.

[228] Rual J-F, Venkatesan K, Hao T, Hirozane-Kishikawa T, Dricot A, Li N, et al. Towards a proteome-scale map of the human protein-protein interaction network. Nature 2005; 437:1173–8.

[229] Futschik ME, Chaurasia G, Herzel H. Comparison of human protein-protein interaction maps. Bioinformatics 2007; 23:605–11.

[230] Mann M, Hendrickson RC, Pandey A. Analysis of proteins and proteomes by mass spectrometry. Annu Rev Biochem 2001; 70:437–73.

[231] Pertl-Obermeyer H, Schulze WX, Obermeyer G. In vivo cross-linking combined with mass spectrometry analysis reveals receptor-like kinases and Ca(2+) signalling proteins as putative interaction partners of pollen plasma membrane H(+) ATPases. J Proteomics 2014; 108:17–29.

[232] Kaboord B, Perr M. Isolation of Proteins and Protein Complexes by Immunoprecipitation. In: Posch A (ed.), 2D PAGE: Sample Preparation and Fractionation. Totowa, NJ: Humana Press; 2008:349–364.

[233] Berggård T, Linse S, James P. Methods for the detection and analysis of protein-protein interactions. Proteomics 2007; 7:2833–42.

[234] Lee C. Coimmunoprecipitation assay. Methods Mol Biol 2007; 362:401–6.

[235] Dunn WB. Mass spectrometry in systems biology an introduction. Methods Enzymol 2011; 500:15–35.

[236] Perkins JR, Diboun I, Dessailly BH, Lees JG, Orengo C. Transient protein-protein interactions: structural, functional, and network properties. Structure 2010; 18:1233–43.

[237] Kastritis PL, Moal IH, Hwang H, Weng Z, Bates PA, Bonvin AMJJ, et al. A structure-based benchmark for protein-protein binding affinity. Protein Sci 2011; 20:482–91.

[238] Estojak J, Brent R, Golemis EA. Correlation of two-hybrid affinity data with in vitro measurements. Mol Cell Biol 1995; 15:5820–9.

[239] EMBL-EBI. Primary and secondary databases | EMBL-EBI Train online. https://www.ebi.ac.uk/training/online/course/bioinformatics-terrified/what-database/relational-databases/primary-and-secondary-databases. Accessed 27 July 2017.

[240] Huang DW, Sherman BT, Lempicki RA. Bioinformatics enrichment tools: paths toward the comprehensive functional analysis of large gene lists. Nucleic Acids Res 2009; 37:1–13.

[241] Pavlopoulos GA, Wegener A-L, Schneider R. A survey of visualization tools for biological network analysis. BioData Min 2008; 1:12.

[242] Felgueiras J, Silva JV, Fardilha M. Adding biological meaning to human protein-protein interactions identified by yeast two-hybrid screenings: A guide through bioinformatics tools. J Proteomics 2017.

[243] Böckmann B, Heiden K. PathGuide - model-based generation of guideline-compliant pathways for the use in different hospital information systems. Stud Health Technol Inform 2013; 192:1089.

[244] Koh GCKW, Porras P, Aranda B, Hermjakob H, Orchard SE. Analyzing protein-protein interaction networks. J Proteome Res 2012; 11:2014–31.

[245] Orchard S, Ammari M, Aranda B, Breuza L, Briganti L, Broackes-Carter F, et al. The MIntAct project--IntAct as a common curation platform for 11 molecular interaction databases. Nucleic Acids Res 2014; 42:D358-63.

[246] Cusick ME, Yu H, Smolyar A, Venkatesan K, Carvunis A-R, Simonis N, et al. Literature-curated protein interaction datasets. Nat Methods 2009; 6:39–46.

[247] Orchard S, Kerrien S, Abbani S, Aranda B, Bhate J, Bidwell S, et al. Protein interaction data curation: the International Molecular Exchange (IMEx) consortium. Nat Methods 2012; 9:345–50.

[248] Hermjakob H, Montecchi-Palazzi L, Bader G, Wojcik J, Salwinski L, Ceol A, et al. The HUPO PSI's molecular interaction format--a community standard for the representation of protein interaction data. Nat Biotechnol 2004; 22:177–83.

[249] Kerrien S, Aranda B, Breuza L, Bridge A, Broackes-Carter F, Chen C, et al. The IntAct molecular interaction database in 2012. Nucleic Acids Res 2012; 40:D841-6.

[250] Salwinski L, Miller CS, Smith AJ, Pettit FK, Bowie JU, Eisenberg D. The Database of Interacting Proteins: 2004 update. Nucleic Acids Res 2004; 32:D449-51.

[251] Ammari MG, Gresham CR, McCarthy FM, Nanduri B. HPIDB 2.0: a curated database for host-pathogen interactions. Database (Oxford) 2016; 2016.

[252] Goll J, Rajagopala S V, Shiau SC, Wu H, Lamb BT, Uetz P. MPIDB: the microbial protein interaction database. Bioinformatics 2008; 24:1743–4.

[253] Licata L, Briganti L, Peluso D, Perfetto L, Iannuccelli M, Galeota E, et al. MINT, the molecular interaction database: 2012 update. Nucleic Acids Res 2012; 40:D857-61.

[254] Chatr-aryamontri A, Ceol A, Palazzi LM, Nardelli G, Schneider MV, Castagnoli L, et al. MINT: the Molecular INTeraction database. Nucleic Acids Res 2007; 35:D572-4.

[255] Launay G, Salza R, Multedo D, Thierry-Mieg N, Ricard-Blum S. MatrixDB, the extracellular matrix interaction database: updated content, a new navigator and expanded functionalities. Nucleic Acids Res 2015; 43:D321-7.

[256] Brown KR, Jurisica I. Online predicted human interaction database. Bioinformatics 2005; 21:2076–82.

[257] Brown KR, Jurisica I. Unequal evolutionary conservation of human protein interactions in interologous networks. Genome Biol 2007; 8:R95.

[258] Breuer K, Foroushani AK, Laird MR, Chen C, Sribnaia A, Lo R, et al. InnateDB: systems biology of innate immunity and beyond--recent updates and continuing curation. Nucleic Acids Res 2013; 41:D1228-33.

[259] Apweiler R, Bairoch A, Wu CH, Barker WC, Boeckmann B, Ferro S, et al. UniProt: the Universal Protein knowledgebase. Nucleic Acids Res 2004; 32:D115-9.

[260] Alanis-Lobato G, Andrade-Navarro MA, Schaefer MH. HIPPIE v2.0: enhancing meaningfulness and reliability of protein-protein interaction networks. Nucleic Acids Res 2017; 45:D408–D414.

[261] Schaefer MH, Fontaine J-F, Vinayagam A, Porras P, Wanker EE, Andrade-Navarro MA. HIPPIE: Integrating protein interaction networks with experiment based quality scores. PLoS One

2012; 7:e31826.

[262] del-Toro N, Dumousseau M, Orchard S, Jimenez RC, Galeota E, Launay G, et al. A new reference implementation of the PSICQUIC web service. Nucleic Acids Res 2013; 41:W601-6.

[263] Santos A, Tsafou K, Stolte C, Pletscher-Frankild S, O'Donoghue SI, Jensen LJ. Comprehensive comparison of large-scale tissue expression datasets. PeerJ 2015; 3:e1054.

[264] Nagaraj SH, Gasser RB, Ranganathan S. A hitchhiker's guide to expressed sequence tag (EST) analysis. Brief Bioinform 2007; 8:6–21.

[265] Harrington CA, Rosenow C, Retief J. Monitoring gene expression using DNA microarrays. Curr Opin Microbiol 2000; 3:285–91.

[266] Uhlen M, Oksvold P, Fagerberg L, Lundberg E, Jonasson K, Forsberg M, et al. Towards a knowledge-based Human Protein Atlas. Nat Biotechnol 2010; 28:1248–50.

[267] Wu C, Jin X, Tsueng G, Afrasiabi C, Su AI. BioGPS: building your own mash-up of gene annotations and expression profiles. Nucleic Acids Res 2016; 44:D313-6.

[268] Wu C, Orozco C, Boyer J, Leglise M, Goodale J, Batalov S, et al. BioGPS: an extensible and customizable portal for querying and organizing gene annotation resources. Genome Biol 2009; 10:R130.

[269] Pan J-B, Hu S-C, Shi D, Cai M-C, Li Y-B, Zou Q, et al. PaGenBase: a pattern gene database for the global and dynamic understanding of gene function. PLoS One 2013; 8:e80747.

[270] Petryszak R, Keays M, Tang YA, Fonseca NA, Barrera E, Burdett T, et al. Expression Atlas update--an integrated database of gene and protein expression in humans, animals and plants. Nucleic Acids Res 2016; 44:D746-52.

[271] Wagner L, Agarwala R. UniGene. The NCBI Handbook [Internet]. 2nd ed. Bethesda (MD): National Center for Biotechnology Information; 2013.

[272] Keshava Prasad TS, Goel R, Kandasamy K, Keerthikumar S, Kumar S, Mathivanan S, et al. Human Protein Reference Database--2009 update. Nucleic Acids Res 2009; 37:D767-72.

[273] Brookes AJ, Robinson PN. Human genotype-phenotype databases: aims, challenges and opportunities. Nat Rev Genet 2015; 16:702–15.

[274] Eppig JT, Richardson JE, Kadin JA, Ringwald M, Blake JA, Bult CJ. Mouse Genome Informatics (MGI): reflecting on 25 years. Mamm Genome 2015; 26:272–84.

[275] Amberger JS, Bocchini CA, Schiettecatte F, Scott AF, Hamosh A. OMIM.org: Online Mendelian Inheritance in Man (OMIM®), an online catalog of human genes and genetic disorders. Nucleic Acids Res 2015; 43:D789-98.

[276] Yu W, Clyne M, Khoury MJ, Gwinn M. Phenopedia and Genopedia: disease-centered and gene-centered views of the evolving knowledge of human genetic associations. Bioinformatics 2010; 26:145–6.

[277] Piñero J, Queralt-Rosinach N, Bravo À, Deu-Pons J, Bauer-Mehren A, Baron M, et al. DisGeNET: a discovery platform for the dynamical exploration of human diseases and their genes. Database (Oxford) 2015; 2015:bav028.

[278] Piñero J, Bravo À, Queralt-Rosinach N, Gutiérrez-Sacristán A, Deu-Pons J, Centeno E, et al. DisGeNET: a comprehensive platform integrating information on human disease-associated genes and variants. Nucleic Acids Res 2017; 45:D833–D839.

[279] Pletscher-Frankild S, Pallejà A, Tsafou K, Binder JX, Jensen LJ. DISEASES: text mining and data integration of disease-gene associations. Methods 2015; 74:83–9.

[280] Huang DW, Sherman BT, Lempicki RA. Systematic and integrative analysis of large gene lists using DAVID bioinformatics resources. Nat Protoc 2009; 4:44–57.

[281] Rivals I, Personnaz L, Taing L, Potier M-C. Enrichment or depletion of a GO category within a class of genes: which test? Bioinformatics 2007; 23:401–7.

[282] van den Berg BHJ, Thanthiriwatte C, Manda P, Bridges SM. Comparing gene annotation enrichment tools for functional modeling of agricultural microarray data. BMC Bioinformatics 2009; 10 Suppl 1:S9.

[283] Alexanderson GL. ABOUT THE COVER: EULER AND ONIGSBERG'S BRIDGES: A HISTORICAL VIEW. Bull New Ser Am Math Soc 2006; 43:567–573.

[284] Birlutiu A, Heskes T. Using Topology Information for Protein-Protein Interaction Prediction. In: Comin M, Käll L, Marchiori E, Ngom A, Rajapakse J (eds.), Pattern Recognition in Bioinformatics: 9th IAPR International Conference, PRIB 2014, Stockholm, Sweden, August 21-23, 2014. Proceedings. Cham: Springer International Publishing; 2014:10–22.

[285] Newman ME. Scientific collaboration networks. II. Shortest paths, weighted networks, and centrality. Phys Rev E Stat Nonlin Soft Matter Phys 2001; 64:16132.

[286] Yoon J, Blumer A, Lee K. An algorithm for modularity analysis of directed and weighted biological networks based on edge-betweenness centrality. Bioinformatics 2006; 22:3106–8.

[287] Ma'ayan A. Introduction to network analysis in systems biology. Sci Signal 2011; 4:tr5.

[288] Lotia S, Montojo J, Dong Y, Bader GD, Pico AR. Cytoscape app store. Bioinformatics 2013; 29:1350–1.

[289] Cytoscape Consortium. Cytoscape 3.5.0 User Manual — Cytoscape User Manual 3.5.0 documentation. http://manual.cytoscape.org/en/stable/. Accessed 28 July 2017.

[290] Li Z, Qiao Z, Zheng W, Ma W. Network Cluster Analysis of Protein-Protein Interaction Network-Identified Biomarker for Type 2 Diabetes. Diabetes Technol Ther 2015; 17:475–81.

[291] Saito R, Smoot ME, Ono K, Ruscheinski J, Wang P-L, Lotia S, et al. A travel guide to Cytoscape plugins. Nat Methods 2012; 9:1069–76.

[292] Sato T, Katagiri K, Gohbara A, Inoue K, Ogonuki N, Ogura A, et al. In vitro production of functional sperm in cultured neonatal mouse testes. Nature 2011; 471:504–7.

[293] Lindeboom F. A tissue-specific knockout reveals that Gata1 is not essential for Sertoli cell function in the mouse. Nucleic Acids Res 2003; 31:5405–5412.

[294] Narisawa S, Hecht NB, Goldberg E, Boatright KM, Reed JC, Millán JL. Testis-specific cytochrome c-null mice produce functional sperm but undergo early testicular atrophy. Mol Cell Biol 2002; 22:5554–62.

[295] Baldi E, Luconi M, Muratori M, Forti G. A novel functional estrogen receptor on human sperm membrane interferes with progesterone effects. Mol Cell Endocrinol 2000; 161:31–5.

[296] Luconi M, Muratori M, Forti G, Baldi E. Identification and characterization of a novel functional estrogen receptor on human sperm membrane that interferes with progesterone effects. J Clin Endocrinol Metab 1999; 84:1670–8.

[297] Lavitrano M, Giovannoni R, Cerrito MG. Methods for sperm-mediated gene transfer. Methods Mol Biol 2013; 927:519–29.

[298] Jamur MC, Oliver C. Permeabilization of cell membranes. Methods Mol Biol 2010; 588:63–6.

[299] Díaz A, Domínguez L, Fornés MW, Burgos MH, Mayorga LS. Acrosome content release in streptolysin O permeabilized mouse spermatozoa. Andrologia n.d.; 28:21–6.

[300] Johnson LR, Moss SB, Gerton GL. Maintenance of motility in mouse sperm permeabilized with streptolysin O. Biol Reprod 1999; 60:683–90.

[301] Bustos MA, Roggero CM, De la Iglesia PX, Mayorga LS, Tomes CN. GTP-bound Rab3A exhibits consecutive positive and negative roles during human sperm dense-core granule exocytosis. J Mol Cell Biol 2014; 6:286–98.

[302] Bustos MA, Lucchesi O, Ruete MC, Mayorga LS, Tomes CN. Rab27 and Rab3 sequentially regulate human sperm dense-core granule exocytosis. Proc Natl Acad Sci U S A 2012; 109:E2057-66.

[303] Ruete MC, Lucchesi O, Bustos MA, Tomes CN. Epac, Rap and Rab3 act in concert to mobilize calcium from sperm's acrosome during exocytosis. Cell Commun Signal 2014; 12:43.

[304] Akbarzadeh A, Rezaei-Sadabady R, Davaran S, Joo SW, Zarghami N, Hanifehpour Y, et al. Liposome: classification, preparation, and applications. Nanoscale Res Lett 2013; 8:102.

[305] Garrett FE, Goel S, Yasul J, Koch RA. Liposomes fuse with sperm cells and induce activation by delivery of impermeant agents. Biochim Biophys Acta 1999; 1417:77–88.

[306] Sullivan R, Saez F. Epididymosomes, prostasomes and liposomes; their role in mammalian male reproductive physiology. Reproduction 2013; 146:R21-35.

[307] Arts EG, Kuiken J, Jager S, Hoekstra D. Fusion of artificial membranes with mammalian spermatozoa. Specific involvement of the equatorial segment after acrosome reaction. Eur J Biochem 1993; 217:1001–9.

[308] Coward K, Kubota H, Parrington J. In vivo gene transfer into testis and sperm: developments and future application. Arch Androl n.d.; 53:187–97.

[309] Parrington J, Coward K, Gadea J. Sperm and testis mediated DNA transfer as a means of gene therapy. Syst Biol Reprod Med 2011; 57:35–42.

[310] Bachiller D, Schellander K, Peli J, Rüther U. Liposome-mediated DNA uptake by sperm cells. Mol Reprod Dev 1991; 30:194–200.

[311] Ball BA, Sabeur K, Allen WR. Liposome-mediated uptake of exogenous DNA by equine spermatozoa and applications in sperm-mediated gene transfer. Equine Vet J 2008; 40:76–82.

[312] Lu J-K, Fu B-H, Wu J-L, Chen TT. Production of transgenic silver sea bream (Sparus sarba) by different gene transfer methods. Mar Biotechnol (NY) 2002; 4:328–37.

[313] Miraglia SJ, Glabe CG. Characterization of the membrane-associating domain of the sperm adhesive protein, bindin. Biochim Biophys Acta 1993; 1145:191–8.

[314] Arias ME, Sánchez-Villalba E, Delgado A, Felmer R. Effect of transfection and co-incubation of bovine sperm with exogenous DNA on sperm quality and functional parameters for its use in sperm-mediated gene transfer. Zygote 2017; 25:85–97.

[315] Hoseini Pajooh K, Tajik P, Karimipoor M, Behdani M. Techniques for augmentation of exogenous DNA uptake by ovine spermatozoa. Iran J Vet Res 2016; 17:25–30.

[316] Gromadzka-Ostrowska J, Dziendzikowska K, Lankoff A, Dobrzyńska M, Instanes C, Brunborg G, et al. Silver nanoparticles effects on epididymal sperm in rats. Toxicol Lett 2012; 214:251–8.

[317] De Jong WH, Borm PJA. Drug delivery and nanoparticles:applications and hazards. Int J Nanomedicine 2008; 3:133–49.

[318] Bhatia S. Nanoparticles Types, Classification, Characterization, Fabrication Methods and Drug Delivery Applications. Natural Polymer Drug Delivery Systems: Nanoparticles, Plants, and Algae. Cham: Springer International Publishing; 2016:33–93.

[319] Barkalina N, Jones C, Wood MJA, Coward K. Extracellular vesicle-mediated delivery of molecular compounds into gametes and embryos: learning from nature. Hum Reprod Update n.d.; 21:627–39.

[320] Lehner R, Wang X, Marsch S, Hunziker P. Intelligent nanomaterials for medicine: carrier platforms and targeting strategies in the context of clinical application. Nanomedicine 2013; 9:742–57.

[321] Makhluf SB-D, Abu-Mukh R, Rubinstein S, Breitbart H, Gedanken A. Modified PVA-Fe3O4 nanoparticles as protein carriers into sperm cells. Small 2008; 4:1453–8.

[322] Feugang JM, Youngblood RC, Greene JM, Fahad AS, Monroe WA, Willard ST, et al. Application of quantum dot nanoparticles for potential non-invasive bio-imaging of mammalian spermatozoa. J Nanobiotechnology 2012; 10:45.

[323] Guidotti G, Brambilla L, Rossi D. Cell-Penetrating Peptides: From Basic Research to Clinics. Trends Pharmacol Sci 2017; 38:406–424.

[324] Vivès E, Brodin P, Lebleu B. A truncated HIV-1 Tat protein basic domain rapidly translocates through the plasma membrane and accumulates in the cell nucleus. J Biol Chem 1997; 272:16010–7.

[325] Järver P, Langel U. The use of cell-penetrating peptides as a tool for gene regulation. Drug Discov Today 2004; 9:395–402.

[326] Morris MC, Depollier J, Mery J, Heitz F, Divita G. A peptide carrier for the delivery of biologically active proteins into mammalian cells. Nat Biotechnol 2001; 19:1173–6.

[327] Nagahara H, Vocero-Akbani AM, Snyder EL, Ho A, Latham DG, Lissy NA, et al. Transduction of full-length TAT fusion proteins into mammalian cells: TAT-p27Kip1 induces cell migration. Nat Med 1998; 4:1449–52.

[328] Snyder EL, Meade BR, Dowdy SF. Anti-cancer protein transduction strategies: reconstitution of p27 tumor suppressor function. J Control Release 2003; 91:45–51.

[329] Zender L, Kühnel F, Köck R, Manns M, Kubicka S. VP22-mediated intercellular transport of p53 in hepatoma cells in vitro and in vivo. Cancer Gene Ther 2002; 9:489–96.

[330] Snyder EL, Meade BR, Saenz CC, Dowdy SF. Treatment of terminal peritoneal carcinomatosis by a transducible p53-activating peptide. PLoS Biol 2004; 2:E36.

[331] Fåhraeus R, Paramio JM, Ball KL, Laín S, Lane DP. Inhibition of pRb phosphorylation and cell-cycle progression by a 20-residue peptide derived from p16CDKN2/INK4A. Curr Biol 1996; 6:84–91.

[332] Moulton HM, Hase MC, Smith KM, Iversen PL. HIV Tat peptide enhances cellular delivery of antisense morpholino oligomers. Antisense Nucleic Acid Drug Dev 2003; 13:31–43.

[333] Cutrona G, Carpaneto EM, Ulivi M, Roncella S, Landt O, Ferrarini M, et al. Effects in live cells of a c-myc anti-gene PNA linked to a nuclear localization signal. Nat Biotechnol 2000; 18:300–3.

[334] Simeoni F, Morris MC, Heitz F, Divita G. Insight into the mechanism of the peptide-based gene delivery system MPG: implications for delivery of siRNA into mammalian cells. Nucleic Acids Res 2003; 31:2717–24.

[335] Wender PA, Mitchell DJ, Pattabiraman K, Pelkey ET, Steinman L, Rothbard JB. The design, synthesis, and evaluation of molecules that enable or enhance cellular uptake: peptoid molecular transporters. Proc Natl Acad Sci U S A 2000; 97:13003–8.

[336] El-Andaloussi S, Holm T, Langel U. Cell-penetrating peptides: mechanisms and applications. Curr Pharm Des 2005; 11:3597–611.

[337] Matsuzaki K, Yoneyama S, Miyajima K. Pore formation and translocation of melittin. Biophys J 1997; 73:831–8.

[338] Oren Z, Shai Y. Mode of action of linear amphipathic alpha-helical antimicrobial peptides. Biopolymers 1998; 47:451–63.

[339] Jones S, Uusna J, Langel Ü, Howl J. Intracellular Target-Specific Accretion of Cell Penetrating Peptides and Bioportides: Ultrastructural and Biological Correlates. Bioconjug Chem 2016; 27:121–9.

[340] Howl J, Matou-Nasri S, West DC, Farquhar M, Slaninová J, Ostenson C-G, et al. Bioportide: an emergent concept of bioactive cell-penetrating peptides. Cell Mol Life Sci 2012; 69:2951–66.

[341] Howl J, Jones S. Proteomimetic Cell Penetrating Peptides. Int J Pept Res Ther 2008; 14:359.

[342] Giorello L, Clerico L, Pescarolo MP, Vikhanskaya F, Salmona M, Colella G, et al. Inhibition of cancer cell growth and c-Myc transcriptional activity by a c-Myc helix 1-type peptide fused to an internalization sequence. Cancer Res 1998; 58:3654–9.

[343] Lukanowska M, Howl J, Jones S. Bioportides: bioactive cell-penetrating peptides that modulate cellular dynamics. Biotechnol J 2013; 8:918–30.

[344] Yoshida T, Tomioka I, Nagahara T, Holyst T, Sawada M, Hayes P, et al. Bax-inhibiting peptide derived from mouse and rat Ku70. Biochem Biophys Res Commun 2004; 321:961–6.

[345] Östlund P, Kilk K, Lindgren M, Hällbrink M, Jiang Y, Budihna M, et al. Cell-Penetrating Mimics of Agonist-Activated G-Protein Coupled Receptors. Int J Pept Res Ther 2005; 11:237–247.

[346] Angeletti RH, Aardal S, Serck-Hanssen G, Gee P, Helle KB. Vasoinhibitory activity of synthetic peptides from the amino terminus of chromogranin A. Acta Physiol Scand 1994; 152:11–9.

[347] Howl J, Jones S, Farquhar M. Intracellular delivery of bioactive peptides to RBL-2H3 cells induces beta-hexosaminidase secretion and phospholipase D activation. Chembiochem 2003; 4:1312–6.

[348] Jones S, Lukanowska M, Suhorutsenko J, Oxenham S, Barratt C, Publicover S, et al. Intracellular translocation and differential accumulation of cell-penetrating peptides in bovine spermatozoa: evaluation of efficient delivery vectors that do not compromise human sperm motility. Hum Reprod 2013; 28:1874–89.

[349] Dravland E, Meizel S. Stimulation of hamster sperm capacitation and acrosome reaction in vitro by glucose and lactate and inhibition by the glycolytic inhibitor ?-chlorohydrin. Gamete Res 1981; 4:515–523.

[350] Vandevoort CA, Overstreet JW. Effects of glucose and other energy substrates on the hyperactivated motility of macaque sperm and the zona pellucida-induced acrosome reaction. J Androl n.d.; 16:327–33.

[351] Parrish JJ, Susko-Parrish JL, First NL. Capacitation of bovine sperm by heparin: inhibitory effect of glucose and role of intracellular pH. Biol Reprod 1989; 41:683–99.

[352] Albarracin J, Mogas T, Palomo M, Pena A, Rigau T, Rodriguez-Gil J. In vitro Capacitation and Acrosome Reaction of Dog Spermatozoa can be Feasibly Attained in a Defined Medium Without Glucose. Reprod Domest Anim 2004; 39:129–135.

Aims

Sperm motility is a crucial event for oocyte fertilization by the sperm. Thus, modulation of sperm motility, specifically inhibition represents a perfect target for a reversible male contraceptive. Moreover, since sperm motility it is a post-testicular process, targeting does not affect sperm production. To achieve such goal, we need to understand how sperm motility is acquired during sperm epididymis transit. This work aimed to enrich the knowledge on the signaling events involved in human sperm motility with the final goal of identify potential targets for male contraception. We approached this general goal by focusing on the characterization and modulation of the signaling pathway GSK3/PPP1R2/PPP1 in human sperm.

To this end the following aims were proposed:

Aim 1: Modulate protein-protein interactions in human spermatozoa involved in human spermatozoa motility

Results: Sperm motility modulation by using a bioportide based on PPP1/PPP1R2 interaction interface (Chapter B1)

Aim 2: Identify and characterize protein-protein interactions involved in human sperm motility as potential targets for male contraceptives

Results: Identification and characterization of GSK3 human testis and spermatozoa interactome

B. Results

B1. Sperm motility modulation using a bioportide based on PPP1/PPP1R2 interaction interface

Maria João Freitas[1], Joana Vieira Silva[2], John Howl[3], Sarah Jones[3], Barbara Regadas-Correia[2]; Sofia Guimarães[2], Srinivasan Vijayaraghavan[4] and Magarida Fardilha[2]

1. Signal Transduction Laboratory, Institute for Research in Biomedicine – iBiMED, Biology PhD Program, University of Aveiro, Aveiro, Portugal;

2. Signal Transduction Laboratory, Institute for Research in Biomedicine – iBiMED, Health Sciences Program, University of Aveiro, Aveiro, Portugal;

3. Molecular Pharmacology Group, University of Wolverhampton, Wolverhampton, UK;

4. Department of Biological Sciences, Kent State University, Kent, OH 44242, USA.

In the process of patent application (UK patent application number 1711620.3, submitted on 19th of July 2017)

Acknowledgments

This work was financed by FEDER funds through the "Programa Operacional Competitividade e Internacionalização- COMPETE 2020" and by National Funds through the FCT- Fundação para a Ciência e Tecnologia (PTDB/BBB-BQB/3804/2014). We are thankful to Institute for Biomedicine – iBiMED (UID/BIM/04501/2013) for supporting this project. iBiMED is supported by the Portuguese Foundation for Science and Technology (FCT), Compete2020 and FEDER fund. This work was also supported by an individual grant from FCT of the Portuguese Ministry of Science and Higher Education to M.J.F. (SFRH/BD/84876/2012).

B1.1. Abstract

The limited options available for male contraception reflect the necessity of a new group of male contraceptives. The sperm motility acquisition mechanism is an optimal target for a new male contraceptive since is essential for fertilization and a post-testicular sperm maturation process. Sperm motility relies on phosphorylation of key proteins. Phosphoprotein phosphatase 1 catalytic subunit gamma 2 (PPP1CC2) is a central player on controlling the phosphorylation state of proteins and consequently sperm motility. On human sperm, PPP1CC2 activity is partially controlled by PPP1 regulatory subunit 2 (PPP1R2). We hypothesized that disruption of PPP1R2/PPP1CC2 interaction would have a deleterious effect on sperm motility. In order to modulate sperm motility, we designed peptides sequences capable of disrupting PPP1R2/PPP1CC2 interactions based on PPP1R2/PPP1CC2 interaction interference. To insure sperm intracellular delivery, the peptides were coupled with cell penetrating peptides (CPPs) originating bioportides. We demonstrated that the disruptive bioportide was able to interfere with PPP1R2/PPP1CC2 interaction, translocate to human sperm and significantly reduced sperm motility. In conclusion, we proved that rationally designed peptides can target protein-protein interactions in spermatozoa and development of a new type of male contraceptive based on sperm motility modulations is possible.

B1.2. Introduction

Currently, contraception is mainly limited to female contraceptives. Condom and vasectomy are the foremost methods used by males [1,2]. Although research on hormonal male contraceptives has been reported, severe secondary side effects have discouraged further investment. [3]. Since sperm motility is a post-testicular acquisition process and it appears to be hormonal independent, we consider that targeting the mechanism of sperm motility acquisition may be the future on male contraceptives.

Sperm motility is acquired in the epididymis and relies mostly on intracellular signaling events, since sperm cells are transcriptionally silent. Reversible phosphorylation is essential to motility acquisition and Phosphoprotein phosphatase 1 (PPP1) is a key player in this process [4]. In mammalian sperm PPP1CC2, a testis-enriched PPP1 isoform, appears to be the sole responsible for PPP1 activity [5,6]. Furthermore, PPP1CC2 is distributed along the entire flagellum [7,8] and inhibition of PPP1 by phosphatase inhibitors (calyculin A and okadaic acid) induces caput sperm motility [5]. Smith et al showed that in epididymis caput, bovine immotile sperm present a two-fold higher activity of PPP1 compared with fully mature sperm [5,9]. Control of PPP1 catalytic activity is achieved through binding to regulatory subunits, the PPP1 interacting proteins. In mammalian sperm, Phosphoprotein phosphatase 1 regulatory subunit 2 (PPP1R2), a PPP1 inhibitor, is central in controlling PPP1 activity. PPP1R2 is a highly intrinsically disordered protein that only acquires a defined structure when associated with PPP1 [7,10,11]. In human sperm, Korrodi-Gregório et al demonstrated that part of PPP1 population is bound to PPP1R2 and within these complex PPP1 is inactive [10].

The interaction between PPP1 and PPP1R2 has been solved by crystallography. PPP1R2 interacts with PPP1 in 3 regions: between residues 12-17 (site 1); 44-56 (site 2) and 130-169 (site 3) of PPP1R2. PPP1R2 contains two degenerated RVxF motifs, the most common motif among PPP1 interactors. The first RVxF motif, ^{44}KSQKW^{48} sites on top of PPP1 RVxF pocket, far away from the catalytic center, while the ^{145}KLHY^{148} motif sites on top of PPP1 catalytic center. PPP1R2 site 3 of interaction is unique, since it extends on top of the active site of PPP1 resulting in complete inhibition of PPP1, by displacement of metal ions (Mn^{2+} and Fe^{2+}) crucial for phosphatase activity [12,14].

The interface between PPP1 and PPP1R2 present an opportunity for pharmacological interventions, specifically to modulate sperm motility. However, target intracellular complexes can be challenging due to cells bilayred lipid membrane. Cell penetrating peptides (CPPs) are short peptide sequences

that are able to rapid translocate into mammalian cells and deliver biological active molecules [15]. In 2015, Jones and colleagues proved that CPPs translocate into human and bovine sperm without affecting viability and motility [16].

The goal of this study was to design and synthetize peptides capable of translocating the sperm membrane and disrupting PPP1/PPP1R2 complex, as well as, evaluate their ability to modulate sperm motility.

B1.3. Methods

B1.3.1. Bioportide design

With the goal of disrupting the complex PPP1/PPP1R2 in human sperm, the following bioportides were designed (Table B1.1):

Table B1.1. Peptide sequence, peptide designation and length of the bioportides (BP) used in this study. To enable quantitative and qualitative uptake studies, TAMRA fluorophore was added. Underline, C105Y (CPP); Red PPP1 binding motif; Bold, PPP1R2 RVxF flanking sequence.

Peptide Designation	Sequence	Length
BP-PPP1R2 RVxF	H-^{36}**VDEELSK**^{44}**KSQKW**^{48}**DEMNILA**^{54}CSIPPEVKFNKPFVYLI-NH_2	36
BP-PPP1R2 RVxF SC	H-^{36}**VDEELSK**^{44}**QWKKS**^{48}**DEMNILA**^{54}CSIPPEVKFNKPFVYLI-NH_2	36

The BP-PPP1R2 RVxF bioportide was designed by coupling the PPP1R2 RVxF motif- ^{44}KSQKW^{48}- and the adjacent 7 aminoacids with C105Y CPP. The BP-PPP1R2 RVxF SC is similar to the BP-PPP1R2 RVxF peptide, yet the RVxF was scrambled to QWKKS to prevent disruption of PPP1/PPP1R2 complex.

B1.3.2. Microwave-assisted solid phase peptide synthesis

Fmoc-protected aminoacids were purchased from Novabiochem (Beeston, UK). Microwave-assisted solid phase peptide syntheses were performed using a Discover SPS Microwave Peptide Synthsizer (CEM Microwave Technology Ltd, Buckingham, UK) with fibre optic temperature control. Peptides were synthesized (0.1 mmol scale) using Rink amide MBHA resins pre-loaded with the first amino acid (AnaSpec, Inc., Cambridge Bioscience Ltd, Cam- bridge, UK) and employed an N-a-Fmoc protection strategy with HCTU activation. Deprotection with 7 mL of 20% piperidine was performed for 3 min at 50 W/75ºC. A majority of AA coupling reactions were accomplished with a 4-fold molar excess of Fmoc-protected AA with HCTU and diisopropylethylamine (DIPEA), molar ratio of 1:1:2 (AA/HCTU/ DIPEA), in 4 mL for 10 min at 25 W/75ºC. Arg coupling was performed in two stages: 30 min 0W/≈25ºC followed by 5 min at 17 W/75ºC. To reduce racemization of Cys and His, coupling conditions were 5 min at 0 W/≈25ºC followed by 6 min at 17 W/50ºC with the hindered base collidine (TMP) at a molar ratio of 1:1:2 (AA/HCTU/TMP) [17]. Aspartimide formation was reduced by the substitution of piperidine for 5% piperazine and 0.1 M 1-hydroxybenztriazole hydrate (HOBt) in the deprotection solution [17]. Fluorescent peptides, to be used in cell imaging and quantitative

uptake analyses, were synthesized by amino-terminal acylation with 6-carboxy-tetramethylrhodamine (TAMRA) (Novabiochem, Beeston, UK) as previously described. Peptides were purified by semi-preparative scale high-performance liquid chromatography, and the predicted masses of all peptides were confirmed by matrix-assisted laser desorption ionization (MALDI) time of flight mass spectrometry.

B1.3.3. *In vitro* effect of Bioportides

A concentration range of commercial PPP1R2 (New England Biolabs, Herts, UK) was incubated with purified PPP1CC2 (1:20; 1:200 and 1:2000) and either BP-PPP1R2 RVxF or BP-PPP1R2 RVxF SC for 30 min (ratio of 1:200:0.5 of PPP1R2, PPP1CC2 and bioportides). PPP1CC2 activity was measured during 30 min, in 5 min breaks, using the SensoLyte® pNPP Protein Phosphatase Assay Kit *Colorimetric*(AnaSpec, Inc., Cambridge Bioscience Ltd, Cambridge, UK) and a PPP1 specific assay buffer according to manufactures instructions. Negative control (only assay buffer) was included. Four replicas were performed.

B1.3.4. Sperm cells preparation

This study was approved by the Ethics and Internal Review Board of the Hospital Infante D. Pedro E.P.E. (Aveiro, Portugal) (Process number: 36/AO) and was conducted in accordance with the ethical standards of the Helsinki Declaration. All donors signed an informed consent allowing the samples to be used for scientific purposes. Human semen samples were obtained from a randomized group of donors and collected by masturbation into a sterile container. Basic semen analysis was conducted in accordance with World Health Organization (WHO) guidelines [18] and only normospermic samples were further used. Fresh semen from Holstein Friesian bulls was obtained from LusoGenes, LDA, Aveiro, Portugal. Semen was collected by artificial vagina and assessed by a certified veterinarian. Human and bovine sperm were isolated and washed three times in PBS 1x (Fisher Scientific, Loures, Portugal) from seminal plasma by centrifugation (600 g for 10 min at RT) using AllGrade Wash medium (LifeGlobal, Brussels, Belgium). Pellet was resuspended in medium to a final concentration of $40x10^6$ sperm cells/mL and incubated at 37 ºC with 5% CO_2 until further treatment.

B1.3.5. Microscopy evaluation of intracellular accumulation of bioportides

Washed bovine and human sperm cells ($40x10^6$) were resuspended and incubated with 10 μM TAMRA-labeled bioportides for 1 h at 37 ºC in a humidified atmosphere of 5% CO_2. After, cells were washed 3 times in PBS 1x (800 g for 5 min) in AllGrade Wash medium (LifeGlobal, Brussels, Belgium). To confirm that the fluorescently labeled peptides were not merely surface associated, sperm cell were treated with trypsin. Briefly, sperm cells were divided into two populations and half of the cells were fixed in 4% of paraformaldehyde (PFA) (Fisher Scientific, Loures, Portugal) for 20 min. The other half was incubated with 1% of trypsin (wt/vol) (Promega, Madison, Wisconsin, USA) at 37 ºC, centrifuged at 3000 g, washed in AllGrade Wash medium (LifeGlobal, Brussels, Belgium) and resuspended in 4% of PFA for 20min. Fixed cells from both populations were spread into coverslips, allowed to air dry and mounted. Negative controls (only cells) were processed in parallel. Slides were assessed using an Imager Z1, Axio-Cam HRm camera and AxioVision software (Zeiss, Jena, Germany).

B1.3.6. Quantitative evaluation of intracellular accumulation of bioportides

Quantitative assessment of bioportide translocation into sperm was based on a previously described method [19]. Washed bovine and human sperm cells were incubated with 10 μM TAMRA-labeled bioportide for 1 h 37 ºC in a humidified atmosphere of 5% CO_2. Cells were then washed 3 times with PBS 1x, incubated with 1% trypsin (Promega, Madison, Wisconsin, USA) at 37 ºC and collected by centrifugation at 3000 g. Next, cells were lysed in 300 μL 0.1 M NaOH (Fisher Scientific, Loures, Portugal) for 2 h on ice. The lysate (250 μL) was placed into a black 96-well plate and analyzed using an Infinite® 200 PRO plate reader (Tecan, Switzerland) (λAbs 544 nm/ λEm 590 nm).

B1.3.7. Sperm viability assays

Bovine sperm was incubated for 1 min in a 1:1 proportion of Trypan Blue (Fisher Scientific, Loures, Portugal) and 10 μL spread in a slide and left to dry. Dead sperm present a compromised plasma membrane, enabling the Trypan Blue to stain the cell. Live sperm have intact plasma membrane and appear translucid. Two hundred sperm cells were counted per condition using a Zeiss Primo Star microscope (Zeiss, Jena, Germany). Experiments were performed on samples form 3 individual bulls.

B1.3.8. Motility assays

Bioportides were prepared in AllGrade Wash medium (LifeGlobal, Brussels, Belgium) in individual volumes. Washed bovine sperm cells ($20x10^6$) were added to the medium to a final volume of 500 μL. Control samples included sperm cells in medium. All samples were incubated at 37 ºC for 1 or 2 h in a humidified atmosphere of 5%CO_2. Sperm motility, was evaluated using the Sperm Class Analyzer CASA System (Microptic S L, Barcelona, Spain) with SCA® v5.4 software. Briefly, 2 μL of samples were loaded into individual chambers of Leja Standart Count 8 chamber slide 20 μm depth (Leja Products B. V., The Netherlands) pre-heated to 37 ºC. This temperature was kept while at least 500 sperm/condition were evaluated. Experiments were performed on samples form 3 individual bulls and all the conditions were performed in triplicate.

B1.3.9. Molecular modelling and dynamic studies

Computer simulation studies of PPP1R2 RVxF and scrambled RVxF and the 7 flanking aminoacids were performed by the MD (molecular dynamics) simulation package Amber v14 applying Amber-ff14SB force field [20]. The two systems were solvated, in a simulation octahedral box of explicit water molecules (TIP3P model) [21], counter ions were added to neutralize the system and periodic boundary conditions imposed in the three dimensions (12 A^o). After minimizations, systems were subjected to an equilibration phase where water molecules position were restrained, then unrestrained systems were simulated for a total of 5 microseconds, in a NPT ensemble; Langevin equilibration scheme and Berendsen thermostat were used to keep constant temperature (300 K) and pressure (1 atm), respectively. Electrostatic forces were evaluated by Particle Mesh Ewald method and Lennard-Jones forces by a cutoff of 10 Å. All bonds involving hydrogen atoms were constrained using the SHAKE algorithm. Figures were extracted using VMD and prepared in Maestro [22]. Simulation was run for 200 ns in each system.

To perform the trajectory analysis, GROMACS [23], more specifically g_cluster command, was used .For each system, a conformational cluster analysis using gromos algorithm was carried out using a cut-off of 0.2 nm. Using a threshold, the algorithm finds the neighbouring structure and forms clusters with the structure with the largest number of neighbours. The cluster is removed from the frames and the process repeated for the remaining frames. Each of the cluster centroids is used as a representative structure. Change in binding affinity or stability toward PPP1CC2 caused by mutations to alanine or residues within the RVxF motif were calculated using the Residue Scanning functionality in BioLuminate [22] which incorporates the Prime MM-GBSA approach [24].

The PDB format file of rat PPP1CC complexed with mouse PPP1R2 (ref:2O8A) [12] freely available

at protein data bank [25] was modified in MacPymolEdu software to create Figure B1.5.

B1.3.10. Biostatistics analysis

In vitro effect of the CPP: To characterize the sample statistical measures, line graphs and bars graphs were used. For each condition (11 conditions), a Pos Hoc analysis of the Friedman test to detect differences over time (pairwise comparisons) was performed. For each time (0 m, 5 m, 15 m, 20 m, 25 m and 30 m), the Kruskall Wallis test was used to detect differences between the conditions (independent groups). Finally, a pairwise comparisons of conditions test was applied to identify between differences (Mann-Whitney U test).

CPPs impact on sperm motility: To summarize the information contained in the sample a descriptive analysis was performed (central tendency, dispersion measures and bar graph). To decide between parametric or non-parametric methods, a Shapiro-Will test analyzed the existence of outliers. Finally, the differences between the means of two independent groups were tested. In the parametric case, after the Levene's test for equality of variances, the Student's T test was performed to assess for equality of means.

For all tests, the significance level was set at 0.05. Statistical analysis was conducted using IBM SPSS Statistics Software 22.

B1.4. Results

A bioportide was synthesized by coupling a peptide with the potential of disrupting the PPP1/PPP1R2 complex was with a CPPs, with the goal of translocating to sperm cells and affecting their motility. The peptide sequence mimics the PPP1 binding motif of human PPP1R2 (^{44}KSQKW^{48}), which is conserved among bovine, mouse and rat. A bioportide presenting a scrambled PPP1R2 RVxF motif (QWKKS) was used as a control in all experiments.

B1.4.1. Bioportides can disrupt PPP1/PPP1R2 complex *in vitro*

To assess the disruptive capacity of the bioportides, PPP1 activity was evaluated in the presence of the BP--PPP1R2 RVxF and BP--PPP1R2 RVxF SC. The results show that PPP1R2 inhibited PPP1CC2 in a concentration dependent manner [increasing amounts of PPP1R2 led to higher PPP1CC2 inhibition (Supplementary Figure B1.1)]. After 15 min and until 30 min, PPP1R2 inhibited significantly around 50% of PPP1CC2 activity (ratio of 1:200) (Figure B1.1 A and D). Upon adding BP-PPP1R2 RVxF (1:200:0.5), PPP1CC2 activity is restored to original values starting at 15 min (Figure B1.1 B and D) showing that the bioportide that mimics the RVxF PPP1R2 motif was able to disrupt, *in vitro*, the PPP1CC2/PPP1R2 complex. Also, when BP-PPP1R2 RVxF SC was added, PPP1CC2 activity was also restored (time point 25 min and 30 min) (Figure B1.1 C and D). PPP1R2 alone does not present any phosphatase activity (Supplementary Figure B1.1). Descriptive and statistical analysis can be consulted in Supplementary Table B1.1 and Supplementary Table B1.2, respectively.

B1.4.2. Bioportides translocate into human and bovine spermatozoa

Fluorescent cell imaging analysis revealed that fluorescently labeled BP-PPP1R2 RVxF and BP-PPP1R2 RVxF SC (10 μM) were able to translocate and accumulate in human and bovine sperm (Figure B1.2 A and B). In human and bovine sperm, both CPPs accumulated preferentially at the midpiece (* in Figure B1.2 A and B) and, occasionally, in sperm´s head (+ in Figure B1.2 A and B) and along the length of the flagellum. Quantitative uptake comparisons demonstrated that BP-PPP1R2 presented a higher cellular uptake, when compared with BP-PPP1R2 RVxF SC (human 2.9 times; bovine 10.7 times) (Figure B1.2 C). In contrast, bioportides accumulation was similar between species. Higher concentrations were also analyzed (20 μM and 50 μM) and the pattern of bioportides distribution was similar (data not showed).

B1. Sperm motility modulation using a bioportide based on PPP1/PPP1R2 interaction interface

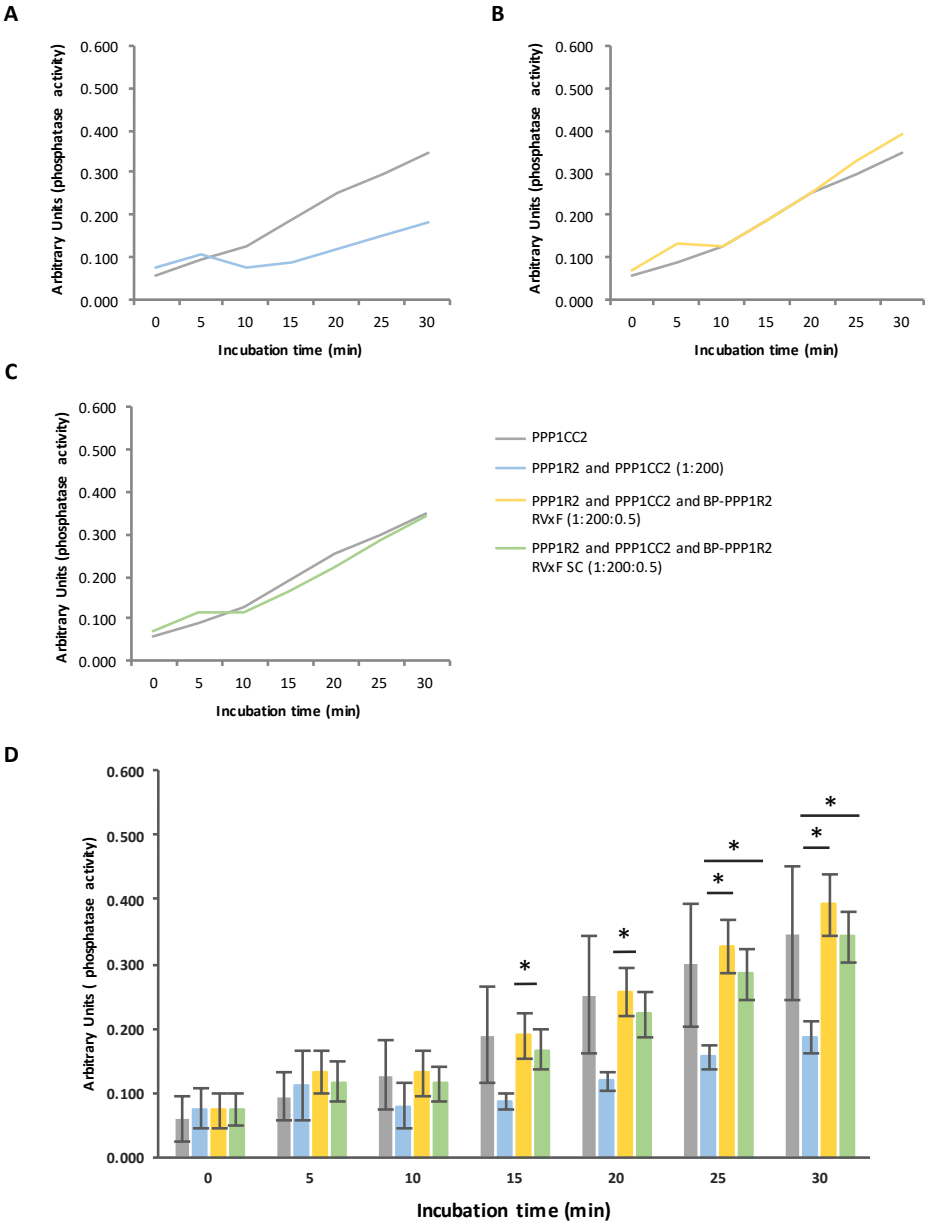

Figure B1.1. Effect of bioportides on PPP1 activity. Effect of BP-PPP1R2 RVxF SC and BP-PPP1R2 RVxF SC on PPP1 activity during 30min **A**. PPP1CC2 and PPP1R2/PPP1CC2 (1:200) phosphatase activity. **B**. PPP1CC2 and PPP1R2/PPP1CC2/BP-PPP1R2 RVxF (1:200:0.5) phosphatase activity. **C**. PPP1CC2 and PPP1R2/PPP1CC2/BP-PPP1R2 RVxF SC (1:200:0.5) phosphatase activity. **D**. Comparison of phosphatase activity mean of PPP1CC2; PPP1R2/PPP1CC2 (1:200); PPP1R2/PPP1CC2/BP-PPP1R2 RVxF and PPP1R2/PPP1CC2/BP-PPP1R2 RVxF SC (1:200:0.5). Data is expressed as arbitrary units of phosphatase activity (minus negative control). Graph bars and lines represent the mean values of 4 replicas. Error bars represent the SEM (standard error of the mean). Statistically significant findings are indicated with a (*). * P<0.05.

B1. Sperm motility modulation using a bioportide based on PPP1/PPP1R2 interaction interface

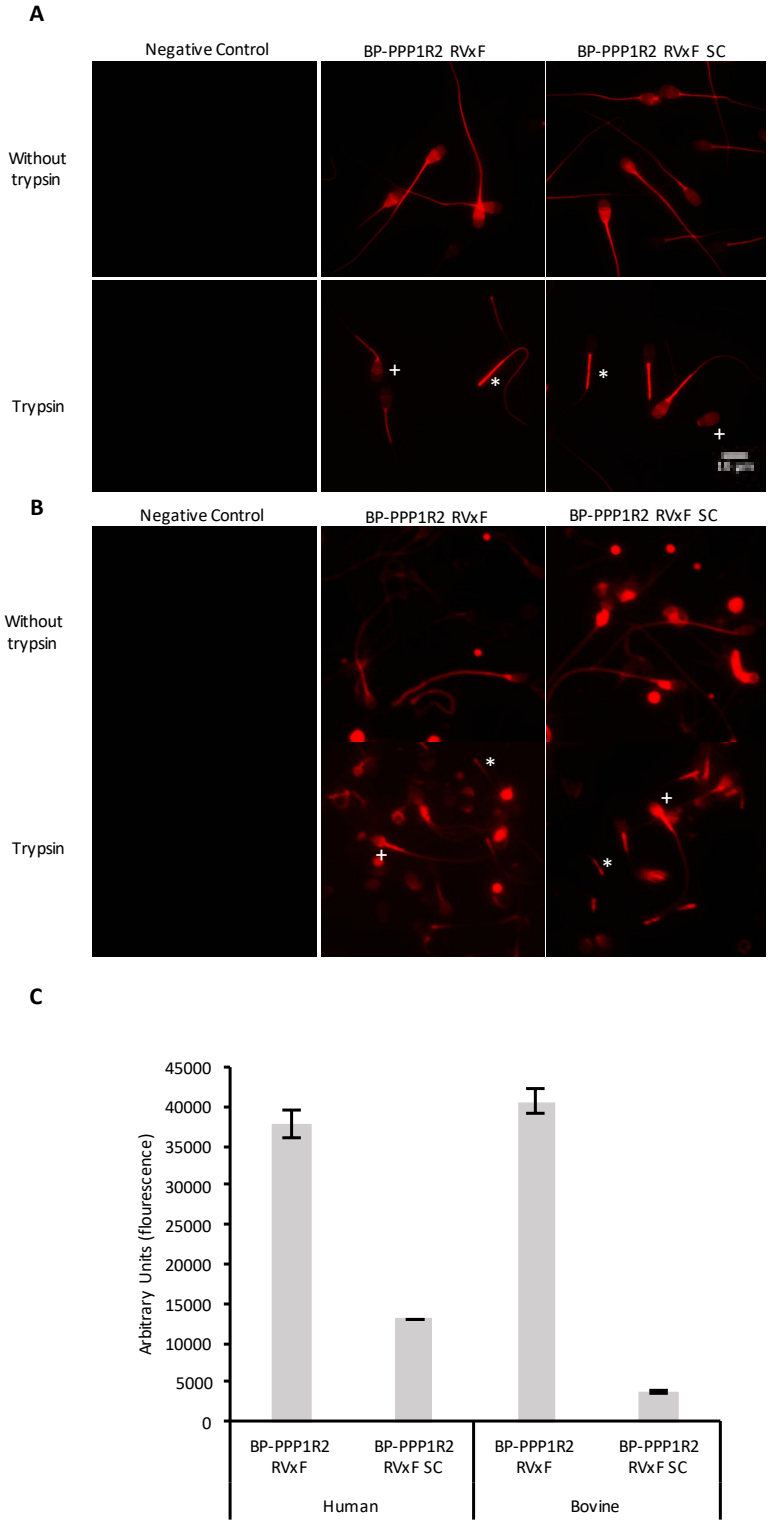

Figure B1.2. Bioportides translocation into bovine and human spermatozoa (previous page). BP-PPP1R2 RVxF and BP-PPP1R2 RVxF SC were synthesized and complexed TAMRA to assess the delivery of the bioportides. **A.** Bovine spermatozoa**.** bioportides accumulation in midpiece (*), head of spermatozoa (+) and occasionally along the flagellum. **B.** Human spermatozoa. Both bioportides also accumulate in midpiece (*) and occasionally in the head (+) and along the flagellum. Scale bar in is 10 μm. Bovine spermatozoa were acquired at 150 ms and human spermatozoa were acquired at 50 ms. **C**. Quantification of CPP translocation into bovine and human spermatozoa. Graph bars represent the mean values of four independent replicas. Error bars represent the SEM (standard error of the mean).

B1.4.3. Bioportides decrease sperm motility

Bovine sperm were exposed to a range of bioportides concentration (20, 50 and 100 μM) and motility parameters were evaluated at 1 h and 2 h. Negative controls were performed in the absence of bioportides. Sperm viability was evaluated after bioportides exposure (100 μM, 1 and 2 h) and no significant changes were observed for both bioportides (Supplementary Figure B1.2).

To assess the effect of the bioportides on sperm physiology, bovine sperm were exposed to 20 μM, 50 μM and 100 μM of both peptides. Exposure of bovine sperm to 20 and 50 μM of both bioportides did not induce any significant alterations in the motility parameters (data not shown). Yet, exposure of bovine sperm to 100 μM BP-PPP1R2 RVxF reduced significantly the percentage of progressive fast motile sperm at 1 h and 2 h (mean decrease of 36.3%, p=0.007 for 1 h and 47.6% p=0.001 for 2 h) compared with the negative control (Figure B1.3 A). In contrast, the percentage of immotile sperm increased significantly at 1 h and 2 h (mean increase of 45.5%, p=0.015 and 49.2%, p=0.007) (Figure B1.3 B). BP-PPP1R2 RVxF SC also significantly decreased the percentage of progressive fast motile sperm at 1 h and 2 h compared with the negative control (mean decrease of 53.2%, p=0.000 and 49.6%, p=0.000) (Figure B1.3 A) and increased the percentage of immotile sperm (mean increase of 73.2%, p=0.000 and 55.7%, p=0.002) (Figure B1.3 B) at both time points tested. No significant alterations were observed in slow progressive motility and non-progressive motility (Figure B1.3 C and D). Descriptive and statistical analysis can be consulted in Supplementary Table B1.3 and Supplementary Table B1.4, respectively.

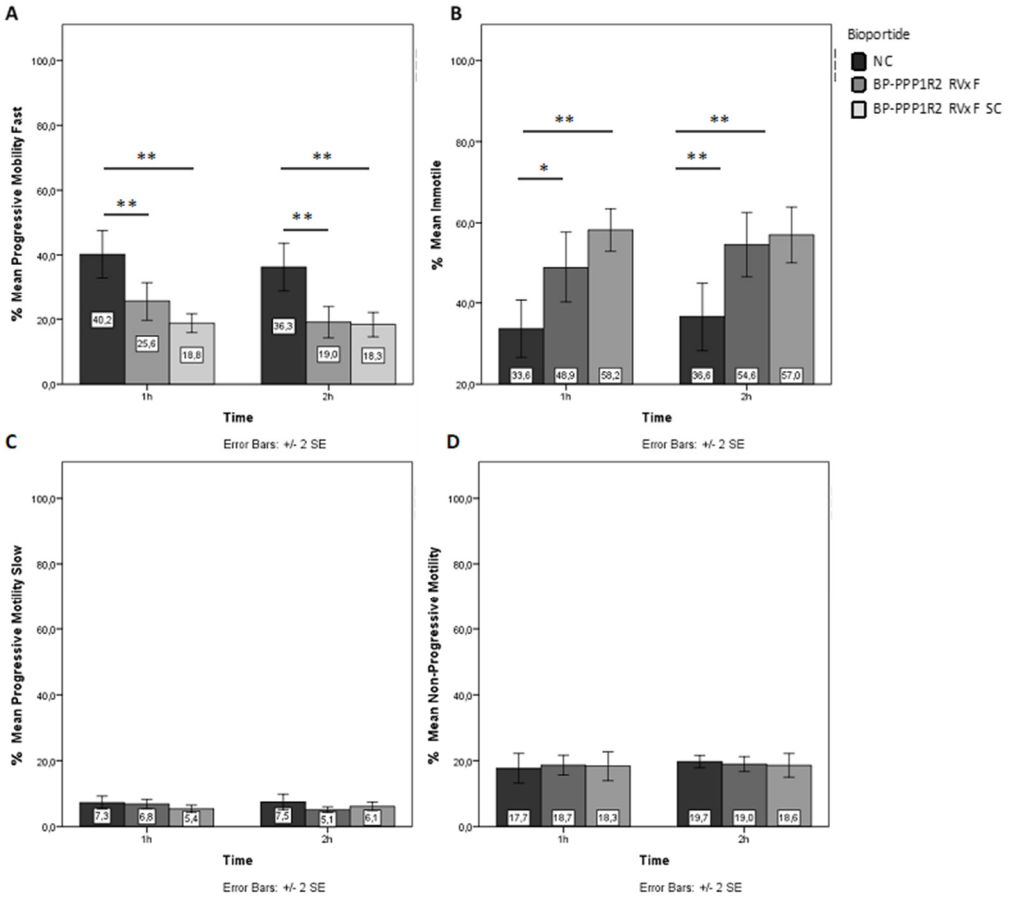

Figure B1.3. Impact of the bioportides in bovine spermatozoa motility parameter. **A**. Impact of bioportides (100µM) on the percentage fast progressive motility, **B.** on the percentage immotile spermatozoa, **C**. on the percentage slow progressive motility, **D.** on the percentage of non-progressive spermatozoa. Graph bars represent the mean values of three independent experiments performed in triplicate. Error bars +/- SE (standard error). Statistically significant findings are indicated with a (*). * P<0.05; ** P<0.01.

B1.4.4. PPP1R2 RVxF and PPP1R2 RVxF scrambled have different stabilities and affinities towards PPP1 RVxF pocket

Molecular dynamics simulations were performed with the peptide sequence, which comprised the PPP1R2 RVxF binding motif and 7 aminoacids flanking at N- and C-termini. Figure B1.4 A shows that the RVxF binding motif forms a rigid secondary structure, an α-helix, while the remaining sequence showed no secondary structure. In the case of PPP1R2 RVxF SC binding motif peptide, the most frequent cluster presented a pronounced α-helix at the N- term and a tendency to form a α-helix at the C-term. The middle region, comprising the scrambled RVxF binding motif, showed no evident secondary structure with an apparently higher flexibility (Figure B1.4 B).

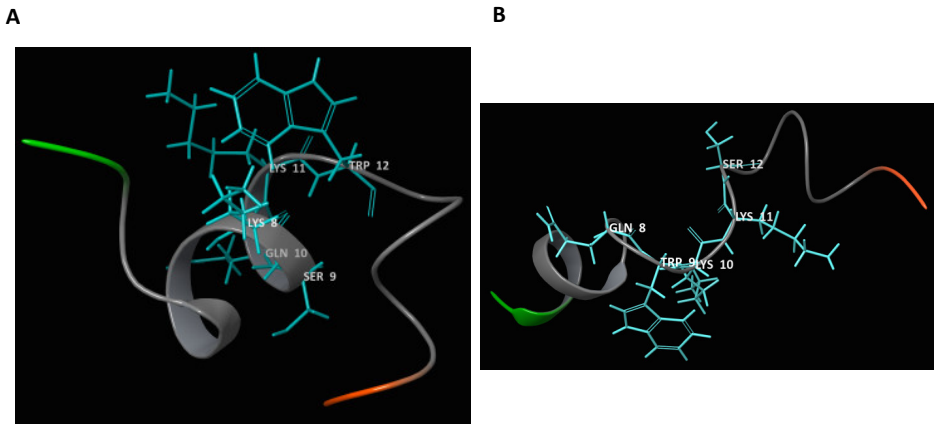

Figure B1.4. Molecular dynamics of PPP1R2 RVxF and PPP1R2 RVxF SC peptide. **A.** RVxF and the 7 flanking aminoacids of the BP-PPP1R2 RVxF bioportide. **B.** Scrambled RVxF and the 7 flanking aminoacids of the BP-PPP1R2 RVxF SC bioportide. Note that the number of the aminoacids correspond to their position within the peptide not within PPP1R2. Green: N-terminus; Orange: C-terminus; Blue: RVxF aminoacids side chains.

Next, aminoacid substitution studies using previous crystallography studies (PDB code 2O8G) revealed that the peptide with RVxF scrambled may bind more stably and with more affinity with the core region of the PPP1 RVxF pocket. The substitution of lysine to a glutamine in the first aminoacid of RVxF motif appears to provide more stability to the peptide (Table B1.2) while the change in the second aminoacid from a serine to a tryptophan confers more affinity to the PPP1 RVxF pocket (Table B1.2).

Table B1.2. Aminoacids substitution studies of RVxF motif. The substitutions studies were performed using previous experimental data no PPP1/PPP1R2 interaction. The more negative the Δ affinity and Δ stability (kcal/mol), the stronger the affinity and stability, respectively*. In the scrambled peptide, the lysine present at position 47 was not changed. In the substitutions studies this lysine was changed for an alanine.

PPP1R2 Residue	RVxF Original	RVxF scrambled	Δ Affinity	Δ Stability
44	LYS	GLN	3.59	-6.89
45	SER	TRP	-4.33	3.16
46	GLN	LYS	6.54	9.27
47	LYS	ALA*	7.34	-3.84
48	TRP	SER	25.3	0.91

B1.5. Discussion

PPP1 has a broad activity spectrum, but is restrained *in vivo* by numerous PPP1 interacting proteins (PIPs) [26]. One of the major set-backs for the design of selective inhibitors for PPP1 lies in the similarity of the catalytic pocket between PPP1 and other serine/threonine phosphatases [27]. Even more challenging is to selective inhibit PPP1 isoforms activity, since the catalytic pocket of all PPP1 isoforms is identical. A promising approach for development of PPP1 selective inhibitors is targeting specific interfaces between PPP1 and PIPs. Around 90% of all PIPs present a PPP1 binding motif, the RVxF [28]. In 1997, Egloff and colleagues, used a short peptide based on p53BP2, a PIP, to disrupt PPP1/PPP1R2 interaction *in vitro* [28] and more recently Chatterjee and colleagues proved that a peptide based on NIPP1 RVxF can, *in vivo,* release PPP1 from PPP1R2 (among other interactors) and restore PPP1 activity. This resulted in enhanced histone H3 dephosphorylation that leaded to loss of centromeric dynamic [27].

Targeting intracellular protein-protein interactions is dependent on delivering protein-protein interactions disruptor drugs to the intracellular environment. Cell penetrating peptides (CPPs) can be employed to carry various cargo molecules across the highly impermeable cellular lipid bilayer. CPPs are short peptides sequences (typically less than 40 aminoacids) that are rapidly translocated into mammalian cells [15]. In 2015, Jones and colleagues proved that CPPs enter mammalian spermatozoa at different rates depending on the CPP [16]. Coupling CPPs with a biological active peptide originates a bioportide [29,30]. With the purpose of disrupting the interaction between PPP1CC2 and PPP1R2 in human sperm, we designed a disruptive bioportide that mimics the PPP1R2 RVxF and the flanking 7 aminoacids coupled with a CPP (C105Y). The C105Y peptide was used in this study, since it has an enhanced and quick translation efficacy into bovine sperm [16]. Two bioportides were synthesized: the BP-PPP1R2 RVxF which is expected to be biological active and the BP-PPP1R2 RVxF SC which should be biological inactive (scrambled RVxF) (Table B1.1)

In vitro studies proved that BP-PPP1R2 RVxF disrupted PPP1CC2/PPP1R2 interaction restoring PPP1CC2 activity (Figure B1.1). Also, the fact that half the amount of BP-PPP1R2 RVxF released PPP1CC2 from PPP1R2 inhibition suggests that the peptide can have a high affinity towards PPP1CC2 RVxF pocket. These results indicate that of BP-PPP1R2 RVxF competitively binds to PPP1, displacing PPP1R2 and thereby increasing PPP1CC2 enzymatic activity. Surprisingly, the BP-PPP1R2 RVxF SC also restored PPP1CC2 activity, upon incubation with PPP1CC2/PPP1R2 (Figure B1.1). BP-PPP1R2 RVxF SC was designed by scrabbling the RVxF motif (QWKKS instead of KSQKW) with the goal of not interfering with PPP1CC2/PPP1R2 interaction and keep the peptide chemical features

(Table B1.1). Computationally studies revealed that the peptide sequence alterations that characterizes the BP-PPP1R2 RVxF SC may resulted in higher stability and affinity of the bioportide towards the PPP1 RVxF pocket and consequently explain the observed biological effect of BP-PPP1R2 RVxF SC (Figure B1.4 and Table B1.4). Nevertheless, docking studies of PPP1/bioportides are pivotal to understand these preliminary results as well to determine optimal peptide sequence to achieve higher affinity towards the PPP1 RVxF pocket, translocation across the plasma membrane and stability within sperm cells.

Translocation and intracellular accumulation of BP-PPP1R2 RVxF and BP-PPP1R2 RVxF SC were verified by qualitative and quantitative fluorescence detection. Subcellular localization of the bioportides was similar in bovine (Figure B1.2 A) and human (Figure B1.2 B) sperm and not attributed to surface-associated bioportides. Bioportides accumulated preferentially at the midpiece and posterior head, analogous to previously described for C105Y [16] (Figure B1.2. A and B). BP-PPP1R2 RVxF presented a higher sperm intracellular accumulation (either bovine or human) when compared with BP-PPP1R2 RVxF SC (Figure B1.2 C). This may result from different rates of translocation, intracellular stability and/or metabolic cleavage of the bioportides in sperm, as described in other studies [31,32]. Further studies using a range of CPPs concentration must be performed in order determine the external concentrations necessary to achieve a similar intracellular uptake and accumulation.

The effect of the bioportides on bovine sperm motility was evaluated. Both BP-PPP1R2 RVxF and BP-PPP1R2 RVxF SC induced significant alterations in motility parameters without altering cell viability. We demonstrated that the BP-PPP1R2 RVxF decreased significantly the percentage of fast motile sperm and increased significantly the percentage of immotile sperm (Figure B1.3). Our *in vitro* studies, support the idea that BP-PPP1R2 RVxF, which mimics the PPP1R2 RVxF, competed with PPP1R2 for PPP1CC2 and prevented PPP1CC2/PPP1R2 interaction (Figure B1.1). Since it is not expected that the CPP interferes with PPP1CC2 catalytic center, in contrary to PPP1R2, PPP1CC2 becomes active and capable of dephosphorylate key proteins involved in sperm motility (Figure B1.5).

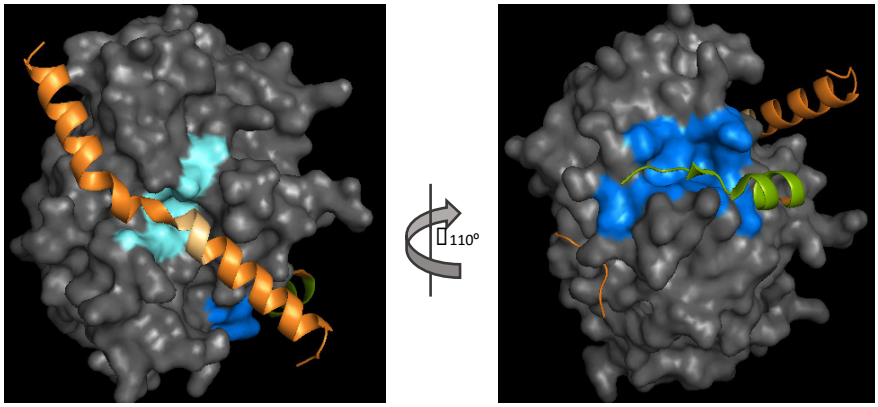

Figure B1.5. Schematic representation of the structure of PPP1CC complexed with PPP1R2. PPP1R2 interacts with PPP1CC in three regions (orange). The PPP1R2 sequence used in the BP-PPP1R2 RVxF is represented as part of PPP1R2 (green). Unlike PPP1R2, the bioportide BP-PPP1R2 RVxF is expected to only cover the PPP1 RVxF pocket and not interfere with PPP1 catalytic center (light blue). Please note that PPP1R2 presents a second RVxF motif (wheat) that sites on top of the catalytic center. Light blue: PPP1 catalytic center; Dark blue: PPP1 RVxF pocket; Orange: PPP1R2; Wheat: second PPP1 RVxF; Green: PPP1R2 RVxF and flanking aminoacids used on the bioportide BP-PPP1R2 RVxF.

Consequently, sperm becomes immotile. Similarly to our work, earlier studies targeted PPP1 interactions successfully. Salubrinal, a small molecule that blocks PPP1/GADD34 interaction prevents eIF2α dephosphorylation by PPP1 [33]. Trichostatin A disrupts the interactions between PPP1 and HDAC6 in glioblastoma and prostate cancer cells [34]. Nevertheless, since RVxF mediated PPP1 interactions are common to most PIPs, the bioportides used in this study may be interfering with most PPP1 sperm interactions. Further studies are required to determine the impact of BP-PPP1R2 RVxF and BP-PPP1R2 RVxF SC in human sperm motility, in PPP1CC2 sperm interactome and phosphorylation levels of sperm proteins. Moreover, identify specific PPP1CC2 interactors that are expressed uniquely in testis/sperm would be perfect for pharmacologic intervention and overcome the issue of ubiquitous expressed PPP1 regulators, such as PPP1R2. In 2017, Silva et al proved that disruption of PPP1CC2/AKAP4 interface may be a potential sperm specific pharmacological target [35].

Although in somatic cells the role of PPP1/PPP1R2 complex is well explored, in sperm cells, the role of PPP1/PPP1R2 complex is still unclear. Yet, it has been suggested that the PPP1/PPP1R2 is essential for regulation of sperm motility [10]. PPP1CC2 activity is inversely associated to human sperm motility in human epididymis [5]. In human sperm, it is hypothesized that in caput epididymis PPP1CC2 is active due to PPP1R2 inability to interact with PPP1CC2. This results from GSK3 phosphorylation on threonine 73 of PPP1R2 rendering it unable to interact with PPP1CC2 [36]. Throughout epididymis transit, GSK3 activity decreases, resulting in decreased PPP1R2 phosphorylation. Consequently, PPP1R2 blocks the catalytic center of PPP1CC2 rendering it inactive and leading to sperm motility [5,12]. PPP1CC2 inhibition is required for sperm motility and PPP1R2

is necessary for PPP1CC2 activity inhibition, it is reasonable to assume that loss of PPP1CC2/PPP1R2 interaction due to the competitive bioportide is associated with immotile sperm. Further studies are needed to determine the alterations of PPP1 activity in human sperm upon exposure to competitive BP-PPP1R2 RVxF. Additionally, competitive assays will be used to conclusively determine that the effect of the BP-PPP1R2 RVxF is due to PPP1CC2/PPP1R2 interaction interference.

Although we observe a decreased sperm motility upon exposure to disruptive peptide, motility is not completely abolished (around 18% of sperm still present a fast-progressive motility) (Figure B1.3). To completely abolish sperm motility, we believe that instead of targeting one PPP1CC2/PPP1R2 interface, a multi interface targeting approach must be undertaken. This will increase the percentage of immotile human sperm and decrease the amount of peptide necessary to achieve complete immotile sperm. In conclusion, we significantly reduced sperm motility by using disruptive bioportides that target PPP1/PIPs interaction interface instead of interfering with PPP1 itself.

B1.6. References

[1] Kogan P, Wald M. Male contraception: history and development. Urol Clin North Am 2014; 41:145–61.

[2] Chao J, Page ST, Anderson RA. Male contraception. Best Pract Res Clin Obstet Gynaecol 2014; 28:845–57.

[3] Nya-Ngatchou J-J, Amory JK. New approaches to male non-hormonal contraception. Contraception 2013; 87:296–9.

[4] Fardilha M, Esteves SLC, Korrodi-Gregório L, Pelech S, da Cruz E Silva OAB, da Cruz E Silva E. Protein phosphatase 1 complexes modulate sperm motility and present novel targets for male infertility. Mol Hum Reprod 2011; 17:466–77.

[5] Smith GD, Wolf DP, Trautman KC, da Cruz e Silva EF, Greengard P, Vijayaraghavan S. Primate sperm contain protein phosphatase 1, a biochemical mediator of motility. Biol Reprod 1996; 54:719–27.

[6] Vijayaraghavan S, Stephens DT, Trautman K, Smith GD, Khatra B, da Cruz e Silva EF, et al. Sperm motility development in the epididymis is associated with decreased glycogen synthase kinase-3 and protein phosphatase 1 activity. Biol Reprod 1996; 54:709–18.

[7] Fardilha M, Esteves SLCC, Korrodi-Gregório L, Vintém AP, Domingues SC, Rebelo S, et al. Identification of the human testis protein phosphatase 1 interactome. Biochem Pharmacol 2011; 82:1403–1415.

[8] Fardilha M, Ferreira M, Pelech S, Vieira S, Rebelo S, Korrodi-Gregorio L, et al. 'Omics' of human sperm: profiling protein phosphatases. OMICS 2013; 17:460–72.

[9] Smith GD, Wolf DP, Trautman KC, Vijayaraghavan S. Motility potential of macaque epididymal sperm: the role of protein phosphatase and glycogen synthase kinase-3 activities. J Androl n.d.; 20:47–53.

[10] Korrodi-Gregório L, Ferreira M, Vintém AP, Wu W, Muller T, Marcus K, et al. Identification and characterization of two distinct PPP1R2 isoforms in human spermatozoa. BMC Cell Biol 2013; 14:15.

[11] Vijayaraghavan S, Mohan J, Gray H, Khatra B, Carr DW. A role for phosphorylation of glycogen synthase kinase-3alpha in bovine sperm motility regulation. Biol Reprod 2000; 62:1647–54.

[12] Hurley TD, Yang J, Zhang L, Goodwin KD, Zou Q, Cortese M, et al. Structural basis for regulation of protein phosphatase 1 by inhibitor-2. J Biol Chem 2007; 282:28874–83.

[13] Wakula P, Beullens M, Ceulemans H, Stalmans W, Bollen M. Degeneracy and function of the ubiquitous RVXF motif that mediates binding to protein phosphatase-1. J Biol Chem 2003; 278:18817–23.

[14] Yang J, Hurley TD, DePaoli-Roach AA. Interaction of inhibitor-2 with the catalytic subunit of type 1 protein phosphatase. Identification of a sequence analogous to the consensus type 1 protein phosphatase-binding motif. J Biol Chem 2000; 275:22635–44.

[15] Guidotti G, Brambilla L, Rossi D. Cell-Penetrating Peptides: From Basic Research to Clinics. Trends Pharmacol Sci 2017; 38:406–424.

[16] Jones S, Lukanowska M, Suhorutsenko J, Oxenham S, Barratt C, Publicover S, et al. Intracellular translocation and differential accumulation of cell-penetrating peptides in

bovine spermatozoa: evaluation of efficient delivery vectors that do not compromise human sperm motility. Hum Reprod 2013; 28:1874–89.

[17] Palasek SA, Cox ZJ, Collins JM. Limiting racemization and aspartimide formation in microwave-enhanced Fmoc solid phase peptide synthesis. J Pept Sci 2007; 13:143–8.

[18] Organization WH. Examination and processing of human semen. vol. Fifth Edit. 2010.

[19] Holm T, Johansson H, Lundberg P, Pooga M, Lindgren M, Langel U. Studying the uptake of cell-penetrating peptides. Nat Protoc 2006; 1:1001–5.

[20] Maier JA, Martinez C, Kasavajhala K, Wickstrom L, Hauser KE, Simmerling C. ff14SB: Improving the Accuracy of Protein Side Chain and Backbone Parameters from ff99SB. J Chem Theory Comput 2015; 11:3696–713.

[21] Jorgensen WL, Chandrasekhar J, Madura JD, Impey RW, Klein ML. Comparison of simple potential functions for simulating liquid water. J Chem Phys 1983; 79:926–935.

[22] Schrödinger. LLC. New York 2014.

[23] Hess B, Kutzner C, van der Spoel D, Lindahl E. GROMACS 4: Algorithms for Highly Efficient, Load-Balanced, and Scalable Molecular Simulation. J Chem Theory Comput 2008; 4:435–47.

[24] Beard H, Cholleti A, Pearlman D, Sherman W, Loving KA. Applying physics-based scoring to calculate free energies of binding for single amino acid mutations in protein-protein complexes. PLoS One 2013; 8:e82849.

[25] Berman HM, Battistuz T, Bhat TN, Bluhm WF, Bourne PE, Burkhardt K, et al. The Protein Data Bank. Acta Crystallogr D Biol Crystallogr 2002; 58:899–907.

[26] Bollen M, Peti W, Ragusa MJ, Beullens M. The extended PP1 toolkit: designed to create specificity. Trends Biochem Sci 2010; 35:450–8.

[27] Chatterjee J, Beullens M, Sukackaite R, Qian J, Lesage B, Hart DJ, et al. Development of a peptide that selectively activates protein phosphatase-1 in living cells. Angew Chem Int Ed Engl 2012; 51:10054–9.

[28] Egloff MP, Johnson DF, Moorhead G, Cohen PT, Cohen P, Barford D. Structural basis for the recognition of regulatory subunits by the catalytic subunit of protein phosphatase 1. EMBO J 1997; 16:1876–87.

[29] Howl J, Matou-Nasri S, West DC, Farquhar M, Slaninová J, Ostenson C-G, et al. Bioportide: an emergent concept of bioactive cell-penetrating peptides. Cell Mol Life Sci 2012; 69:2951–66.

[30] Howl J, Jones S. Proteomimetic Cell Penetrating Peptides. Int J Pept Res Ther 2008; 14:359.

[31] Foerg C, Weller KM, Rechsteiner H, Nielsen HM, Fernández-Carneado J, Brunisholz R, et al. Metabolic cleavage and translocation efficiency of selected cell penetrating peptides: a comparative study with epithelial cell cultures. AAPS J 2008; 10:349–59.

[32] Palm C, Jayamanne M, Kjellander M, Hällbrink M. Peptide degradation is a critical determinant for cell-penetrating peptide uptake. Biochim Biophys Acta 2007; 1768:1769–76.

[33] Boyce M, Bryant KF, Jousse C, Long K, Harding HP, Scheuner D, et al. A selective inhibitor of eIF2alpha dephosphorylation protects cells from ER stress. Science 2005; 307:935–9.

[34] Chen C-S, Weng S-C, Tseng P-H, Lin H-P, Chen C-S. Histone acetylation-independent effect of histone deacetylase inhibitors on Akt through the reshuffling of protein phosphatase 1 complexes. J Biol Chem 2005; 280:38879–87.

[35] Silva JV, Yoon S, De Bock P-J, Goltsev A V, Gevaert K, Mendes JFF, et al. Construction and analysis of a human testis/sperm-enriched interaction network: Unraveling the PPP1CC2 interactome. Biochim Biophys Acta 2017; 1861:375–385.

[36] Hemmings BA, Resink TJ, Cohen P. Reconstitution of a Mg-ATP-dependent protein phosphatase and its activation through a phosphorylation mechanism. FEBS Lett 1982; 150:319–24.

B1.7. Supplementary Material

B1.7.1. Tables

Supplementary Table B1.1. Descriptive and statistical measures of the effect of bioportide in PPP1 activity. Mean and standard deviation (SD) associated with BP-PPP1R2 RVxF and BP-PPP1R2 RVxF SC peptides in PPP1 activity.

Condition		0min	5min	10min	15min	20min	25min	30min
PPP1CC2	Mean	0.058	0.093	0.127	0.189	0.252	0.298	0.348
	Std. Deviation	0.069	0.076	0.107	0.148	0.186	0.194	0.209
PPP1R2 and PPP1CC2 (1:200)	Mean	0.074	0.111	0.079	0.087	0.118	0.155	0.184
	Std. Deviation	0.064	0.111	0.069	0.023	0.030	0.040	0.051
PPP1R2 and PPP1CC2 and BP-PPP1R2 RVxF (1:200:0.5)	Mean	0.072	0.131	0.130	0.188	0.256	0.328	0.392
	Std. Deviation	0.053	0.068	0.072	0.071	0.077	0.085	0.093
PPP1R2 and PPP1CC2 and BP-PPP1R2 RVxF SC (1:200:0.5)	Mean	0.074	0.116	0.113	0.166	0.222	0.284	0.342
	Std. Deviation	0.048	0.063	0.056	0.063	0.071	0.076	0.081

Supplementary Table B1.2. Inferential statistics of the effect of bioportide in PPP1 activity. Mann-Whitney U test (grouping variable: condition; exact sig. (2-tailed)) was performed to evaluate the diference between means of two idependet grupos associated with BP-PPP1R2 RVxF and BP-PPP1R2 RVxF SC peptides in PPP1 activity

0m	PPP1R2 and PPP1CC2 (1:200)	PPP1R2 and PPP1CC2 and BP-PPP1R2 RVxF (1:200:0.5)	PPP1R2 and PPP1CC2 and BP-PPP1R2 RVxF SC (1:200:0.5)
PPP1CC2	0.384	0,772	0.554
PPP1R2 and PPP1CC2 (1:200)	-	0.456	0.101
PPP1R2 and PPP1CC2 and BP-PPP1R2 RVxF (1:200:0.5)	-	-	0.765
5m	PPP1R2 and PPP1CC2 (1:200)	PPP1R2 and PPP1CC2 and BP-PPP1R2 RVxF (1:200:0.5)	PPP1R2 and PPP1CC2 and BP-PPP1R2 RVxF SC (1:200:0.5)
PPP1CC2	0.712	0.890	0.890
PPP1R2 and PPP1CC2 (1:200)	-	0.546	0.067
PPP1R2 and PPP1CC2 and BP-PPP1R2 RVxF (1:200:0.5)	-	-	0.109
10m	PPP1R2 and PPP1CC2 (1:200)	PPP1R2 and PPP1CC2 and BP-PPP1R2 RVxF (1:200:0.5)	PPP1R2 and PPP1CC2 and BP-PPP1R2 RVxF SC (1:200:0.5)
PPP1CC2	0.234	0.234	0.345
PPP1R2 and PPP1CC2 (1:200)	-	1.00	0.345
PPP1R2 and PPP1CC2 and BP-PPP1R2 RVxF (1:200:0.5)	-	-	0.091
15m	PPP1R2 and PPP1CC2 (1:200)	PPP1R2 and PPP1CC2 and BP-PPP1R2 RVxF (1:200:0.5)	PPP1R2 and PPP1CC2 and BP-PPP1R2 RVxF SC (1:200:0.5)

PPP1CC2	0.234	1.00	1.00
PPP1R2 and PPP1CC2 (1:200)	-	**0.029**	0.901
PPP1R2 and PPP1CC2 and BP-PPP1R2 RVxF (1:200:0.5)	-	-	0.234
20m	PPP1R2 and PPP1CC2 (1:200)	PPP1R2 and PPP1CC2 and BP-PPP1R2 RVxF (1:200:0.5)	PPP1R2 and PPP1CC2 and BP-PPP1R2 RVxF SC (1:200:0.5)
PPP1CC2	0.234	1.00	0.990
PPP1R2 and PPP1CC2 (1:200)	-	**0.029**	0.101
PPP1R2 and PPP1CC2 and BP-PPP1R2 RVxF (1:200:0.5)	-	-	0.191
25m	PPP1R2 and PPP1CC2 (1:200)	PPP1R2 and PPP1CC2 and BP-PPP1R2 RVxF (1:200:0.5)	PPP1R2 and PPP1CC2 and BP-PPP1R2 RVxF SC (1:200:0.5)
PPP1CC2	0.234	1.00	0.125
PPP1R2 and PPP1CC2 (1:200)	-	**0.029**	**0.029**
PPP1R2 and PPP1CC2 and BP-PPP1R2 RVxF (1:200:0.5)	-	-	0.121
30m	PPP1R2 and PPP1CC2 (1:200)	PPP1R2 and PPP1CC2 and BP-PPP1R2 RVxF (1:200:0.5)	PPP1R2 and PPP1CC2 and BP-PPP1R2 RVxF SC (1:200:0.5)
PPP1CC2	0.101	0.235	0.201
PPP1R2 and PPP1CC2 (1:200)	-	**0.029**	**0.029**
PPP1R2 and PPP1CC2 and BP-PPP1R2 RVxF (1:200:0.5)	-	-	0.901

Supplementary Table B1.3. Descriptive and statistical measures of the effect of bioportide in bovine sperm motility at 1 and 2 hours of incubation. Mean and standard deviation (SD) associated with BP-PPP1R2 RVxF and BP-PPP1R2 RVxF SC effect on bovine sperm motility

Time 1h					
Bioportide		% Progressive Mobility Fast	% Progressive Motility Slow	% Non-Progressive Motility	% Immotile
NC	Mean	40.23	7.28	17.70	33.64
	Std. Deviation	10.95	2.96	6.80	10.61
BP-PPP1R2 RVxF	Mean	25.57	6.84	18.66	48.94
	Std. Deviation	8.88	2.21	4.53	13.09
BP-PPP1R2 RVxF SC	Mean	18.76	5.42	18.30	58.19
	Std. Deviation	4.37	1.67	6.56	7.84
Time 2h					
Bioportide		% Progressive Mobility Fast	% Progressive Motility Slow	% Non-Progressive Motility	% Immotile
NC	Mean	36.33	7.48	19.74	36.64
	Std. Deviation	10.97	3.54	2.83	12.59
BP-PPP1R2 RVxF	Mean	19.04	5.13	18.97	54.58
	Std. Deviation	7.23	1.28	3.41	11.88

BP-PPP1R2 RVxF SC	Mean	18.31	6.13	18.58	56.98
	Std. Deviation	5.58	1.92	5.45	10.28

Supplementary Table B1.4. Inferential statistics of the effect of bioportides on bovine sperm motility at 1 and 2 hours of incubation. T-tests of equality of means (grouping variable: condition; exact sig. (2-tailed)) was performed to evaluate the diference between means of two independent groups associated with BP-PPP1R2 RVxF and BP-PPP1R2 RVxF SC peptides in bovine sperm motility. Bold: statistically significant values at p< 0.05

Condition	Variable	Sig (2-tailed)	% of sperm on variable is higer in
1h NC vs BP-PPP1R2 RVxF	Progressive Mobility Fast	**0.007**	NC
	Progressive Motility Slow	0.730	
	Non-Progressive Motility	0.730	
	Immotile	**0.015**	BP-PPP1R2 RVxF SC
2h NC vs BP-PPP1R2 RVxF	Progressive Mobility Fast	**0.001**	NC
	Progressive Motility Slow	0.080	
	Non-Progressive Motility	0.606	
	Immotile	**0.007**	BP-PPP1R2 RVxF SC

B1.7.2. Figures

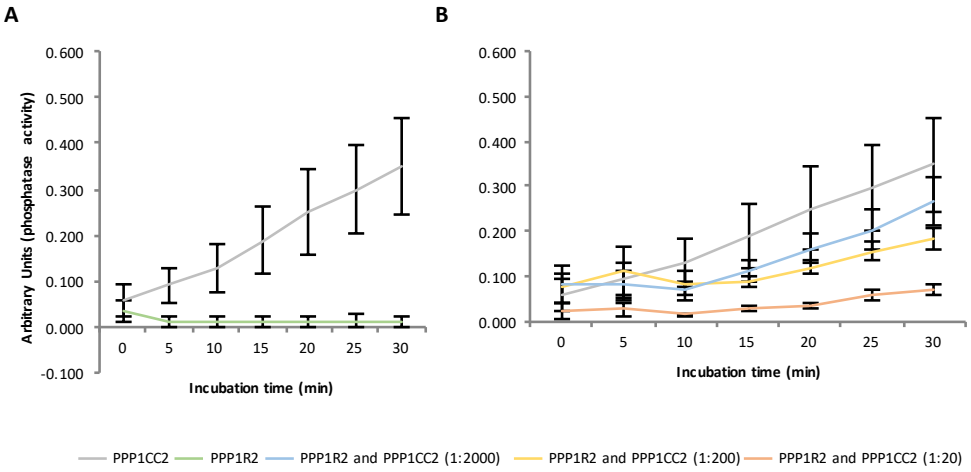

Supplementary Figure B1.1. Effect of PPP1R2 on PPP1 activity. To evaluate the effect of on PPP1 activity, PPP1CC2 was incubated with a range of PPP1R2 concentrations during 30min. **A**. PPP1CC2 and PPP1R2 phosphatase activity. **B**. PPP1CC2, PPP1R2/PPP1CC2 (1:20), PPP1R2/PPP1CC2 (1:200) and PPP1R2/PPP1CC2 (1:2000) phosphatase activity. Graph lines represent the mean values of 4 independent experiments. Error bars represent the SEM (standard error of the mean).

B1. Sperm motility modulation using a bioportide based on PPP1/PPP1R2 interaction interface

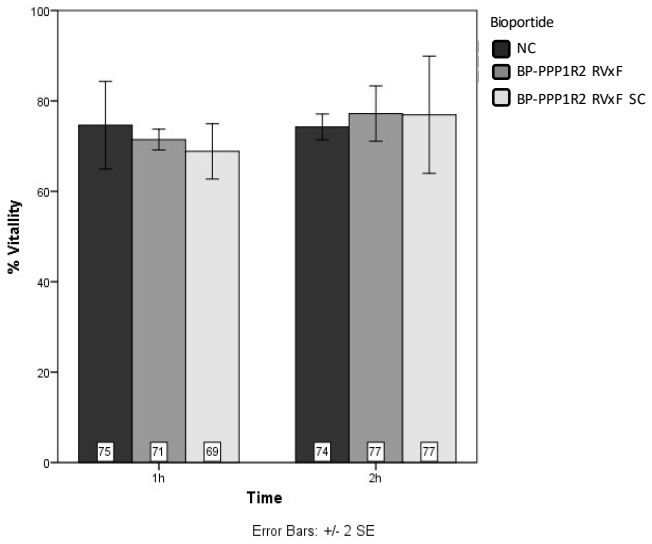

Supplementary Figure B1.2. Impact of bioportides on bovine spermatozoa viability. Graph bars represent the mean values of three independent experiments (at least 200 cells count per experiment). Error bars +/- 2 SE.

B2. Identification and characterization of GSK3 human testis and spermatozoa interactome

Maria João Freitas[1], Cameron Brothag[2], Joana Vieira Silva[3], Margarida Fardilha[3], Srinivasan Vijayaraghavan[2].

1. Signal Transduction Laboratory, Institute for Research in Biomedicine – iBiMED, Biology PhD Program, University of Aveiro, Aveiro, Portugal;

2. Kent State University, Kent, OH 44242, USA;

3. Signal Transduction Laboratory, Institute for Research in Biomedicine – iBiMED, Health Sciences Program, University of Aveiro, Aveiro, Portugal.

Acknowledgments

This work was financed by FEDER funds through the "Programa Operacional Competitividade e Internacionalização- COMPETE 2020" and by National Funds through the FCT- Fundação para a Ciência e Tecnologia (PTDB/BBB-BQB/3804/2014). We are thankful to Institute for Biomedicine – iBiMED (UID/BIM/04501/2013) for supporting this project. iBiMED is supported by the Portuguese Foundation for Science and Technology (FCT), Compete2020 and FEDER fund. Also, this worked was financed by the NIH grant R15 HD068971-01. This work was also supported by an individual grant from FCT of the Portuguese Ministry of Science and Higher Education to M.J.F. (SFRH/BD/84876/2012).

B2.1. Abstract

The signaling protein glycogen synthase kinase 3 (GSK3) exists in two isoforms, GSK3α and GSK3β. In male the male reproduction system, GSK3 is a prominent player on mammalian sperm motility signaling pathways. In mouse and bovine sperm, its activity is negatively correlated with motility. Moreover, it has been suggested an isoform-specific function of GSK3α, since GSK3α KO mice are infertile due to reduced sperm motility and metabolism, while GSK3β KO present no fertility alterations. With the goal of investigate the role of GSK3 in human sperm, we determine expression and activity levels of both GSK3 isoforms in asthenozoospermic and normozoospermic human samples in both human testis and sperm. We showed that sperm human sperm motility appears to be associated specifically with GSK3α expression and activity. Since this isoform-specific function may arise from GSK3α interactors that pay central roles in sperm motility, we unravel the GSK3 interactome in human testis and sperm. By constructing GSK3α-centered motility network, we showed 26 GSK3α direct interactors involved in sperm motility annotations, and from those one highly expressed in testis/sperm, the PRSS37 (probable inactive serine protease 37). Moreover, GSK3α and its interactors appears to be highly associated with protein expression processes revealing other possible functions for this protein, in both testis and sperm. Finally, given the reported relevance of GSK3 PPIs in sperm motility, we hypothesized that they stand as potential targets for

target for male contraceptive strategy based on sperm motility modulation.

B2.2. Introduction

Glycogen synthase kinase 3 (GSK3), a serine/threonine kinase, has been involved in a wide range of cellular processes such as apoptosis, mitosis, and proliferation [1,2]. Moreover, deregulation of GSK3 functions has been associated with pathological conditions such as cancer, Alzheimer's disease, and diabetes [3,4]. GSK3 is ubiquitously expressed and is encoded by two genes giving rise to two isoforms: GSK3α and GSK3β. Both isoforms differ in their N-termini with GSK3α having a unique glycine-rich N-terminus which is highly conserved in mammals, suggesting an isoform-specific function [5].

GSK3 plays a central role in the male reproductive system. In mouse testis, GSK3α is expressed in the seminiferous tubules and its expression increases during the onset of spermatogenesis, peaking in adult testis [6]. GSK3β expression is present in cells entering meiosis, spermatids and Sertoli cells [7]. Curiously, with target disruption of the gene for GSK3α, in testis spermatogenesis is normal, but mature sperm present a reduced motility and metabolism, rendering male mice infertile [6]. On the other hand, GSK3β testis-specific KO is fertile. In sperm, GSK3 activity is inversely proportional to motility; in immotile caput sperm, GSK3 activity is 6 times higher than that of motile caudal sperm. GSK3 activity is controlled by its phosphorylation state. When serine phosphorylated, GSK3 catalytic activity is low (GSK3α Ser9 and GSK3β Ser21) but when tyrosine phosphorylated, it is activated (GSK3α Tyr 279 and GSK3β Tyr 216) [8]. In bovine sperm, GSK3 is present in the posterior area of the head and along the entire flagellum [9,10]. In mouse sperm, GSK3 localizes to the peri-acrosomal area and tail [11].

Knowledge on GSK3 in human sperm is limited. The observation that mouse GSK3β cannot substitute for GSK3α, it implies that GSK3α is essential for normal sperm physiology. We considered that the unique role of GSK3α in sperm motility is reliant on its interactors. With that in mind, we performed a GSK3 characterization, by determining its activity levels in asthenozoospermic and normozoospermic human samples, subcellular location on human sperm, and identifying the GSK3α and GSK3β interactomes in both human testis and sperm.

B2.3. Methods

B2.3.1. Ethical approval

This study was approved by the Ethics and Internal Review Board of the Hospital Infante D. Pedro E.P.E. (Aveiro, Portugal) ((Process number: 36/AO) and was conducted in accordance with the ethical standards of the Helsinki Declaration. All donors signed an informed consent forms allowing the samples to be used for scientific purposes.

All procedures using mice used in the present study were performed at the Kent State University animal facility and were approved by the National Institute of Environmental Health Sciences institutional Animal Care and Use Committee (IACUC) and the Kent State Animal Ethics Committee under the IACUC protocol number 362DK 13-11. Immediately after CO_2 euthanization, testis and epididymis of 3-4-month-old wild type and Gsk3a$^{-/-}$ CD1 mice (*mus musculus*) were removed.

B2.3.2. Sperm extracts

Human ejaculate semen samples were obtained from healthy donors by masturbation into a sterile container. Basic semen analysis was performed by qualified technicians according to World Health Organization (WHO) guidelines [12]. After semen liquefaction, sperm cells were washed three times in phosphate buffered saline (PBS, Fisher Scientific, Loures, Portugal) and centrifugation at 600xG for 5min at 4°C. Mouse epididymis was punctured several times with a 26-G (45-mm) needle allowing the sperm to swim out (helped by squeezing with surgical scissors) into PBS1x. Sperm were also extruded from the *vas deferens* by squeezing it along its length. Afterwards, sperm concentration was determined by counting in a Neubauer hemocytometer (Fisher Scientific, Loures, Portugal). Finally, the sperm cells were washed three times in PBS1x followed by centrifugation at 600xG, 5 min, 4°C.

To obtain enriched human motile and immotile sperm fractions, sperm cells were separated according to their motility using the density gradient method (ORIGIO, Denmark) according to manufacturer instructions. Briefly, 1mL of 55% gradient medium was underlayed with 1mL of 80% gradient medium and pre-equilibrated at 5% CO_2 at 37ºC. 1mL of homogenized sperm was dispense on top of the gradient and centrifuged at 300xG, 20min. Then, the supernatant was removed (immotile fraction) and transferred to a clean tube. The pellet was resuspended in 5mL of pre-equilibrated sperm preparation medium (ORIGIO, Denmark), centrifuged at 300g, 10min and the supernatant was removed (the washing step was repeated once more). Sperm preparation medium

was added to the pellet then concentration and motility were assessed (motile fraction). The human albumin and sodium bicarbonate present in the sperm preparation medium are known inducers of sperm capacitation.

B2.3.3. Western blot of human and mouse sperm and testis

After washing, human sperm was lysed in either Tris buffer (20mM Tris-HCl, pH 7.4, 1mM EDTA, 1mM EGTA) (Fisher Scientific, Loures, Portugal); 1xRIPA (0.05M Tris-HCl, pH 7.4, 0.150M NaCl, 0.25% deoxycholic acid, 1% NP-40, 1mM EDTA) (Millipore Iberica, Madrid, Spain); 1xRIPA modified (0.05M Tris-HCl, pH 7.4, 0.150M NaCl, 0.25% deoxycholic acid, 2% NP-40, 1mM EDTA); or 1%SDS (Fisher Scientific, Loures, Portugal) during 30min on ice and centrifuged at 16,000xG, 15min, 4°C. The supernatant was recovered (soluble fraction). For mouse sperm, after washing, cells were normalized by sperm cell number and lysed in 1xRIPA and centrifuged at 16,000xG, 15min, 4°C. The supernatant was recovered (soluble fraction). Human testis protein extract was acquired from Takara, Enzifarma, Lisboa, Portugal (ref: 635309). Testis from wild-type mice were homogenized in 1xRIPA and centrifuged at 16,000xG, 15min, 4°C. The supernatants were recovered (soluble fraction).

Extracts were either mass normalized using BCA assay (ref: 23225, Pierce, Fisher Scientific, Loures, Portugal) or sperm cell number. After, sperm protein extracts were separated by SDS-PAGE and electrotransferred to a nitrocellulose membrane. Afterwards, the membrane was incubated with primary antibody. The following antibodies were used for western blot: mouse anti-GSK3α/β (Invitrogen, Fisher Scientific, Loures, Portugal, ref: 44-610, 1:2000, 4ºC, ON); rabbit anti-GSK3α (Cell Signaling Technology, Danvers, MA, USA, ref: #9338, 1:1000, 4ºC; ON); rabbit anti-GSK3β (Cell Signaling ref: #9315, 1:1000, 4ºC; ON); mouse anti-GSK3α pS21 (Santa Cruz Technologies, Heidelberg, Germany, ref: sc-365483, 1:1000, 4ºC, ON), mouse anti-GSK3β pS9 (Santa Cruz Technologies ref: sc-373800, 1:1000, 4ºC, ON), rabbit anti-LRP6 (Cell Signaling, ref: #2560, 1:1000) and rabbit anti-AKAP11 (Invitrogen, ref: PA5-39868, 1:1000). Finally, the membrane was incubated with the appropriate infrared secondary antibodies (1:5000, Li-Cor Biosciences UK Ltd, Cambridge, UK). The images were obtained using Odyssey Infrared Imaging Bands System (Li-Cor Biosciences UK Ltd, Cambridge, UK). Bands were quantified with the Quantity One 1-D Analysis Software (Bio-Rad, Amadora, Portugal). Phosphoserine GSK3 levels are calculated by determining the ratio between phosphoserine signal and total GSK3 signal. Data is expressed as mean ± SEM (standard error of the mean). Statistical analysis was conducted using IBM SPSS Statistics Software 22. A test

of normality (Shapiro- Wilk test) was performed to assess normality of samples and the Pearson correlation coefficient, r, was determined to assess the relationship between two variables. The significance level was set at $p<0.05$.

B2.3.4. Immunocytochemistry of human sperm

Washed sperm was spread onto a glass coverslip and dried at room temperature in a six well plate. Sperm cells were fixed in 4% formaldehyde (Fisher Scientific, Loures, Portugal) for 10 min. After, sperm was washed and permeabilized in 0.1% Tween (Fisher Scientific, Loures, Portugal) in 1% goat serum (Sigma-Aldrich Química, S.A., Sintra) and 5% BSA (NZYTech, Lisboa,Portugal) was added to the sperm and incubated for 20min. Blocking was performed with 1% goat serum and 5% BSA for 1h30min and then incubated with primary antibodies: rabbit anti-GSK3α (Cell Signaling ref: #9338, 1:50) and rabbit anti-GSK3β (Cell Signaling ref: #9315, 1:50) overnight at 4°C in a moisture environment; rabbit anti-LRP6 (Cell Signaling, ref: #2560, 1:50), rabbit anti-pLRP6 1490 (Cell Signaling, ref: #2568, 1:50) and rabbit anti-AKAP11 (Invitrogen, ref: PA5-39868, 1:100) for 1h20min in a moisture environment. The sperm cells were incubated with a fluorescently-labeled secondary antibody against rabbit (Alexa 594nm 1:800, Life Technologies S.A., Madrid, Spain) for 45min at room temperature. Coverslips were washed in PBSx1 + 0.1 Tween three times, followed by one wash step in PBS1x. Finally, Hoechst was added and coverslips were mounted with ProLong™ Gold Antifade Mountant (Invitrogen, ref: 10144). Negative controls (only secondary antibody) were processed in parallel. Fluorescence images were obtained using an Imager.Z1, Axio-Cam HRm camera and AxioVision software (Zeiss, Jena, Germany).

B2.3.5. Yeast two-hybrid screen of human testis

Homo Sapiens GSK3α cDNA (NM_019884.2) was subcloned using EcoRI and BamHI (New England Biolabs, Herts, UK) into pAS2-1, and *Homo Sapiens* GSK3β (NM_002093.3) was subcloned using NdeI and SalI (New England Biolabs, Herts, UK) into pAS2-1. Both vectors were sequenced to ensure that GSK3α and GSK3β were in frame with Gal-AD. The original vectors were a kind gift from Dr. Phiel. The pAS2-1-GSK3α and pAS2-1-GSK3β vectors were transformed into AH109 yeast strain by a standard lithium acetate method (Clontech, Takara, Enzifarma, Lisboa, Portugal). GSK3α and GSK3β are not cytotoxic to AH109 yeast cells. Expression of GSK3α and GSK3β was confirmed and both proteins did not activate *per se* the reporter genes (Supplementary Figure 1). For library

screening, the yeast strain AH109 transformed with either pAS2-1-GSK3α or pAS2-1-GSK3β was mated with yeast strain Y187 expressing human testis cDNA library in pGADT7-Rec (Mate&Plate Library – Human testis ref. 630470, Clontech, Takara, Enzifarma, Lisboa, Portugal) according to manufacture instructions. Half of the mating mixture was plated onto high-stringency medium (Quadruple dropout medium: SD/-Ade/-His/-Leu/-Trp) and the other half onto low-stringency medium (Triple dropout medium: SD/-His/-Leu/-Trp) and the plates were incubated at 30ºC. Colonies obtained in the low stringency plates were replica plated onto medium with X-α-Gal and incubated at 30ºC to check for MEL-1 expression (blue color colonies). Positive clones were numbered and kept in culture until identification.

B2.3.6. Identification of yeast two-hybrid positive clones

Yeast plasmid DNA (pGADT7-Rec) containing the cDNA of the positive clones was analyzed using the Matchmaker Insert Check PCR mix 2 (Clontech, Takara, Enzifarma, Lisboa, Portugal, ref:630497) and DNA sequence analysis was performed using a specific primer for pGADT7-Rec. The DNA sequences obtained were compared to the GeneBank database to identify the corresponding protein. Moreover, every DNA sequence was check if it was in frame with SV40-AD CDS.

B2.3.7. Yeast co-transformation

AH109 yeast cells transformed with either LRP6, AKAP11, PTMA or LRRC37A2 in pGADT7-Rec (recovered from the human cDNA testis library) or co-transformed with pAS2-1-GSK3α or pAS2-1-GSK3β and LRP6, AKAP11, PTMA or LRRC37A2 in pGADT7-Rec using a standard lithium acetate method (Clontech, Takara, Enzifarma, Lisboa, Portugal) to reconfirm the interaction. Co-transformation of pAS2-1 and pGADT7-Rec was used as a negative control and co-transformation of pAS2-1-p53 and pACT2-SV40 was used as positive control. The co-transformation were plated in either quadruple dropout medium or triple dropout medium.

B2.3.8. Co-immunoprecipitation of GSK3 interactors from human sperm

After washing, $50x10^6$ sperm cells were lysed in 1xRIPA (Millipore Iberica, Madrid, Spain) supplemented with 1mM of Phenylmethylsulfonyl fluoride (PMSF) (Fisher Scientific, Loures, Portugal) and 0.2mM of sodium orthovanadate (Na_3VO_4) (Fisher Scientific, Loures, Portugal) for 60min on ice and centrifuged at 16.000xG, 4°C, 15min. Sperm extracts were pre-cleared using

Dynabeads Protein G (ref: 10003D, Invitrogen, Fisher Scientific, Loures, Portugal) and incubated with either rabbit anti-GSK3α (Cell Signaling ref: #9338, 1:50), rabbit anti-GSK3β (Cell Signaling ref: #9315, 1:50) or rabbit anti-IgG (ref: sc-2027, Santa Cruz Biotechnology) at 4ºC ON with rotation. After incubation, 50µL of Dynabeads Protein G were added and incubated for 2h. After washing three times with PBS1x at 4°C, 10min with rotation. The beads were resuspended in 50mM glycine (Fisher Scientific, Loures, Portugal) for 5min. Finally, the supernatant was recovered and 1%SDS was added to the dynabeads, incubated 5min, boiled and recovered.

Alternatively, rabbit anti-GSK3α (Cell Signaling ref: #9338, 1:50) or rabbit anti-GSK3β (Cell Signaling ref: #9315, 1:50) were crosslinked using BS3 (bis(sulfosuccinimidyl)suberate) (Invitrogen, Fisher Scientific, Loures, Portugal ref: 21580) to Dynabeads Protein G, according to manufacturer instructions. After, sperm extracts were pre-cleared using Dynabeads Protein G, they were incubated with crosslinked beads for 1h. After washing the beads were resuspended in trypsin digestion buffer (20 mM Tris-HCl pH 8.0, 2 mM $CaCl_2$) and stored at -20ºC. One quarter of the Dynabeads were eluted in 1%SDS (for western blot).

For both protocols, western blot was performed using a mouse anti-GSK3α/β (Invitrogen, ref: 44-610, 1:2000), ON, 4ºC, with shaking and the corresponding secondary antibodies, 1h RT (1:5000, Li-Cor Biosciences UK Ltd, Cambridge, UK). The images were obtained using Odyssey Infrared Imaging System.

B2.3.9. Mass spectrometry

Mass spectrometry studies of GSK3 human sperm interactors were performed in two facilities.

The Lerner Research Institute's Proteomics and Metabolomics Laboratory: The LC-MS system was a Dionex Ultimate 3000 nano-flow HPLC interfacing with a Finnigan Orbitrap LTQ Elite hybrid ion trap mass spectrometer system. The HPLC system used an Acclaim PepMap 100 precolum (75 µm x 2 cm, C18, 3 µm, 100 A) followed by an Acclaim PepMap RSLC analytical column (75 µm x 15 cm, C18, 2 µm, 100 A). The data was analyzed by using all CID spectra collected in the experiment to search the human UniProtKB protein database with the search programs Sequest and Mascot. Only results with mascot score $p<0.05$ and at least two identifying peptides with mascot ion scores of at least 40 were considered. Specifically, GSK3α and GSK3β sequences searches were performed in Sequest program.

VIB Proteomics Core Facility: The LC-MS/MS system was Ultimate 3000 RSLCnano system (Thermo) in-line connected to a Q Exactive mass spectrometer (Thermo, Fisher Scientific, Loures, Portugal). Peptides were loaded on a reverse-phase column (made in-house, 75 µm I.D. x 20 mm, 3 µm beads C18 Reprosil-Pur, Dr. Maisch). Each sample was injected 3 times and analyzed in triplicate. Data analysis was performed with MaxQuant (version 1.5.6.5) [13] using the Andromeda search engine with default search settings including a false discovery rate set at 1% on both the peptide and protein level. Spectra were searched against the human proteins in the UniProt/Swiss-Prot database (database release version of January 2017 containing 20,172 human protein sequences). Only proteins with at least one unique or razor peptide were retained. Proteins were quantified by the MaxLFQ algorithm integrated in the MaxQuant software [14]. A minimum ratio count of two unique or razor peptides was required for quantification. Further data analysis was performed with the Perseus software (version 1.5.5.3) [15] after loading the protein groups file from MaxQuant. Proteins only identified by site, reverse database hits and contaminants were removed and technical replicate samples of GSK3α, GSK3β, and the negative control were grouped. Proteins with less than three valid values in at least one group were removed and missing values were imputed from a normal distribution around the detection limit. Then, t-tests were performed (FDR=0.0001 and S0=5) to compare samples of GSK3α and GSK3β with the negative control.

B2.3.10. *In silico* analysis of human GSK3α and GSK3β interactors: gene expression; phenotype; disease association and Gene Ontology.

To characterize human GSK3α and GSK3β interactors, either UniProtKB or FASTA sequence was retrieved for all interactors and used for subsequent *in silico* analysis (only *Homo sapiens* information was considered).

For presence of GSK3 consensus phosphorylation site (xxx[ST]xxx[ST]P) [16] in the identified interactors, the following bioinformatics tools were used: Eukaryotic Linear Motif (ELM) resource [17]; PhosphoSitePlus [18]; Kinase Net (http://www.kinasenet.ca); NetPhos 3.1 Server [19] ; ScanProsite [20] and GPS 3.0 [21]. Only data obtained with high threshold, high conservation scores and using the specific GSK3 phosphorylation site were used. Also, we only consider the presence of GSK3 phosphorylation site in the interactors if at least 3 of the tools supported this information. All tools were consulted in the April 2017.

To determine if any of the GSK3α and GSK3β interactions identified were new interactions, GSK3α and GSK3β interactomes were retrieved from IMEx-curated databases (DIP; DIP-IMEx; I2D-IMEx;

InnateDB-IMEx; MPIDB; MolCon; MatrixDB, MINT; MBinfo; Uniprot, IntAct; bhf-ucl) [22] and Human Integrated Protein-Protein Interaction rEference (HIPPIE) database [23] and compared with the identified GSK3 interactome. Only interactions for human GSK3α and GSK3β with human proteins were considered. The GSK3 interactome retrieved from the databases was used for further *in silico* analysis.

Gene expression patterns (mRNA) for all interactors (whether identified in this study or obtained from databases) were retrieved from: The Human Protein Atlas [24]; Pattern Gene Database (PaGenBase) [25] Expression atlas EMBL-EBI (68 FANTOM5 project-adult; 32 Uhlen´s Lab and GTEx) [26]; BioGPS [27] and UniGene [28]. Specifically, for the Human Protein Atlas and PaGenBase, since these databases have subsets list, only mRNA expression patterns of already classified as testis-enriched, testis-enhanced and group-enriched (that included testis) were retrieved. Also, only human gene expression patterns were considered. mRNA expression values for all databases (Transcripts per million or fragments per kilobase of exon model per million mapped reads) were retrieved and testis expression values were normalized by calculating the percentage of testis expression taking into account the expression of all tissues (Supplementary Table B2.1). Only interactors that presented more than 50% of expression in testis in at least 2 of the 5 databases used were considered highly expressed in testis. Furthermore, these interactors were classified in three categories: 50-75%, 75-90%, and >90%. Differently expressed proteins in asthenozoospermic samples were collected from peer reviewed papers and compared with GSK3 interactors [29–41].

Phenotypes associated with all interactors (genes) were retrieved form Mouse Genome Informatics (MGI) [42] and OMIM [43]. Manually curated genes associated with phenotypes of male infertility were retrieved from DisGeNet [44] and Phenopedia [45]. These genes were compared with GSK3 interactome. Also, the DISEASE database was consulted, specifically the experimental data of disease-gene associations [46]. Only phenotypes or diseases related with sperm, testis, epididymis and spermatogenesis defects; general defects of the male productive system; infertility (including litter size) and ciliary defects were included. Altered accessory glands; genetic disorders, sexual behavior and tumor incidence were excluded. Phenotypes were categorized into 10 groups: Male infertility; Morphological male reproductive system defects; Germ cell line abnormalities; Spermatogenesis abnormalities; Male hormonal abnormalities; Inflammation of male reproductive system components; Asthenozoospermia and flagellum, cilium and mitochondrial abnormalities; Oligozoospermia and Teratozoospermia (Suplementary Table 2). Also, GSK3α and GSK3β interactors annotated to testis and sperm physiology on GeneOntology enrichment tool (PANTHER

version 12.0, 25 August 2017) [47] were classified according to those annotations (Supplementary Table B2.2). All databases were consulted June, July, and August of 2017

To determine the enrichment of GSK3α and GSK3β testis and sperm interactors, the Gene Ontology enrichment analysis was performed (PANTHER version 12.0, 25 August 2017) [47]. All genes annotated from *Homo sapiens* were used as reference list and the GO complete lists as annotation data set. Only results with $p<0.05$ were considered. Analysis tool was used on August 2017

B2.3.11. Construction of GSK3 PPIs network

GSK3α and GSK3β protein-protein interaction networks were built using Cytoscape v 3.4 [48]. Also, the inner connections between those proteins were captured. In order to construct sperm motility and testis GSK3α and GSK3β PPI networks, GSK3α and GSK3β interactors associated with motility annotations and phenotypes and testis annotations and phenotypes were extracted from GSK3α and GSK3β interactome network.

B2.4. Results

B2.4.1. GSK3 is present in human testis and sperm and its activity is differently correlated with ejaculated and capacitated spermatozoa motility

First, we evaluated the expression and activation of both GSK3 isoforms in human testis and ejaculated and capacitated human sperm.

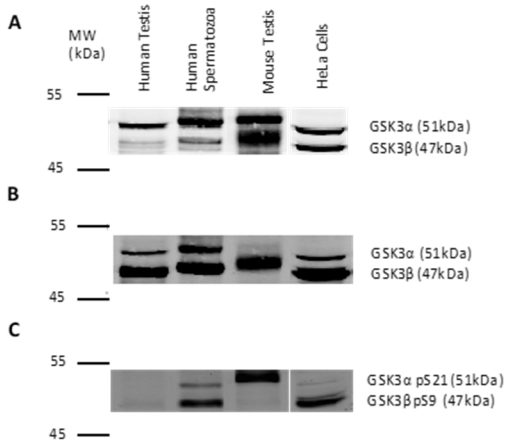

Figure B2.1. GSK3 in human testis and sperm. Western blot analysis of GSK3 isoforms in human testis and sperm, mouse testis and HeLa cells. Human sperm, mouse testis and HeLa cells were homogenized in 1xRIPA. 30µg of protein were loaded per sample. A. GSK3α and GSK3β were detected using an anti-GSK3α/β antibody (Invitrogen, ref: 44-610, 1:2000). B. GSK3α was immunodetected using an anti-GSK3α antibody (Cell Signaling ref: #9338, 1:1000) and GSK3β was immunodetected using an anti-GSK3β antibody (Cell Signaling ref: #9315, 1:1000). Blots were cropped.

In order to demonstrates that both GSK3α and GSK3β are expressed in human testis and sperm, these proteins were immunodetected in human testis and sperm, similar to what was previously described in mouse and bovine (n=1). Moreover, human sperm, different strength recovered different amounts of both GSK3 isoforms (Supplementary Figure B2.2). The levels of inhibited GSK3α and GSK3β (serine phosphorylation) were assessed in human testis and sperm. In human testis, it appears that no serine phosphorylated GSK3 was detected, while in human sperm both phosphorylated GSK3 isoforms were detected (Figure B2.1 C).

To assess if in human sperm GSK3 activity is correlated with sperm motility, serine phosphorylated GSK3α and GSK3β (low activity) were evaluated in ejaculated normospermic and asthenozoospermic samples. Total GSK3α and serine phosphorylated GSK3α levels were lower in asthenozoospermic samples compared to normospermic (Figure B2.2 A and B). Also, it appears that the higher the percentage of immotile sperm the lower are the levels of total GSK3α and

phosphorylated GSK3α (r= -0.910, p=0.012 and r= -0.872, p=0.023, respectively) (Figure B2.2 C and D and Supplementary Table B2.3). Therefore, these results suggest that in human sperm there is a strong negative correlation between the percentage of immotile sperm and the levels of total and phosphorylated (low activity) GSK3α. Regarding GSK3β, it seems that the expression of total and phosphorylated levels of GSK3β were similar in both normospermic and asthenozoospermic samples (Figure B2.2 A and B). It appears that there is no correlation between total GSK3β and sperm motility and between phosphorylated (low activity) GSK3β and the percentage of immotile sperm (Supplementary Table B2.3) (Figure B2.2 C and D).

The correlation between motility and levels of total GSK3 and serine phosphorylated GSK3 (low activity) in capacitated sperm was also assessed. Ejaculated sperm was subjected to density gradients in capacitating conditions, and enriched motile and immotile fractions were recovered. Contrary to the situation in ejaculated sperm, total and phosphorylated GSK3α slightly increased in immotile sperm compared to the motile sperm, and the higher the percentage of immotile sperm the higher the levels of total GSK3α (Figure B2.2 E, F and G). Similarly to GSK3α, there was also an increase in total and phosphorylated GSK3β in immotile compared to motile sperm. Here again, higher the percentage of immotile sperm higher were the levels of total and phosphorylated GSK3β (low activity) (r= 0.848, p=0.033) (Figure B2.2 H and Supplementary Table B2.3).

B2. Identification and characterization of GSK3 human testis and spermatozoa interactome

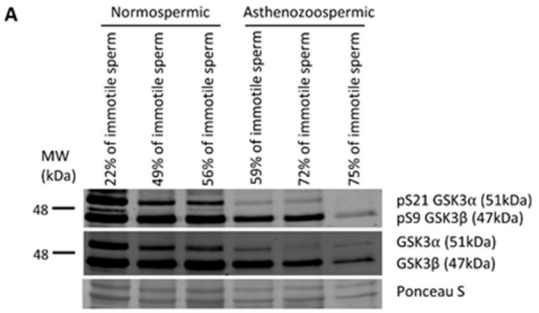

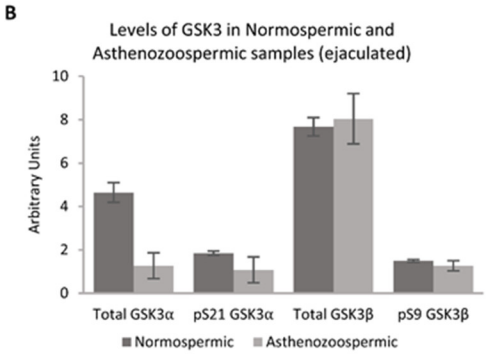

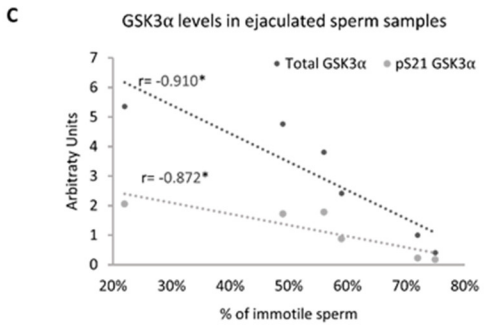

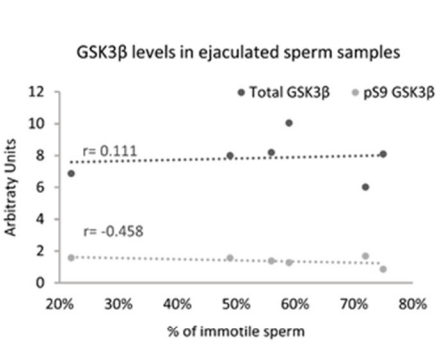

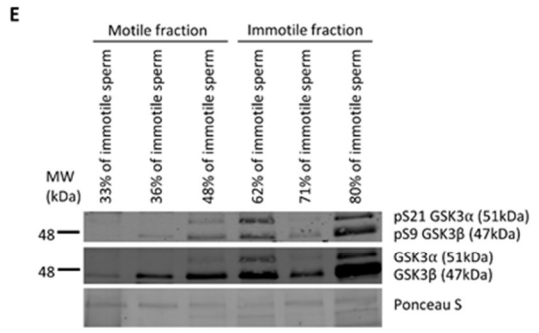

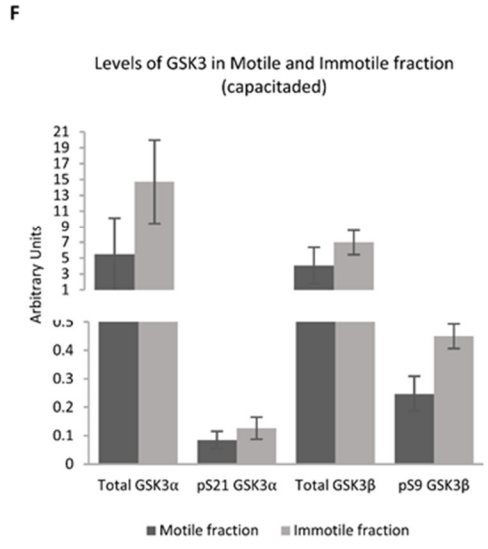

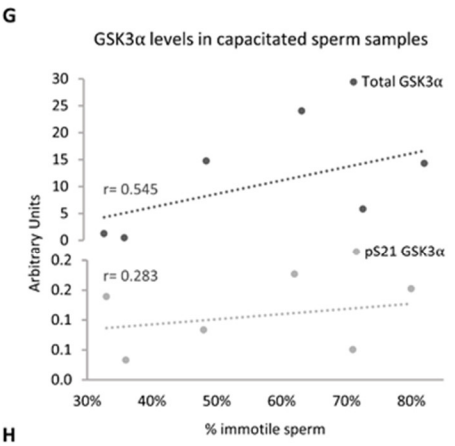

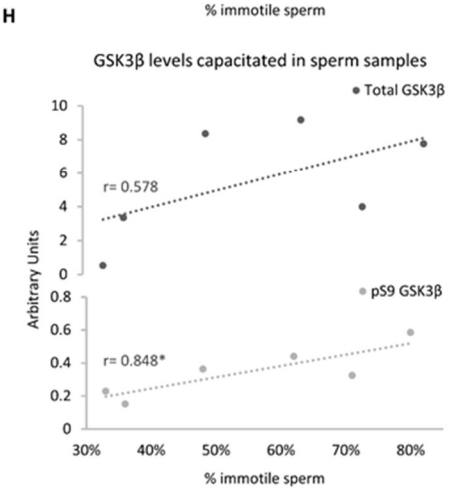

Figure B2.2. Total and serine phosphorylated GSK3 levels in human sperm (previous page). **A**. Immunoblot of total and serine phosphorylated GSK3 isoforms in human normo and asthenozoospermic ejaculated sperm. **B**. GSK3 isoforms protein levels in human normo and asthenozoospermic ejaculated sperm (n=3). **C**. Correlation between percentage of immotile ejaculated sperm and protein levels of total and serine phosphorylated GSK3α. **D**. Correlation between percentage of immotile ejaculated sperm and protein levels of total and serine phosphorylated GSK3β. **E**. Immunoblot of total and serine phosphorylated GSK3 isoforms in motile and immotile capacitated sperm. **F**. GSK3 isoforms protein levels in motile and immotile capacitated sperm (n=3). **G**. Correlation between percentage of immotile capacitated sperm and protein levels of total and serine phosphorylated GSK3α. **D**. Correlation between percentage of immotile capacitated sperm and protein levels of total and serine phosphorylated GSK3β. Phosphoserine GSK3 levels are calculated by determining the ratio between phosphoserine signal and total GSK3 signal. Error bars represent ±SEM. r= Pearson correlation. * Correlation is significant at the 0.05 level (2-tailed). Blots were cropped.

B2.4.2. GSK3α and GSK3β have distinct spermatozoa subcellular localizations

Given the importance of GSK3 in sperm motility and distinct expression patterns in normospermic and asthenozoospermic samples, the subcellular location of GSK3α and GSK3β in ejaculated human sperm was analyzed. Three normospermic human sperm samples were analyzed and around 300 cells were assessed (total). Figure B2.3 shows that GSK3α was primarily located in the flagellum (100%) and 75.7% of sperm cells also showed immunoreactivity in the head. Curiously, 24.2% of the spermatozoa showed a strong immunoreactivity for GSK3α in the equatorial region, particularly at the edges. In contrast, GSK3β was mainly located in the sperm head (100%), 23.9% of sperm showed GSK3β distributed throughout the entire head and flagellum and in 76.0% of sperm it was present only sperm head (Figure B2.3).

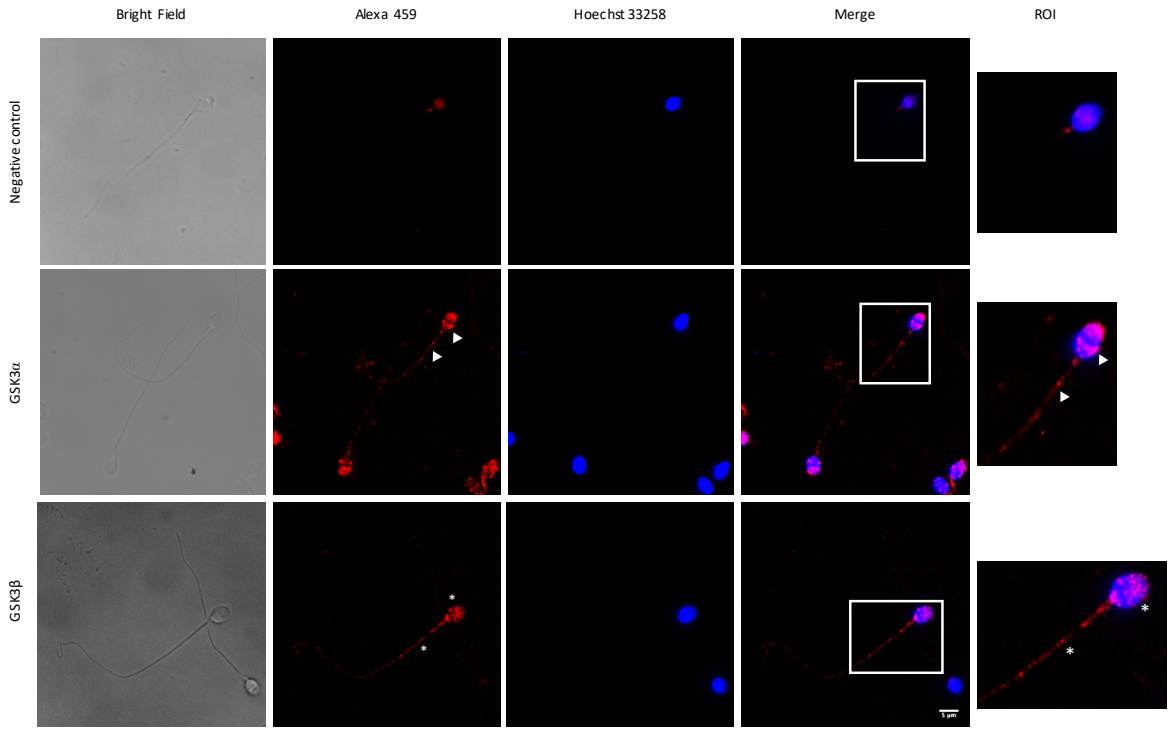

Figure B2.3. Subcelular localization of GSK3α and GSK3β in mature human sperm (previous page). GSK3α is located in the flagellum and head (arrowhead), more specifically in the equatorial region. GSK3β is located through the entire head (star) and occasionally in the flagellum. Scale bar is 5 μm. Nucleus is marked in blue. ROI: region of interest. All images were obtained with 63X magnification in a Imager.Z1, Axio-Cam HRm camera and AxioVision software (Zeiss, Jena, Germany).

B2.4.3. Thirty-five new interactors for GSK3α and fourteen new interactors for GSK3β were identified in human testis

To identify novel GSK3α and GSK3β interactors relevant for fertility, yeast two-hybrid screens were performed using a human testis library and full-length *Homo sapiens* GSK3α and GSK3β. For GSK3α, 93 positive clones were obtained from a total $2.64x10^7$ screened clones. For GSK3β, 54 positive clones were obtained from a total of $2.75x10^7$ screened clones. Nucleotide sequencing of the positive clones, revealed forty-six putative interactors for GSK3α and twenty-one for GSK3β (Table B2.1 and Table B2.2).

For GSK3α, 76% were new putative interactors while 24% were previously described as GSK3 interactors. From the latter, 45.5% were described as interacting with GSK3β in PPI databases (either exclusively or interaction for GSK3α was not tested) and 54.5% interacted with both GSK3 isoforms. Moreover, 58.7% of GSK3α interactors identified contained the GSK3 consensus phosphorylation site (xxx[ST]xxx[ST]P). Finally, 34.8% of GSK3α interactors were already described to be present in either testis and/or sperm of mammals (Table B2.1). For GSK3β, 77.8% were identified for the first time as GSK3β putative interactors, while 22.2% of the interactors were already described as GSK3 interactors in PPI databases, from which 50% interacted with GSK3β (either exclusively or interaction for GSK3α was not tested) and the other half interacted with both GSK3 isoforms. Moreover, around 38% of the GSK3β identified interactors had the GSK3 consensus phosphorylation site and 61.1% were previously reported to be present in testis and/or sperm of mammals (Table B2.2).

To validate the yeast two-hybrid approach and to confirm some of the interactions identified, yeast co-transformations were performed. GSK3α or GSK3β and AKAP11, LRC37A2, LRP6 and PTMA were co-transformed in yeast and plated on highly stringency medium. Also, AKAP11, LRRC37A2, LRP6 and PTMA were transformed in yeast to check for auto-activation of the reporter genes. Figure B2.4 shows that none of the interactors tested activated *per se* the transcription of the reporter genes.

Regarding the interaction between AKAP11 and LRP6 with GSK3, although it was only identified as a GSK3α interactor, they also interacted with GSK3β (Figure B2.4).

B2. Identification and characterization of GSK3 human testis and spermatozoa interactome

Table B2.1. GSK3α human testis interactors. Gene name, UniProtKB, nr of clones, GSK3 phosphorylation site, previously described GSK3 interactor, presence on mammal testis and sperm and alteration on asthenozoospermic samples of testis GSK3α interactors identified by yeast two-hybrid.

GSK3α human testis interactors							
Gene Name	**UniProtKB**	**Name**	**Nr of clones**	**GSK3 phosphorylation site**	**Previously known GSK3 interactor**	**Present in testis and/or sperm**	**Asthenozoospermic alteration**
AKAP11	Q9UKA4	A-kinase anchor protein 11	1	Yes	GSK3β [49–51]	Human testis and human sperm [52]	
ALKBH3	Q96Q83	Alpha-ketoglutarate-dependent dioxygenase alkB homolog 3	1				
AP3D1	O14617	AP-3 complex subunit delta-1	1	Yes			
AURKAIP1	Q9NWT8	Aurora kinase A-interacting protein	2	Yes			
AXIN2	Q9Y2T1	Axin-2	1	Yes	GSK3α and GSK3β [50,51,53,54]	Mouse testis [55]	
BCCIP	Q9P287	BRCA2 and CDKN1A-interacting protein	7	Yes			
C11orf98	E9PRG8	Uncharacterized protein C11orf98	1				
CCDC174	Q6PII3	Coiled-coil domain-containing protein 174	1	Yes			
CHTOP	Q9Y3Y2	Chromatin target of PRMT1 protein	1				
CNTROB	Q8N137	Centrobin	1	Yes		Mouse testis (spermatocyte and spermatids) [56]	
DCAF8	Q5TAQ9	DDB1- and CUL4-associated factor 8	1	Yes			
DCP1B	Q8IZD4	mRNA-decapping enzyme 1B	5	Yes			
DDI1	Q8WTU0	Protein DDI1 homolog 1	1	Yes			
DEAF1	O75398	Deformed epidermal autoregulatory factor 1 homolog	1	Yes	GSK3α and GSK3β [57]		
DNAJB1	P25685	DnaJ homolog subfamily B member 1	1			Human sperm (midpiece and principle piece) [58]	+ [36]

GSK3α human testis interactors							
Gene Name	**UniProtKB**	**Name**	**Nr of clones**	**GSK3 phosphorylation site**	**Previously known GSK3 interactor**	**Present in testis and/or sperm**	**Asthenozoospermic alteration**
DRC1	Q96MC2	Dynein regulatory complex protein 1	1	Yes			
FBXO42	Q6P3S6	F-box only protein 42	1	Yes			
GOLGA6C	A6NDK9	Golgin subfamily A member 6C	1				
H2AFV	Q71UI9	Histone H2A.V	1				
HMBS	P08397	Porphobilinogen deaminase	1				
HMGN1	P05114	Non-histone chromosomal protein HMG-14	1				
HNRNPM	P52272	Heterogeneous nuclear ribonucleoprotein M	1			Mouse testis [59] and human sperm (mRNA) [60]	
HSP90AA1	P07900	Heat shock protein HSP 90-alpha	12	Yes	GSK3α and GSK3β [51,61,62]	Yes, mouse testis (mRNA) [63] and human sperm [64]	+ [36]
HSP90AB1	P08238	Heat shock protein HSP 90-beta	4		GSK3α and GSK3β [51,61]	Rat testis (Sertoli cells) [65] and human sperm (equatorial region) note that does not distinct AA1 from AB1 [66]	+ [36]
LDHA	P00338	L-lactate dehydrogenase A chain	1			Human sperm (principal piece) [67]	- [36]
LRP6	O75581	Low-density lipoprotein receptor-related protein 6	1	Yes	GSK3α and GSK3β [68–70]	Human sperm (flagellum more intense in midpiece) [71]	
LRRC37A2	A6NM11	Leucine-rich repeat-containing protein 37A2	1	Yes			+[36]
MAEA	Q7L5Y9	Macrophage erythroblast attacher	1	Yes			
MTCH1	Q9NZJ7	Mitochondrial carrier homolog 1	1	Yes			
MYL12A	P19105	Myosin regulatory light chain 12A	1				
NBR1	Q14596	Next to BRCA1 gene 1 protein	1	Yes	GSK3α and GSK3β [57,72]	Human testis (mRNA) [73]	

B2. Identification and characterization of GSK3 human testis and spermatozoa interactome

GSK3α human testis interactors							
Gene Name	**UniProtKB**	**Name**	**Nr of clones**	**GSK3 phosphorylation site**	**Previously known GSK3 interactor**	**Present in testis and/or sperm**	**Asthenozoospermic alteration**
PSMD8	P48556	26S proteasome non-ATPase regulatory subunit 8	3			Boar sperm (acrosome) [74]	
PTMA	P06454	Prothymosin alpha	2			Rat testis (Leydig cells, panchytene spermatocyte and spermatids) [75], human sperm (acrosome) [76]	
RPL15	P61313	60S ribosomal protein L15	1				
RPL19	P84098	60S ribosomal protein L19	1		GSK3β [51]	Yes, human sperm [60]	
RPL29	P47914	60S ribosomal protein L29	1		GSK3β [51]	Mouse testis [77]	
RPS15	P62841	40S ribosomal protein S15	1				
RPS19	P39019	40S ribosomal protein S19	1		GSK3β [51]		
RUNX1	Q01196	Runt-related transcription factor 1	1	Yes			
SBNO1	A3KN83	Protein strawberry notch homolog 1	2	Yes			
SMARCA5	O60264	SWI/SNF-related matrix-associated actin-dependent regulator of chromatin subfamily A member 5	1	Yes	GSK3β [51]	Mouse testis [78]	
SMG7	Q92540	Protein SMG7	1	Yes		Mouse testis (spermatocytes and spermatids) [79]	
SUGP2	Q8IX01	SURP and G-patch domain-containing protein 2	1	Yes			
TTC16	Q8NEE8	Tetratricopeptide repeat protein 16	1	Yes			
UBTF	P17480	Nucleolar transcription factor 1	1	Yes			
VCPIP1	Q96JH7	Deubiquitinating protein VCIP135	1	Yes			
Homo Sapiens Chromosome 21 clone CTD-250 3J9 map p11-q21.1			1				

GSK3α human testis interactors							
Gene Name	**UniProtKB**	**Name**	**Nr of clones**	**GSK3 phosphorylation site**	**Previously known GSK3 interactor**	**Present in testis and/or sperm**	**Asthenozoospermic alteration**
Human Dna sequence from clone RP11-543N17			1				
RefSeqGene on chromosome 5 Chromosome 5: 150,401,911-150,402,122			2				

Table B2.2. GSK3β human testis interactors. Gene name, UniProtKB, nr of clones, GSK3 phosphorylation site, previously described GSK3 interactor, presence on mammal testis and sperm and alteration on asthenozoospermic samples of testis GSK3α interactors identified by yeast two-hybrid.

GSK3β human testis interactors							
Gene Name	**UniProtKB**	**Name**	**Nr of clones**	**GSK3 phosphorylation site**	**Previously known GSK3 interactor**	**Present in testis and/or sperm**	**Asthenozoospermic alteration**
AXIN2	Q9Y2T1	Axin-2	1	Yes	GSK3β [50,51,53,54]	Mouse testis [55,71] and mouse sperm (mRNA)	
BCCIP	Q9P287	BRCA2 and CDKN1A-interacting protein	1	Yes		Human testis [80]	
C10orf90	Q96M02	Centrosomal protein C10orf90	1	Yes			
C11orf98	E9PRG8	Uncharacterized protein C11orf98	1				
CASC4	Q6P4E1	Protein CASC4	1	Yes			
CMTM2	Q8TAZ6	CKLF-like MARVEL transmembrane domain-containing protein 2	1			Human testis and sperm (elongating spermatids, pachytene spermatocytes, posterior head of mature sperm) [81,82]	
DCP1B	Q8IZD4	mRNA-decapping enzyme 1B	2	Yes			

B2. Identification and characterization of GSK3 human testis and spermatozoa interactome

GSK3β human testis interactors							
Gene Name	**UniProtKB**	**Name**	**Nr of clones**	**GSK3 phosphorylation site**	**Previously known GSK3 interactor**	**Present in testis and/or sperm**	**Asthenozoospermic alteration**
HNRNPM	P52272	Heterogeneous nuclear ribonucleoprotein M	2			Mouse testis [59] and human sperm [60]	
HSP90AA1	P07900	Heat shock protein HSP 90-alpha	2		GSK3α and GSK3β [51,62]	Mouse testis (mRNA) [63] and human sperm [64]	+[36]
HSP90AB1	P08238	Heat shock protein HSP 90-beta	1		GSK3α and GSK3β [51]	Rat testis (Sertoli cells) [65] and human sperm [83]	+ [36]
LYAR	Q9NX58	Cell growth-regulating nucleolar protein	1			Mouse testis [84]	
MYL6	P60660	Myosin light polypeptide 6	2			Mouse sperm (manchete of elongating spermatids) [85]	+ [36]
PRKRIP1	Q9H875	PRKR-interacting protein 1	2				
PSMD8	P48556	26S proteasome non-ATPase regulatory subunit 8	2			Boar sperm (acrosome) [74]	
RPS15	P62841	40S ribosomal protein S15	2				
SMG7	Q92540	Protein SMG7	1	Yes		Mouse testis (spermatocytes and spermatids) [79]	
TEKT5	Q96M29	Tektin-5	1	Yes		Mouse sperm (flagellum, more intense in midpiece) [86]	- [29,36]
YBX1	P67809	Nuclease-sensitive element-binding protein 1	1		GSK3β [87]		
Human DNA sequence from clone RP11-543N17 on chromosome 10, complete sequence			1				

Table B2.3. GSK3α human sperm interactors. Gene name, UniProtKB, mass spectrometry score, GSK3 phosphorylation site, previously described GSK3 interactor, presence on mammal testis and sperm and alteration on asthenozoospermic samples of testis GSK3α interactors identified by yeast two-hybrid.

GSK3α human spermatozoa interactors								
Gene Name	**UniProtKB**	**Name**	**Spectral Count ratio*†**	**Log of GSK3α/NC ratio±†**	**GSK3 phosphorylation site**	**Previously known GSK3 interactor**	**Present in testis and/or sperm**	**Asthenozoospermic alteration**
ARG1	P05089	Arginase-1	GSK3α only		Yes		Human sperm (activity) [88]	
GGCT	O75223	Gamma-glutamylcyclotransferase	GSK3α only		Yes		Human testis (Sertoli and Leydig cells) and epididymis [89]	
HIST1H2AD	P20671	Histone H2A type 1-D	3					+ [36]
TLR9	Q9NR96	Toll-like receptor 9	GSK3α only				Mouse sperm (acrosome) [90], human testis and sperm(mRNA) [91,92]	
SBSN	Q6UWP8	Suprabasin	GSK3α only					
HIST1H4A	P62805	Histone H4	3				Mouse testis (spermatocyte) [93] human sperm [93]	
HIST1H2BK	A0A024RCL8	Histone H2B	GSK3α only				Human testis (mRNA) and sperm [94]	
HSPA5	P11021	78 kDa glucose-regulated protein	GSK3α only		Yes	GSK3β [51]		+ and – [31,36]
ACR	P10323	Acrosin		8.0		GSK3β [51]	Human testis [95] and sperm (acrosome) [96,97]	-[36]
CPZ	Q66K79	Carboxypeptidase Z		4.8				
EEF1G	P26641	Elongation factor 1-gamma		4.3		GSK3β [51]	Human sperm [98]	-[36]
LTF	P02788	Lactotransferrin		6.7			Human sperm (acrosome) [99]	-[36]

B2. Identification and characterization of GSK3 human testis and spermatozoa interactome

GSK3α human spermatozoa interactors								
Gene Name	**UniProtKB**	**Name**	**Spectral Count ratio*†**	**Log of GSK3α/NC ratio±†**	**GSK3 phosphorylation site**	**Previously known GSK3 interactor**	**Present in testis and/or sperm**	**Asthenozoospermic alteration**
PRSS37	A4D1T9	Probable inactive serine protease 37		4.8				
RPL13	P26373	60S ribosomal protein L13		6.9				
RPL6	Q02878	60S ribosomal protein L6		4.8				
RPS18	P62269	40S ribosomal protein S18		8.1			Human sperm [29]	
RPS8	P62241	40S ribosomal protein S8		4.4			Human testis [95] and sperm (acrosome) [96,97]	

Table B2.4. GSK3β human sperm interactors. Gene name, UniProtKB, mass spectrometry score, GSK3 phosphorylation site, previously described GSK3 interactor, presence on mammal testis and sperm and alteration on asthenozoospermic samples of testis GSK3α interactors identified by yeast two-hybrid.

GSK3β human spermatozoa interactors								
Gene Name	**UniProtKB**	**Name**	**Spectral counts ratio***	**Log of GSK3β/NC ratio±†**	**GSK3 phosphorylation site**	**Previously known GSK3 interactor**	**Present in testis and/or sperm**	**Asthenozoospermic alteration**
ANXA1	P04083	Annexin A1	GSK3β only					
ARG1	P05089	Arginase-1	GSK3β only		Yes		Human sperm [88] (activity)	
BPIFB1	Q8TDL5	BPI fold-containing family B member 1	GSK3β only					

GSK3β human spermatozoa interactors								
Gene Name	**UniProtKB**	**Name**	**Spectral counts ratio***	**Log of GSK3β/NC ratio±†**	**GSK3 phosphorylation site**	**Previously known GSK3 interactor**	**Present in testis and/or sperm**	**Asthenozoospermic alteration**
CASP14	P31944	Caspase 14	GSK3β only					
CAT	P04040	Catalase	GSK3β only				Human sperm (catalase activity) [100]	
CTSG	P08311	Cathepsin G	GSK3β only					
LYZ	B2R4C5	C-type lysozyme	GSK3β only					
DMBT1	Q9UGM3	Deleted in malignant brain tumors 1 protein	GSK3β only		Yes			
GGCT	O75223	Gamma-glutamylcyclotransferase	GSK3β only		Yes		Human testis (Sertoli and Leydig cells) and epididymis [89]	
GSN	P06396	Gelsolin	GSK3β only					
GAPDH	P04406	Glyceraldehyde-3-phosphate dehydrogenase	2			GSK3β [101]	Boar sperm (fibrous sheat of the flagellum) [102]	
HP	P00738	Haptoglobin	GSK3β only			GSK3β [51]	Rat testis (mRNA) [103]	
HSP90AB1	P08238	Heat shock protein HSP 90-beta	GSK3β only			GSK3α and GSK3β [51]	Rat testis (Sertoli cells) [65] and human sperm [83]	
HSPA2	P54652	Heat shock-related 70 kDa protein 2	3					+[29]

B2. Identification and characterization of GSK3 human testis and spermatozoa interactome

GSK3β human spermatozoa interactors								
Gene Name	**UniProtKB**	**Name**	**Spectral counts ratio***	**Log of GSK3β/NC ratio±†**	**GSK3 phosphorylation site**	**Previously known GSK3 interactor**	**Present in testis and/or sperm**	**Asthenozoospermic alteration**
HIST1H2AD	P20671	Histone H2A	4					+ [36]
HIST1H2BK	A0A024RCL8	Histone H2B	GSK3β only					
H3F3B	P84243	Histone 3.3	GSK3β only				Mouse testis (spermatogonia, leptotene spermatocytes, pachytene spermatocytes and elongating spermatids) [104]	
HIST1H4A	P62805	Histone H4	13				Mouse testis (spermatocyte) [93] and human sperm [105]	
HIST1H3A	P68431	**Histone H3**	GSK3β only				Human sperm (nuclear) [106]	
MUC5AC	A7Y9J9	Mucin 5AC, oligomeric mucus/gel-formin	GSK3β only					
MPO	P05164	Myeloperoxidase	GSK3β only		Yes		In seminal plasma [107]	- [36]
PFN1	P07737	Profilin-1	GSK3β only				Rat testis (Leydig and Sertoli cells) [108]	+ [36]
S100A8	P05109	Protein S100-A8	3				Human sperm [109]	-[36]

GSK3β human spermatozoa interactors								
Gene Name	**UniProtKB**	**Name**	**Spectral counts ratio***	**Log of GSK3β/NC ratio±†**	**GSK3 phosphorylation site**	**Previously known GSK3 interactor**	**Present in testis and/or sperm**	**Asthenozoospermic alteration**
DKFZp686J11235	Q6MZW0	Putative uncharacterized protein DKFZp686J11235	GSK3β only		Yes			
SERPINB4	P48594	Serpin B4 (Fragment)	GSK3β only					
TLR9	Q9NR96	Toll-like receptor 9	GSK3β only				Mouse sperm (acrosome) [90] human testis and sperm (mRNA) [91,92]	
n/a	Q6GMV8	Uncharacterized protein	GSk3β only					
ZG16B	Q96DA0	Zymogen granule protein 16 homolog B	GSK3β only					
ACR	P10323	Acrosin		7.70			Yes, human testis [95] and sperm (acrosome) [96,97]	
LTF	P02788	Lactotransferrin		6.45		GSK3β [51]	Human sperm (mRNA) [110]	-[36]
PRSS37	A4D1T9	Probable inactive serine protease 37		4.40			Human sperm [98]	
RPL13	P26373	60S ribosomal protein L13		4.79		GSK3β [51]		
RPL6	Q02878	60S ribosomal protein L6		4.75				
RPS18	P62269	40S ribosomal protein S18	7.31			Human sperm (acrosome) [99]		

B2. Identification and characterization of GSK3 human testis and spermatozoa interactome

* Spectral counts ratios: total number of spectral counts for each protein in GSK3α condition divided by the number of total number of spectral counts for each protein in negative control. Only rations higher than 2 were considered relevant (increase of 100% of number of spectral counts in the condition GSK3α). Please note that "GSK3α only" means that spectral counts were only detected in GSK3α condition.

±†Logarithm of GSK3α/Negative control:

† Mass spectrometry results present distinct scoring methods, since the technique was performed in two different facilities, VIB Proteomics Expertise Center and Proteomic Core Lab, Lerner Research Institute.

As for LRC37A2 and PTMA, both proteins were unable to activate the transcription of the reporter genes in the most stringent medium, which suggests that the interactions between GSK3 isoforms and LRRPC37A2 and PTMA are weaker or more transient (Figure B2.4).

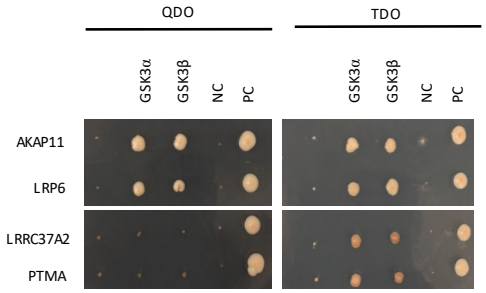

Figure B2.4. Yeast co-transformation of GSK3 and GSK3 interactors. pAS2-1- GSK3α and pAS2-1-GSK3β were co-transformed with the either pGADT7-Rec-AKAP11, pGADT7-Rec-LRP6, pGADT7-Rec-LRRC37A2 or pGADT7-Rec-PTMA recovered from the human testis cDNA library. All proteins interact with both GSK3 isoforms but only AKAP11 and LRP6 maintain the interaction in a more stringency medium. Also, none of the proteins activate per se the reporter genes. Negative (NC) and positive controls (PC) were included.

B2.4.4. Fourteen new interactors for GSK3α and twenty-nine new interactors for GSK3β were identified in human spermatozoa

To identify novel GSK3α and GSK3β interactors essential for sperm physiology, GSK3α and GSK3β interactors were isolated from mature human sperm by co-immunoprecipitation using isoform-specific GSK3 antibodies in two independent experiments (pool of two different samples in each experiment) followed by mass spectrometry analysis. Three different elution methods were used: 1%SDS, 50mM Glycine pH2.5 and no elution (in beads trypsinization was performed). Endogenous GSK3α and GSK3β were successfully immunoprecipitated in all experiments, as seen in Figure B2.5. Additionally, five peptides were identified that matched GSK3α and four that matched GSK3β (Table B2.5). Note that neither GSK3α and GSK3β were detected in the negative control either by western blot or identified by mass spectrometry (Figure B2.5 and Table B2.5).

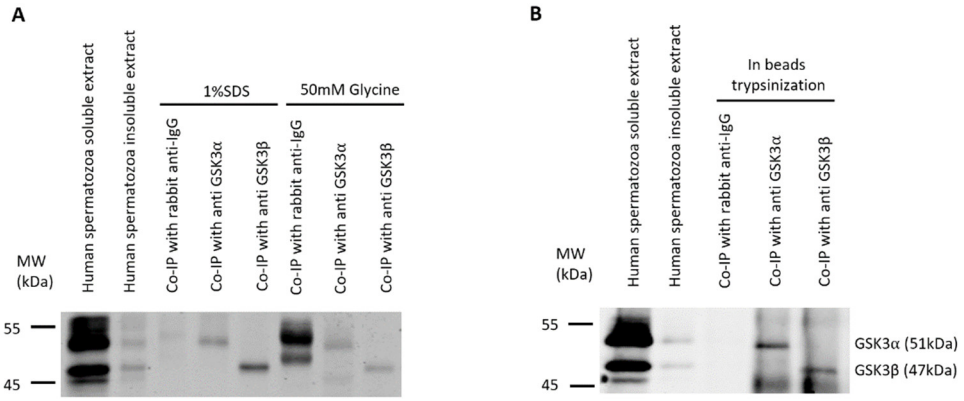

Figure B2.5.Co-Immunoprecipitation of GSK3 from normospermic human sperm sample. Both co-immunoprecipitations were also used for identification of GSK3 interactors by mass spectrometry. GSK3α and GSK3β were detected using a anti-GSK3α/β (Invitrogen, ref: 44-610, 1:2000). **A** After co-immunoprecipitation with either a GSK3α or GSK3β specific antibody, proteins were eluted with 1% SDS or 50mM glycine. Prior to GSK3 immunodetection, APP presence was evaluated by probing with 6E10 antibody. Although the reason is unknown, upon incubation with the 6E10 antibody, two unspecific bands appear on the negative control eluted with 50mM of glycine (Supplementary Figure 3). **B** After co-immunoprecipitation with crosslink of GSK3α or GSK3β antibodies to dynabeads beads, ¼ of the beads were eluted with 1%SDS and GSK3α or GSK3β presence was evaluated. Blots were cropped

Seventeen and thirty-four interactors were identified as sperm GSK3α and for GSK3β interactors, respectively (Table B2.3 and B4). Regarding GSK3α interactors, 82.4% were potentially novel interactors while 17.6% were previously identified as GSK3 interactors in PPI databases. From those, all were described as interacting with GSK3β (either exclusively or interaction for GSK3α was not tested). Also, 58.8% of GSK3α identified interactors were described as expressed in either mammalian testis and/or sperm by previous studies. Lastly, 17.6% of GSK3α identified interactors contained the GSK3 consensus phosphorylation site (Table B2.3).

Table B2.5. GSK3 isoforms peptides detected on mass spectrometry. Peptide sequence, first and last aminoacid of the peptide, peptide % of coverage for the complete protein and peptide spectral count.

Sequence	Start	End	Coverage	Spectral Count
Mass spectrometry eluted with 50mM glycine and 1% SDS				
GSK3α (UniProtKB: P49840)				
TSSFAEPGGGGGGGGGGPGGSASGPGGTGGGK	19	50	10%	5
VTTVVATLGQGPER	100	113		
GSK3β (UniProtKB: P49841)				
TPPEAIALCSR	309	319	3%	1
Mass spectrometry on-bead trypsin digestion				
GSK3α (UniProtKB: P49840)				
VTTVVATLGQGPER	100	113	8%	13
SQEVAYTDIK	114	123		
DIKPQNLLVDPDTAVLK	244	260		
GSK3β (UniProtKB: P49841)				
VTTVVATPGQGPDRPQEVSYTDTK	37	60	17%	32
DTPALFNFTTQELSSNPPLATILIPPHAR	355	383		
IQAAASTPTNATAASDANTGDR	384	405		

For GSK3β interactors, 85.3% were new putative interactors and 14.7% were already described as GSK3 interactors. From the latter, one interaction was reported with both GSK3 isoforms while the remaining were described as interacting with GSK3β. Moreover, 47.1% of GSK3β identified interactors are expressed in either mammalian testis and/or sperm. Finally, the GSK3 consensus phosphorylation site is present in 14.7% of GSK3β interactors (Table B2.3).

B2.4.5. GSK3 testis and spermatozoa interactomes are enriched in gene and protein expression processes

In this study, four distinct GSK3 interactomes were characterized: GSK3α and GSK3β in human testis and human sperm. The Venn diagrams in Figure B2.6 represent the overlap between GSK3α and GSK3β interactomes in human testis, sperm and databases.

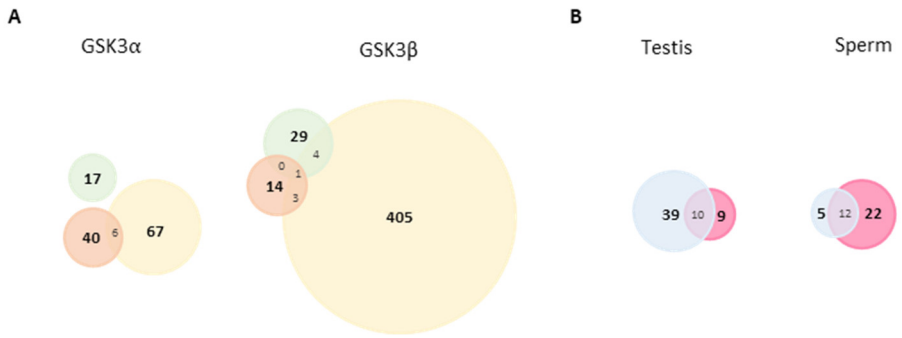

Figure B2. 6. Venn diagram showing the overlap of GSK3α and GSK3β interactomes. The data retrieved from testis, sperm and databases GSK3 interactors was compared and the number of common proteins between two or three categories is shown **A.** Overlap of GSK3α and GSK3β interactomes between interactors reported in databases and identified in testis and sperm. **B**. Overlap of testis and sperm GSK3 interactors. Green: Sperm interactors; Orange: Testis interactors; Yellow: Databases interactors; Blue: GSK3α interactors and Pink: GSK3β interactors.

With the goal of identifying key GSK3 interactors for sperm and testis physiology, gene expression for GSK3 interactors was retrieved from 5 different databases (Supplementary Table B2.1). For GSK3α four proteins were considered testis-enriched, with more than 90% of their expression restricted to testis: DDI1, GOLGA6C (testis interactors), ACR and PRSS37 (sperm interactors). Although not testis-enriched, 50-75% expression of TTC16 is limited to testis. For GSK3β interactors, besides ACR and PRSS37 similarly to GSK3α, TEKT5, CMTM2 (testis interactors), HIST1H1T, PRKACG, TSKS (databases interactors) were classified as highly enriched in testis (>90% expression). CABYR presented 75%-90% of expression in testis while RGS22 only 50-75%. To further characterize GSK3

interactome, differently expressed proteins in asthenozoospermic samples were retrieved from proteomics studies (Tables B2.1-B2.4).

To better understand the role of GSK3 isoforms and their interactors in testis and sperm, an enrichment analysis was performed. Testis GSK3α interactome appears to be highly associated with RNA metabolic processing and located mainly in the nucleus (Supplementary Table B2.4). On the other hand, the GSK3α sperm interactome is enriched in proteins involved in ribosomal function, particularly protein production (Supplementary Table B2.5)

The GSK3β testis interactome it appears to be associated with maintenance of gene quality, particularly telomerase length (Supplementary Table B2.6). The GSK3β sperm interactome is enriched in proteins reported to be involved in immune response (Supplementary Table B2.7).

B2.4.6. The GSK3 interactomes are associated with sperm motility and testis functions

To further characterize the GSK3 interactome, protein-protein interaction networks were constructed using data obtained from this study and GSK3 PPIs retrieved from databases. The GSK3α interactome network (Supplementary Figure B2.4) presents 130 proteins,

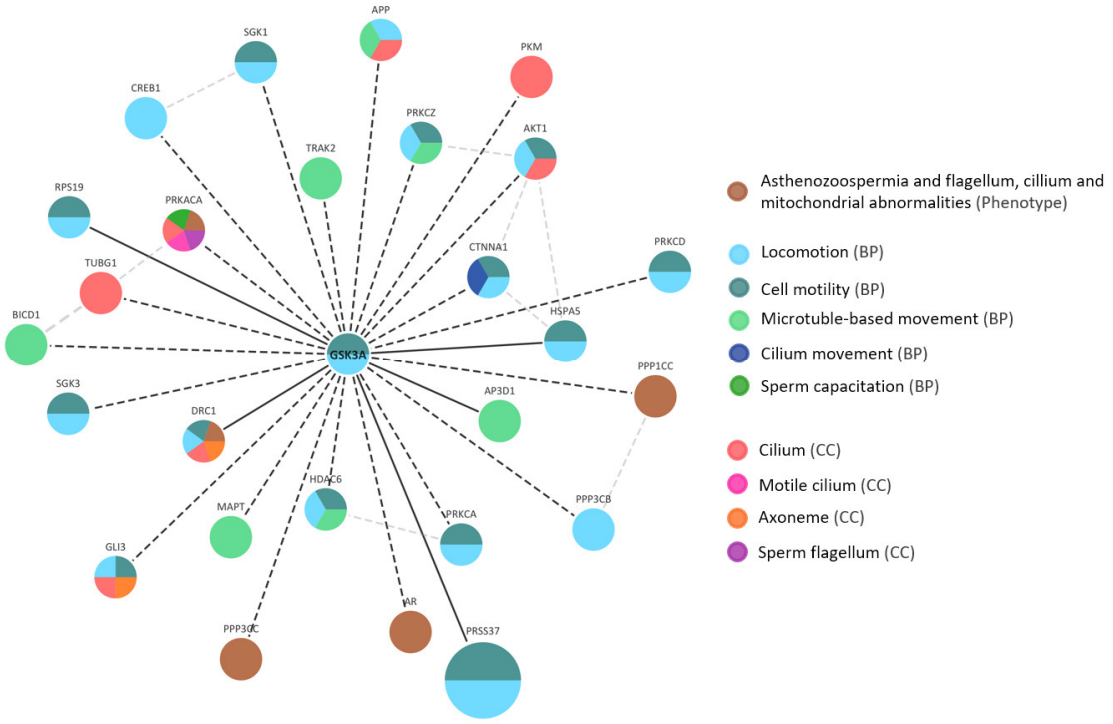

Figure B2.7. GSK3α sperm motility network. GSK3α-centered subnetwork for sperm motility extracted from GSK3α interactome network. All GSK3α interactors associated with motility-related annotations were used to build the network. Solid lines: testis or sperm GSK3α interactions; Dashed lines: Databased retrieved GSK3α interactions. Node size: according to testis expression. Node colors: represent motility-related phenotypes, biological processes (BP) or cellular components (CC).

including GSK3α. Between these GSK3α interactors 257 interactions were formed. The average number of neighbor of a node was 3.9 (ranging from 1 to 130). Around 40% of GSK3α interactors only formed one interaction (with GSK3α). 96% of all GSK3α interactors had five or less interactions. As expected, GSK3α was the protein that presents more interactions, since it is a protein-centered network. The mean clustering coefficient for GSK3α interactome network is 0.462. The GSK3β interactome is composed by 456 proteins that form 1813 interactions among them (Supplementary

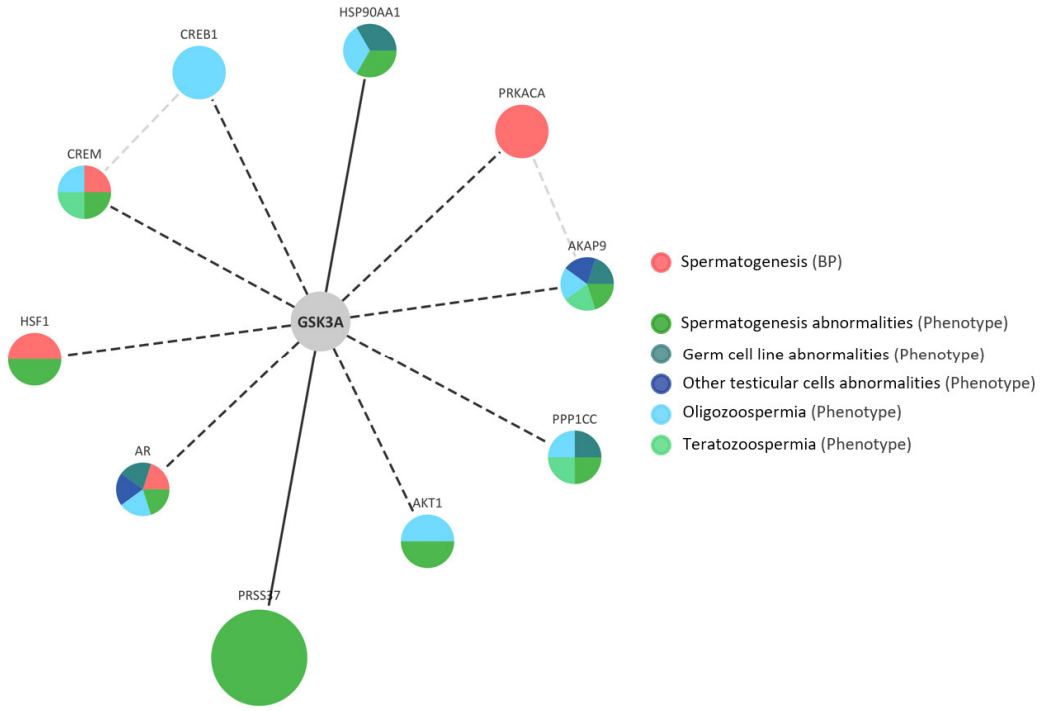

Figure B2.8. GSK3α testis network. GSK3α-centered subnetwork for testis-related annotations extracted from GSK3α interactome network. All GSK3α interactors associated with testis annotations were used to build the network. Solid lines: testis or sperm GSK3α interactions; Dashed lines: Databased retrieved GSK3α interactions. Node size: according to testis expression. Node colors: represent testis related phenotypes, biological processes (BP) or cellular components (CC).

Figure B2.5). The average number of neighbor of a node was 7.815 (ranging from 1 to 455). Seventy-six proteins interacted exclusively with GSK3β and 24% of GSK3β interactors had ten or more interactors. GSK3β network presents a mean clustering coefficient of 0.448 (Supplementary Figure B2.6).

GSK3 subnetworks associated with sperm-motility and testis were extracted from GSK3 isoforms protein-protein networks (Figure B2.7 and B2.8). Twenty-six GSK3α interactors have been associated with motility-related functions, phenotypes and/or subcellular locations (Figure B2.7). From those, five (PRSS37; DRC1; RPS19; HSPA5 and AP3D1) were identified in this study as either testis or sperm GSK3α interactors and only one was classified as testis-enriched protein (PRSS37).

PRKACA and DRC1 stand out by presenting five motility-related functions, phenotypes and/or subcellular locations, followed by GLI3 with four. Note that GSK3α itself has been associated with locomotion and cell motility processes (Figure B2.7). Ten GSK3α interactors were associated with testis-related functions or phenotypes/diseases and two of those were identified in this study (PRSS37 and HSP90AA1) (Figure B2.8). Only PRSS37 was described as highly expressed in testis and associated with testis-related annotations (PRSS37) (Figure B2.8). With five testis-related functions and/or subcellular locations, we highlight AKAP9 and AR. PRSS37 is also the single GSK3α interactor that is with associated with sperm motility, testis annotations, and categorized as enriched in testis (Figure B2.7 and Figure B2.8). For GSK3β, 100 interactors are annotated to motility-related categories, and from those six are highly expressed in testis (CABYR, TEKT5, PRKACG, PRSS37, TSKS, CMTM2) (Figure B2.9). For testis-related categories, GSK3β presents forty-five interactors (Figure B2.10).

Although not directly related to sperm motility and testis function, several GSK3 interactors are related to more general phenotypes or functions related to the male reproductive system (Supplementary Figure B2.6 and B2.7).

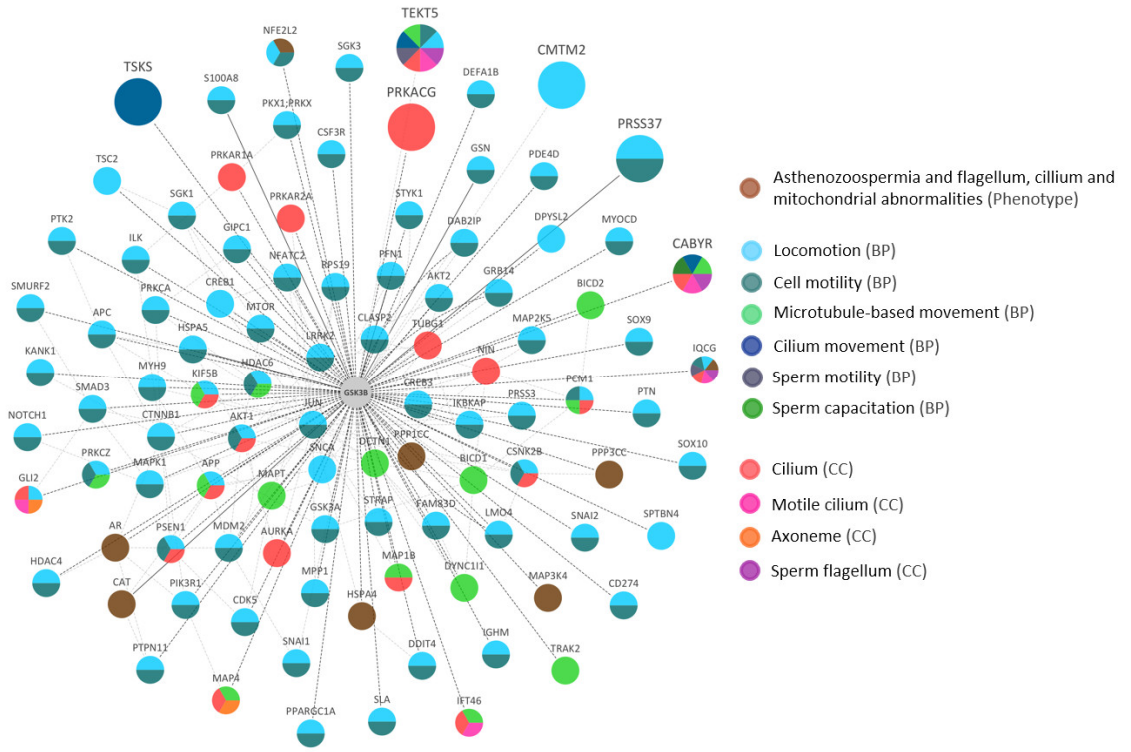

Figure B2.9. GSK3β sperm motility network. GSK3β-centered subnetwork for sperm motility extracted from GSK3β interactome network. All GSK3βinteractors associated with motility-related annotations were used to build the network. Solid lines: testis or sperm GSK3β interactions; Dashed lines: Databased retrieved GSK3β interactions. Node size: according to testis expression. Node colors: represent motility-related phenotypes, biological processes (BP) or cellular components (CC).

B2.4.7. AKAP11 and LRP6 subcellular localization in human sperm

Two GSK3 interactors identified in this study, LRP6 and AKAP11, were chosen for further characterization. Both these proteins were chosen due to their potential involvement in male reproduction. LRP6 was already described as involved in sperm motility and testis physiology and AKAP11 in mouse spermatogenesis. AKAP11 and LRP6 expression in human testis and ejaculated sperm and the subcellular localization in human sperm were assessed. Figure B2.11 A shows that LRP6 is expressed in human testis and in human sperm. Although the expected molecular weight of LRP6 was around 180kDa, in human testis immunoreactivity was detected at around 210kDa. Several studies reported LRP6 at a higher molecular weight possible due to post-translational modification such as glycosylation and phosphorylation [111,112]. In human sperm, LRP6 was also detected at around 180kDa, although the immunoreactivity is weak. No immunoreactivity was detected for p1490LRP6 using Western blot. Regarding AKAP11, no signal was detected. We believe this is due to limitations of the antibody. All commercially available AKAP11 antibodies are

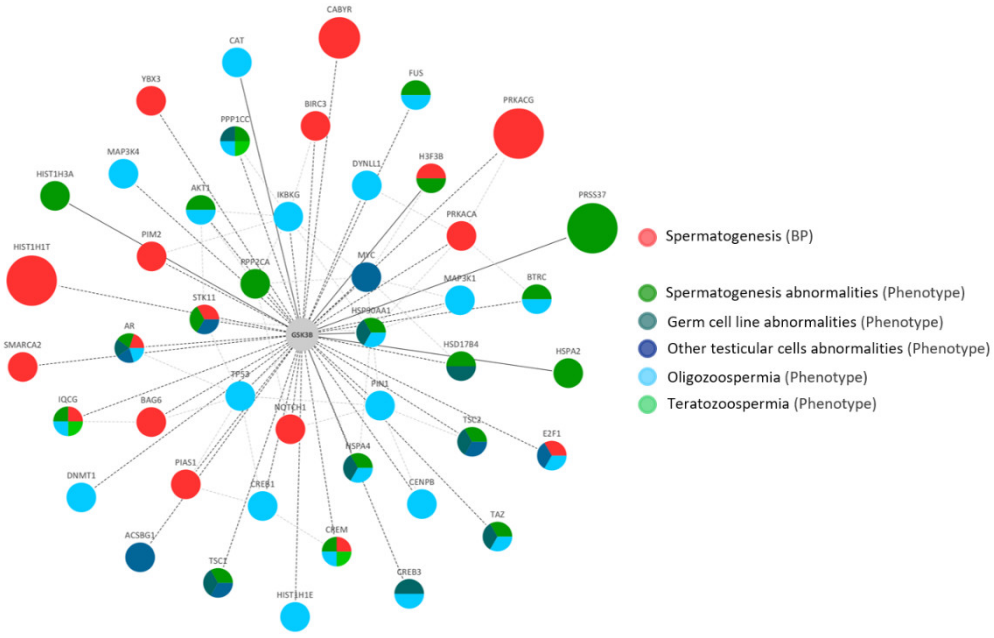

Figure B2.10. GSK3β testis network. GSK3β-centered subnetwork for testis-related annotations extracted from GSK3β interactome network. All GSK3β interactors associated with testis annotations were used to build the network. Solid lines: testis or sperm GSK3β interactions; Dashed lines: Databased retrieved GSK3β interactions. Node size: according to testis expression. Node colors: represent testis related phenotypes, biological processes (BP) or cellular components (CC).

recommended for immunocytochemistry and immunohistochemistry studies and not for Western blot, suggesting that only non-denatured AKAP11 is recognized by the antibodies.

Immunocytochemistry studies (Figure B2.11 B), revealed that total LRP6 is localized to the entire length of the flagellum and occasionally at the post-acrosomal area. However, p1490LRP6 is restricted to the midpiece. Moreover, a closer analysis showed that not all sperm cells present immunoreactivity towards LRP6 and LRP6p1490. Only 18% and 29% of sperm cells present immunoreactivity for LRP6 and p1490LRP6 respectively (Figure B2.11 B). Regarding AKAP11, this protein is localized on the anterior portion of the head and the equatorial area of ejaculated human sperm (Figure B2.11 B).

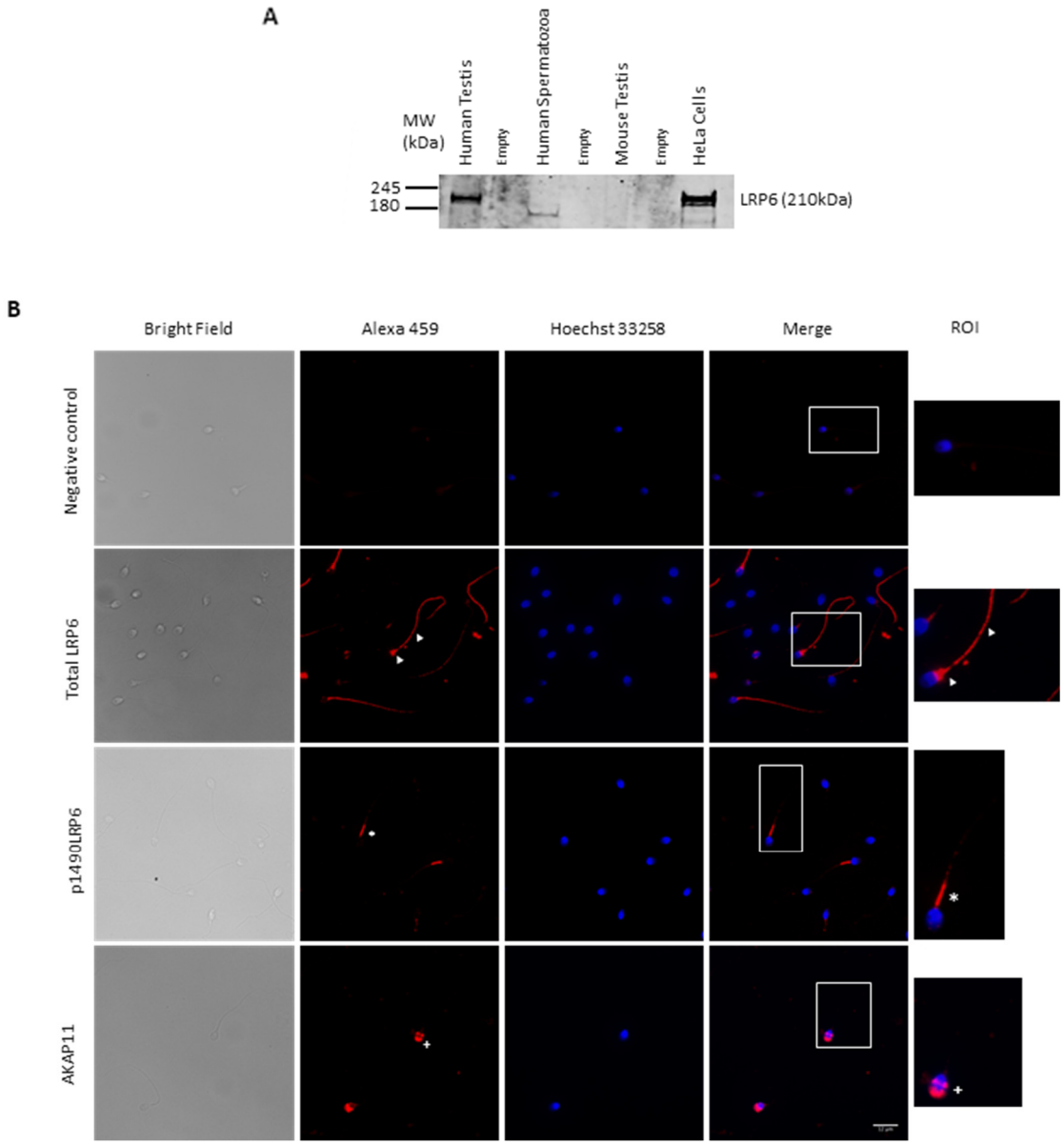

Figure B2.11. LRP6 and AKAP11 in human testis and sperm. A. LRP6 in testis and mature human sperm. Western blot analysis of LRP6 in human testis and mature sperm, mouse testis and HeLa cells. For human testis, mouse testis and HeLa cells 30µg of protein were loaded per sample. For mature human sperm 100µg of proteins were loaded. **B.** subcellular localization of LRP6, p1490LRP6 and AKAP11 in mature human sperm. Total LRP6 is located in the entire flagellum and occasionally in the post-acrosomal area (arrowhead). The phosphorylated form of LRP6 at serine 1490 is restricted to the midpiece (star). AKAP11 is located to the head, specifically to the anterior and equatorial area (plus sign). Scale bar is 10µm. Nucleus is marked in blue. ROI: region of interest. All images were obtained with 63X magnification in a Imager.Z1, Axio-Cam HRm camera and AxioVision software Zeiss, Jena, Germany).

B2.5. Discussion

GSK3 has been long associated with sperm motility acquisition and maintenance in mammals [9,10,113]. In mice sperm, GSK3α seems key for primary motility acquisition since mice testis lacking this protein present low-motility sperm. However, the characterization of both GSK3 isoforms (GSK3α and GSK3β) in human sperm and testis physiology has been sparse. This work aimed to characterize GSK3 isoforms in human sperm as well as identify and analyze GSK3α and GSK3β interactome in human sperm and testis. Ultimately, this can help depict new GSK3 isoform-specific interactions essential for human sperm function.

Similar to other mammals, both GSK3 isoforms are present in human testis and sperm (Figure B2.1) [7,9,10,113,114]. We believe that the observed molecular weight differences between mouse and human GSK3 isoforms arise from protein sequence differences (*Homo sapiens* and *Mus musculus* share 95% identity for GSK3α and 99% identity for GSK3β). Intraspecies differences may be explained by differences in phosphorylation status since this kinase presents multiple phosphorylation sites. Besides, it appears that in human testis, GSK3α and GSK3β are mainly active while in human sperm part of the GSK3 population is inhibited (Figure B2.1).

To evaluate the importance of GSK3 in motility we assessed GSK3 activity in human sperm samples with distinct motility levels. We showed that in ejaculated human sperm, GSK3α activity presents a strong negative correlation with sperm motility, but GSK3β activity does not appear to influence motile sperm (Figure B2.2). Moreover, the fact that 100% of the sperm analyzed presented GSK3α in the flagellum but only around 24% presented GSK3β on the same subcellular location reinforces the possible GSK3α isoforms-specific role in sperm motility (Figure B2.3). Contrary to previously described [115], we showed that in capacitated sperm GSK3β presents a strong positive correlation with sperm motility, while GSK3α has no correlation with motility (Figure B2.3). These findings suggest that human sperm motility acquisition can be a GSK3α isoform-specific function and GSK3 isoforms may have other functions on sperm physiology. In 2015, Koch et al suggested that besides sperm motility, GSK3 may be involved in sperm protein stability and subcellular compartmentalization [71].

Given the reported relevance of GSK3 isoforms in sperm function, specifically GSK3α in motility, the GSK3α and GSK3β interactomes in testis and sperm were identified and characterized (Tables B2. 1-4). The fact that several GSK3 sperm and testis interactions identified in this study were previously described, strengthens the validity of the GSK3 testis interactome. Furthermore, the

known interaction between GSK3 isoforms and AXIN2 was also detected in testis. The interaction between Axin and GSK3 is extensively described in the literature on somatic cells (see Table 1 and [116–119]) and has been target for drug pharmacological approach [120]. Yet to our knowledge, this is the first time the interaction was described in testis.

An enrichment analysis of GSK3 interactome revealed that GSK3α and its testis interactors are mainly involved in gene expression (transcription) (Supplementary Table B2.4). Testis require high and specialized levels of gene expression mainly due to meiosis and the high level of cell differentiation [121,122]. The involvement of GSK3α interactors on these processes suggests that GSK3α may play a role in testis gene expression. This is further supported by the fact that both LRP6 and AXIN2 were identified as GSK3α testis interactors (Table B2.1). LRP6, AXIN2 and GSK3 are involved in the gene expression control by Wnt/β-catenin signaling pathway [116–119]. In mouse testis, Wnt/β-catenin signaling participates in undifferentiated spermatogonia proliferation and regulation [55] and in idiopathic azoospermic cases, β-catenin clusters in Sertoli cells [123]. We further investigated the potential role of LRP6 in human fertility. Bioinformatics analysis revealed that when LRP6 is absent from mice testis, they became infertile due to morphological defects of the reproductive system (Supplementary Figure B2.6 and Supplementary Table B2.2). Expression studies showed that LRP6 is present in human testis and sperm and is localized along the entire flagellum (Figure B2.11). Furthermore, when LRP6 is phosphorylated on S1490 (in somatic cells a GSK3 substrate [124,125]) its subcellular location is restricted to the human sperm midpiece (Figure B2.11). This is in accordance to earlier studies in mice and bovine sperm [71]. In 2015, Koch et al explored the non-genetic effects of β-catenin signaling on human sperm and suggested that the interaction between LRP6 and GSK3 is required for protein stabilization and consequently sperm motility [71]. Therefore, despite the fact that in somatic cells GSK3/LRP6 interaction is involved in gene expression, in human sperm this interaction can have other roles which might deserve further studies.

In sperm, the fact that the GSK3α interactome was involved in protein expression processes (Supplementary Table B2.5) and several ribosomal proteins were identified in this study as sperm GSK3α and GSK3β interactors (Table B2.3 and B2.4) was surprising. Sperm is typically described as a transcriptionally silent cell and being unable to produce proteins due to lack of ribosomes [126]. Yet, several cytoplasmic and mitochondrial ribosomal proteins have been previously described in human sperm (head and flagellum) [127–130]. Moreover, Gur and colleagues demonstrate the translation of mRNA by mitochondrial-type ribosomes [127] in human sperm and inhibition of such

translation leads to reduced levels of several proteins and, consequently, a significantly reduction of sperm motility, capacitation and *in vitro* fertilization [127,131]. These findings further strengthen the idea that GSK3α is a multi-task protein involved in processes other than motility.

With the purpose of constructing the most complete GSK3 interactome, GSK3 interactions annotated on PPIs databases were retrieved. Interestingly, the overlap between testis/sperm interactomes and databases is very small (Figure B2.6). This may be a result of the understudy of GSK3 and its interactors in the male reproductive system. Also, the discrepancy between the number of GSK3α and GSK3β-described interactions in databases may rise from more intense study of GSK3β than of GSK3α, and not from a biological difference in the number of interactors of both isoforms. In both testis and sperm, several proteins were identified exclusively in GSK3α or GSK3β interactomes (Figure B2.6). This may reflect specific GSK3 isoform interactions but further protein-protein interaction validation is necessary. The fact that both GSK3α and GSK3β networks (Supplementary Figure B2.4 and B2.5) presented a clustering coefficient (how nearest neighboring nodes of node are connected to each other) higher than 0.02 suggests a motif-like structure [132]. Network motifs are network patterns that appear more frequently than expected and typically proteins belonging to the same motif share the same function [133,134].

To achieve functional and tissue-specific relationships, tissue-expression, phenotypes and annotations were integrated into the GSK3 networks (Figure B2.7-10). It may be noted that the knowledge of protein tissue expression is still limited and typically does not take into account tissue-specific alternative splicing products. This is particularly relevant for testis, since testis is the tissue with a higher number of alternative transcripts splice variants [135] [24]. None of GSK3α interactors listed on databases showed a testis-specific or enriched expression. However, we identified DDI1, GOLGA6C (testis interactors), ACR and PRSS37 (sperm interactors) that showed a testis-enriched expression pattern (Supplementary Table B2.1). Besides being involved in sperm motility functions (Figure B2.7), our *in silico* analysis revealed that PRSS37 may play a role in spermatogenesis (Figure B2.8). PRSS37 when absent in mice testis compromises spermatogenesis, sperm oviduct-migrating ability, and sperm-zona binding resulting in low percentage of fertilized eggs [136]. AR, PPP1CC, and AKAP9 (identified exclusively in the GSK3α interactome) appear to be highly associated with testis functions since germ cells and other types of testicular cells are greatly affected by their absence (Figure B2.8). These findings are in accordance to former studies [137–139].

AKAP11 was identified as a testis GSK3α interactor (Table B2.1). While the interaction between AKAP11 and GSK3β has been previously described [49], to our knowledge this is the first description

of the interaction with GSK3α. Opposing to earlier studies in human sperm [52], we showed that AKAP11 is localized in the anterior portion of the head and equatorial region (Figure B2.11). In somatic cells, AKAP11 has been associated with cell migration [140] and in 2002, Tanji et al showed that AKAP11, PPP1, PRKACA, and GSK3β formed a multimeric complex in which PPP1 and PRKACA controlled GSK3β activity. Since both PPP1 and PRKACA have been extensively described in mammalian testis [137,141], we may assume that in testis a similar multimeric complex may be formed to control GSK3α activity.

TEKT5 and CMTM2 were identified as GSK3β testis interactors (Table B2.2) and categorized as testis-enriched (Supplementary Table B2.1). TEKT5 is present in mouse testis and expression patterns of this protein suggest a role in flagella formation during spermiogenesis [86]. Further, in mouse sperm TEKT5 is enriched in flagellar accessory structures and has been implicated in sperm motility [86]. The fact that TEKT5 is highly associated with sperm motility phenotypes (Figure B2.9), suggests that the interaction GSK3β/TEKT5 may be involved in sperm motility.

In conclusion, human sperm motility is at least partially regulated by GSK3 activity, particularly the GSK3α isoform. This isoform-specific function may arise from GSK3α interactors that pay central roles in sperm motility. In brain, RACK1 is a GSK3α-specific interactor. Although no GSK3α-specific interaction was identified in testis and sperm, we have identified GSK3α interactors, such as PRSS37, that are potentially involved in sperm motility. Moreover, GSK3α and its interactors appear to be highly associated with protein expression suggesting other possible functions for this protein in both testis and sperm. Finally, the interactions identified in this study could be promising pharmacological targets for a new male contraceptive based on disrupting sperm motility.

B2.6. References

[1] Kaidanovich-Beilin O, Woodgett JR. GSK-3: Functional Insights from Cell Biology and Animal Models. Front Mol Neurosci 2011; 4:40.

[2] Beurel E, Grieco SF, Jope RS. Glycogen synthase kinase-3 (GSK3): regulation, actions, and diseases. Pharmacol Ther 2015; 148:114–31.

[3] Gao C, Hölscher C, Liu Y, Li L. GSK3: a key target for the development of novel treatments for type 2 diabetes mellitus and Alzheimer disease. Rev Neurosci 2011; 23:1–11.

[4] Amar S, Belmaker RH, Agam G. The possible involvement of glycogen synthase kinase-3 (GSK-3) in diabetes, cancer and central nervous system diseases. Curr Pharm Des 2011; 17:2264–77.

[5] Azoulay-Alfaguter I, Yaffe Y, Licht-Murava A, Urbanska M, Jaworski J, Pietrokovski S, et al. Distinct molecular regulation of glycogen synthase kinase-3alpha isozyme controlled by its N-terminal region: functional role in calcium/calpain signaling. J Biol Chem 2011; 286:13470–80.

[6] Bhattacharjee R, Goswami S, Dudiki T, Popkie AP, Phiel CJ, Kline D, et al. Targeted disruption of glycogen synthase kinase 3A (GSK3A) in mice affects sperm motility resulting in male infertility. Biol Reprod 2015; 92:65.

[7] Guo TB, Chan KC, Hakovirta H, Xiao Y, Toppari J, Mitchell AP, et al. Evidence for a role of glycogen synthase kinase-3 beta in rodent spermatogenesis. J Androl n.d.; 24:332–42.

[8] Wang QM, Fiol CJ, DePaoli-Roach AA, Roach PJ. Glycogen synthase kinase-3 beta is a dual specificity kinase differentially regulated by tyrosine and serine/threonine phosphorylation. J Biol Chem 1994; 269:14566–74.

[9] Somanath PR, Jack SL, Vijayaraghavan S. Changes in sperm glycogen synthase kinase-3 serine phosphorylation and activity accompany motility initiation and stimulation. J Androl n.d.; 25:605–17.

[10] Vijayaraghavan S, Mohan J, Gray H, Khatra B, Carr DW. A role for phosphorylation of glycogen synthase kinase-3alpha in bovine sperm motility regulation. Biol Reprod 2000; 62:1647–54.

[11] Reid AT, Anderson AL, Roman SD, McLaughlin EA, McCluskey A, Robinson PJ, et al. Glycogen synthase kinase 3 regulates acrosomal exocytosis in mouse spermatozoa via dynamin phosphorylation. FASEB J 2015; 29:2872–82.

[12] Organization WH. Examination and processing of human semen. vol. Fifth Edit. 2010.

[13] Cox J, Mann M. MaxQuant enables high peptide identification rates, individualized p.p.b.-range mass accuracies and proteome-wide protein quantification. Nat Biotechnol 2008; 26:1367–72.

[14] Cox J, Hein MY, Luber CA, Paron I, Nagaraj N, Mann M. Accurate proteome-wide label-free quantification by delayed normalization and maximal peptide ratio extraction, termed MaxLFQ. Mol Cell Proteomics 2014; 13:2513–26.

[15] Tyanova S, Temu T, Sinitcyn P, Carlson A, Hein MY, Geiger T, et al. The Perseus computational platform for comprehensive analysis of (prote)omics data. Nat Methods 2016; 13:731–40.

[16] Wu G, Huang H, Garcia Abreu J, He X. Inhibition of GSK3 phosphorylation of beta-catenin via phosphorylated PPPSPXS motifs of Wnt coreceptor LRP6. PLoS One 2009; 4:e4926.

[17] Dinkel H, Van Roey K, Michael S, Kumar M, Uyar B, Altenberg B, et al. ELM 2016--data update and new functionality of the eukaryotic linear motif resource. Nucleic Acids Res 2016; 44:D294-300.

[18] Hornbeck P V, Zhang B, Murray B, Kornhauser JM, Latham V, Skrzypek E. PhosphoSitePlus, 2014: mutations, PTMs and recalibrations. Nucleic Acids Res 2015; 43:D512-20.

[19] Blom N, Sicheritz-Pontén T, Gupta R, Gammeltoft S, Brunak S. Prediction of post-translational glycosylation and phosphorylation of proteins from the amino acid sequence. Proteomics 2004; 4:1633–49.

[20] de Castro E, Sigrist CJA, Gattiker A, Bulliard V, Langendijk-Genevaux PS, Gasteiger E, et al. ScanProsite: detection of PROSITE signature matches and ProRule-associated functional and structural residues in proteins. Nucleic Acids Res 2006; 34:W362-5.

[21] Xue Y, Liu Z, Cao J, Ma Q, Gao X, Wang Q, et al. GPS 2.1: enhanced prediction of kinase-specific phosphorylation sites with an algorithm of motif length selection. Protein Eng Des Sel 2011; 24:255–60.

[22] Orchard S, Kerrien S, Abbani S, Aranda B, Bhate J, Bidwell S, et al. Protein interaction data curation: the International Molecular Exchange (IMEx) consortium. Nat Methods 2012; 9:345–50.

[23] Alanis-Lobato G, Andrade-Navarro MA, Schaefer MH. HIPPIE v2.0: enhancing meaningfulness and reliability of protein-protein interaction networks. Nucleic Acids Res 2017; 45:D408–D414.

[24] Uhlén M, Fagerberg L, Hallström BM, Lindskog C, Oksvold P, Mardinoglu A, et al. Proteomics. Tissue-based map of the human proteome. Science 2015; 347:1260419.

[25] Pan J-B, Hu S-C, Shi D, Cai M-C, Li Y-B, Zou Q, et al. PaGenBase: a pattern gene database for the global and dynamic understanding of gene function. PLoS One 2013; 8:e80747.

[26] Petryszak R, Burdett T, Fiorelli B, Fonseca NA, Gonzalez-Porta M, Hastings E, et al. Expression Atlas update--a database of gene and transcript expression from microarray- and sequencing-based functional genomics experiments. Nucleic Acids Res 2014; 42:D926-32.

[27] Wu C, Jin X, Tsueng G, Afrasiabi C, Su AI. BioGPS: building your own mash-up of gene annotations and expression profiles. Nucleic Acids Res 2016; 44:D313-6.

[28] Pontius JU, Wagner L, Schuler GD. UniGene: a unified view of the transcriptome. The NCBI Handbook, vol. 1. 2003:1–12.

[29] Amaral A, Paiva C, Attardo Parrinello C, Estanyol JM, Ballescà JL, Ramalho-Santos J, et al. Identification of proteins involved in human sperm motility using high-throughput differential proteomics. J Proteome Res 2014; 13:5670–84.

[30] Bhagwat S, Dalvi V, Chandrasekhar D, Matthew T, Acharya K, Gajbhiye R, et al. Acetylated α-tubulin is reduced in individuals with poor sperm motility. Fertil Steril 2014; 101:95–104.e3.

[31] Shen S, Wang J, Liang J, He D. Comparative proteomic study between human normal motility sperm and idiopathic asthenozoospermia. World J Urol 2013; 31:1395–401.

[32] Li Y-S, Feng X-X, Ji X-F, Wang Q-X, Gao X-M, Yang X-F, et al. [Expression of SEPT4 protein in the ejaculated sperm of idiopathic asthenozoospermic men]. Zhonghua Nan Ke Xue 2011; 17:699–702.

[33] An C-N, Jiang H, Wang Q, Yuan R-P, Liu J-M, Shi W-L, et al. Down-regulation of DJ-1 protein

in the ejaculated spermatozoa from Chinese asthenozoospermia patients. Fertil Steril 2011; 96:19–23.e2.

[34] Jing X, Xing R, Zhou Q, Yu Q, Guo W, Chen S, et al. [Expressions of cysteine-rich secretory protein 2 in asthenospermia]. Zhonghua Nan Ke Xue 2011; 17:203–7.

[35] Hashemitabar M, Sabbagh S, Orazizadeh M, Ghadiri A, Bahmanzadeh M. A proteomic analysis on human sperm tail: comparison between normozoospermia and asthenozoospermia. J Assist Reprod Genet 2015; 32:853–63.

[36] Saraswat M, Joenväärä S, Jain T, Tomar AK, Sinha A, Singh S, et al. Human Spermatozoa Quantitative Proteomic Signature Classifies Normo- and Asthenozoospermia. Mol Cell Proteomics 2017; 16:57–72.

[37] Zhou J-H, Zhou Q-Z, Lyu X-M, Zhu T, Chen Z-J, Chen M-K, et al. The expression of cysteine-rich secretory protein 2 (CRISP2) and its specific regulator miR-27b in the spermatozoa of patients with asthenozoospermia. Biol Reprod 2015; 92:28.

[38] Salvolini E, Buldreghini E, Lucarini G, Vignini A, Giulietti A, Lenzi A, et al. Interleukin-1β, cyclooxygenase-2, and hypoxia-inducible factor-1α in asthenozoospermia. Histochem Cell Biol 2014; 142:569–75.

[39] Li H, Yu N, Zhang X, Jin W, Li H. Spermatozoal protein profiles in male infertility with asthenozoospermia. Chin Med J (Engl) 2010; 123:2879–82.

[40] Chen J, Wang Y, Xu X, Yu Z, Gui Y, Cai Z. [Differential expression of ODF1 in human ejaculated spermatozoa and its clinical significance]. Zhonghua Nan Ke Xue 2009; 15:891–4.

[41] Cai Z-M, Gui Y-T, Guo X, Yu J, Guo L-D, Zhang L-B, et al. Low expression of glycoprotein subunit 130 in ejaculated spermatozoa from asthenozoospermic men. J Androl n.d.; 27:645–52.

[42] Eppig JT, Richardson JE, Kadin JA, Ringwald M, Blake JA, Bult CJ. Mouse Genome Informatics (MGI): reflecting on 25 years. Mamm Genome 2015; 26:272–84.

[43] Amberger JS, Bocchini CA, Schiettecatte F, Scott AF, Hamosh A. OMIM.org: Online Mendelian Inheritance in Man (OMIM®), an online catalog of human genes and genetic disorders. Nucleic Acids Res 2015; 43:D789-98.

[44] Piñero J, Bravo À, Queralt-Rosinach N, Gutiérrez-Sacristán A, Deu-Pons J, Centeno E, et al. DisGeNET: a comprehensive platform integrating information on human disease-associated genes and variants. Nucleic Acids Res 2017; 45:D833–D839.

[45] Yu W, Clyne M, Khoury MJ, Gwinn M. Phenopedia and Genopedia: disease-centered and gene-centered views of the evolving knowledge of human genetic associations. Bioinformatics 2010; 26:145–6.

[46] Pletscher-Frankild S, Pallejà A, Tsafou K, Binder JX, Jensen LJ. DISEASES: text mining and data integration of disease-gene associations. Methods 2015; 74:83–9.

[47] Gene Ontology Consortium. Gene Ontology Consortium: going forward. Nucleic Acids Res 2015; 43:D1049-56.

[48] Shannon P, Markiel A, Ozier O, Baliga NS, Wang JT, Ramage D, et al. Cytoscape: a software environment for integrated models of biomolecular interaction networks. Genome Res 2003; 13:2498–504.

[49] Tanji C, Yamamoto H, Yorioka N, Kohno N, Kikuchi K, Kikuchi A. A-kinase anchoring protein

AKAP220 binds to glycogen synthase kinase-3beta (GSK-3beta) and mediates protein kinase A-dependent inhibition of GSK-3beta. J Biol Chem 2002; 277:36955–61.

[50] Varjosalo M, Keskitalo S, Van Drogen A, Nurkkala H, Vichalkovski A, Aebersold R, et al. The protein interaction landscape of the human CMGC kinase group. Cell Rep 2013; 3:1306–20.

[51] Varjosalo M, Sacco R, Stukalov A, van Drogen A, Planyavsky M, Hauri S, et al. Interlaboratory reproducibility of large-scale human protein-complex analysis by standardized AP-MS. Nat Methods 2013; 10:307–14.

[52] Reinton N, Collas P, Haugen TB, Skålhegg BS, Hansson V, Jahnsen T, et al. Localization of a novel human A-kinase-anchoring protein, hAKAP220, during spermatogenesis. Dev Biol 2000; 223:194–204.

[53] von Kries JP, Winbeck G, Asbrand C, Schwarz-Romond T, Sochnikova N, Dell'Oro A, et al. Hot spots in beta-catenin for interactions with LEF-1, conductin and APC. Nat Struct Biol 2000; 7:800–7.

[54] Schwarz-Romond T, Asbrand C, Bakkers J, Kühl M, Schaeffer H-J, Huelsken J, et al. The ankyrin repeat protein Diversin recruits Casein kinase Iepsilon to the beta-catenin degradation complex and acts in both canonical Wnt and Wnt/JNK signaling. Genes Dev 2002; 16:2073–84.

[55] Takase HM, Nusse R. Paracrine Wnt/β-catenin signaling mediates proliferation of undifferentiated spermatogonia in the adult mouse testis. Proc Natl Acad Sci U S A 2016; 113:E1489-97.

[56] Liska F, Gosele C, Rivkin E, Tres L, Cardoso MC, Domaing P, et al. Rat hd mutation reveals an essential role of centrobin in spermatid head shaping and assembly of the head-tail coupling apparatus. Biol Reprod 2009; 81:1196–205.

[57] Pilot-Storck F, Chopin E, Rual J-F, Baudot A, Dobrokhotov P, Robinson-Rechavi M, et al. Interactome mapping of the phosphatidylinositol 3-kinase-mammalian target of rapamycin pathway identifies deformed epidermal autoregulatory factor-1 as a new glycogen synthase kinase-3 interactor. Mol Cell Proteomics 2010; 9:1578–93.

[58] Verze P, Cai T, Lorenzetti S. The role of the prostate in male fertility, health and disease. Nat Rev Urol 2016; 13:379–86.

[59] Bao J, Tang C, Li J, Zhang Y, Bhetwal BP, Zheng H, et al. RAN-binding protein 9 is involved in alternative splicing and is critical for male germ cell development and male fertility. PLoS Genet 2014; 10:e1004825.

[60] Bansal SK, Gupta N, Sankhwar SN, Rajender S. Differential Genes Expression between Fertile and Infertile Spermatozoa Revealed by Transcriptome Analysis. PLoS One 2015; 10:e0127007.

[61] Taipale M, Krykbaeva I, Koeva M, Kayatekin C, Westover KD, Karras GI, et al. Quantitative analysis of HSP90-client interactions reveals principles of substrate recognition. Cell 2012; 150:987–1001.

[62] Muller P, Ruckova E, Halada P, Coates PJ, Hrstka R, Lane DP, et al. C-terminal phosphorylation of Hsp70 and Hsp90 regulates alternate binding to co-chaperones CHIP and HOP to determine cellular protein folding/degradation balances. Oncogene 2013; 32:3101–10.

[63] Esakky P, Hansen DA, Drury AM, Moley KH. Molecular analysis of cell type-specific gene

expression profile during mouse spermatogenesis by laser microdissection and qRT-PCR. Reprod Sci 2013; 20:238–52.

[64] Li K, Xue Y, Chen A, Jiang Y, Xie H, Shi Q, et al. Heat shock protein 90 has roles in intracellular calcium homeostasis, protein tyrosine phosphorylation regulation, and progesterone-responsive sperm function in human sperm. PLoS One 2014; 9:e115841.

[65] Tash JS, Chakrasali R, Jakkaraj SR, Hughes J, Smith SK, Hornbaker K, et al. Gamendazole, an orally active indazole carboxylic acid male contraceptive agent, targets HSP90AB1 (HSP90BETA) and EEF1A1 (eEF1A), and stimulates Il1a transcription in rat Sertoli cells. Biol Reprod 2008; 78:1139–52.

[66] Mitchell LA, Nixon B, Aitken RJ. Analysis of chaperone proteins associated with human spermatozoa during capacitation. Mol Hum Reprod 2007; 13:605–13.

[67] Beyler SA, Wheat TE, Goldberg E. Binding of antibodies against antigenic domains of murine lactate dehydrogenase-C4 to human and mouse spermatozoa. Biol Reprod 1985; 32:1201–10.

[68] Mi K, Dolan PJ, Johnson GVW. The low density lipoprotein receptor-related protein 6 interacts with glycogen synthase kinase 3 and attenuates activity. J Biol Chem 2006; 281:4787–94.

[69] Yamamoto H, Komekado H, Kikuchi A. Caveolin is necessary for Wnt-3a-dependent internalization of LRP6 and accumulation of beta-catenin. Dev Cell 2006; 11:213–23.

[70] Piao S, Lee S-H, Kim H, Yum S, Stamos JL, Xu Y, et al. Direct inhibition of GSK3beta by the phosphorylated cytoplasmic domain of LRP6 in Wnt/beta-catenin signaling. PLoS One 2008; 3:e4046.

[71] Koch S, Acebron SP, Herbst J, Hatiboglu G, Niehrs C. Post-transcriptional Wnt Signaling Governs Epididymal Sperm Maturation. Cell 2015; 163:1225–1236.

[72] Nicot A-S, Lo Verso F, Ratti F, Pilot-Storck F, Streichenberger N, Sandri M, et al. Phosphorylation of NBR1 by GSK3 modulates protein aggregation. Autophagy 2014; 10:1036–53.

[73] Dimitrov S, Brennerova M, Forejt J. Expression profiles and intergenic structure of head-to-head oriented Brca1 and Nbr1 genes. Gene 2001; 262:89–98.

[74] Yi Y-J, Manandhar G, Sutovsky M, Jonáková V, Park C-S, Sutovsky P. Inhibition of 19S proteasomal regulatory complex subunit PSMD8 increases polyspermy during porcine fertilization in vitro. J Reprod Immunol 2010; 84:154–63.

[75] Ferrara D, Izzo G, Pariante P, Donizetti A, D'Istria M, Aniello F, et al. Expression of prothymosin alpha in meiotic and post-meiotic germ cells during the first wave of rat spermatogenesis. J Cell Physiol 2010; 224:362–8.

[76] Ferrara D, Pariante P, Di Matteo L, Serino I, Oko R, Minucci S. First evidence of prothymosin α localization in the acrosome of mammalian male gametes. J Cell Physiol 2013; 228:1629–37.

[77] Aravindan RG, Kirn-Safran CB, Smith MA, Martin-DeLeon PA. Ultrastructural changes and asthenozoospermia in murine spermatozoa lacking the ribosomal protein L29/HIP gene. Asian J Androl n.d.; 16:925–6.

[78] Thompson PJ, Norton KA, Niri FH, Dawe CE, McDermid HE. CECR2 is involved in spermatogenesis and forms a complex with SNF2H in the testis. J Mol Biol 2012; 415:793–

806.

[79] Bao J, Vitting-Seerup K, Waage J, Tang C, Ge Y, Porse BT, et al. UPF2-Dependent Nonsense-Mediated mRNA Decay Pathway Is Essential for Spermatogenesis by Selectively Eliminating Longer 3'UTR Transcripts. PLoS Genet 2016; 12:e1005863.

[80] Liu J, Yuan Y, Huan J, Shen Z. Inhibition of breast and brain cancer cell growth by BCCIPalpha, an evolutionarily conserved nuclear protein that interacts with BRCA2. Oncogene 2001; 20:336–45.

[81] Zhang XW, Lan K, Yang WB, Li Q, Zhao YP, Yin HQ, et al. [Expression and localization of transmembrane protein CMTM2 in human testis and sperm]. Beijing Da Xue Xue Bao 2017; 49:575–579.

[82] Liu G, Xin Z-C, Chen L, Tian L, Yuan Y-M, Song W-D, et al. Expression and localization of CKLFSF2 in human spermatogenesis. Asian J Androl 2007; 9:189–98.

[83] Spiridonov NA, Wong L, Zerfas PM, Starost MF, Pack SD, Paweletz CP, et al. Identification and characterization of SSTK, a serine/threonine protein kinase essential for male fertility. Mol Cell Biol 2005; 25:4250–61.

[84] Lee B, Jin S, Choi H, Kwon JT, Kim J, Jeong J, et al. Expression and function of the testis-predominant protein LYAR in mice. Mol Cells 2013; 35:54–60.

[85] Yuan S, Stratton CJ, Bao J, Zheng H, Bhetwal BP, Yanagimachi R, et al. Spata6 is required for normal assembly of the sperm connecting piece and tight head-tail conjunction. Proc Natl Acad Sci U S A 2015; 112:E430-9.

[86] Cao W, Ijiri TW, Huang AP, Gerton GL. Characterization of a novel tektin member, TEKT5, in mouse sperm. J Androl n.d.; 32:55–69.

[87] Coles LS, Lambrusco L, Burrows J, Hunter J, Diamond P, Bert AG, et al. Phosphorylation of cold shock domain/Y-box proteins by ERK2 and GSK3beta and repression of the human VEGF promoter. FEBS Lett 2005; 579:5372–8.

[88] Elgün S, Kaçmaz M, Sen I, Durak I. Seminal arginase activity in infertility. Urol Res 2000; 28:20–3.

[89] Amano T, Eishi Y, Yamada T, Uchida K, Minegishi K, Tamura T, et al. Widespread expression of γ-glutamyl cyclotransferase suggests it is not a general tumor marker. J Histochem Cytochem 2012; 60:76–86.

[90] Mihara T, Fukumoto K, Okazaki T, Shimada M. Murine Sperm Expresses Toll-Like Receptor (TLR) Family that Responds to the Pathogens Released from Virus, and Decreases Fertilization Ability by the Stimuli. J Mamm Ova Res 2010; 27:136–143.

[91] Saeidi S, Shapouri F, Amirchaghmaghi E, Hoseinifar H, Sabbaghian M, Sadighi Gilani MA, et al. Sperm protection in the male reproductive tract by Toll-like receptors. Andrologia 2014; 46:784–90.

[92] Shapouri F, Saeidi S, Ashrafi Kakhki S, Pouyan O, Amirchaghmaghi E, Aflatoonian R. The expression of Toll-Like Receptors (TLRs) in testicular cancer: A case control study. Iran J Reprod Med 2013; 11:919–24.

[93] Shirakata Y, Hiradate Y, Inoue H, Sato E, Tanemura K. Histone h4 modification during mouse spermatogenesis. J Reprod Dev 2014; 60:383–7.

[94] Zalensky AO, Siino JS, Gineitis AA, Zalenskaya IA, Tomilin N V, Yau P, et al. Human

testis/sperm-specific histone H2B (hTSH2B). Molecular cloning and characterization. J Biol Chem 2002; 277:43474–80.

[95] Escalier D, Gallo JM, Albert M, Meduri G, Bermudez D, David G, et al. Human acrosome biogenesis: immunodetection of proacrosin in primary spermatocytes and of its partitioning pattern during meiosis. Development 1991; 113:779–88.

[96] Zaneveld LJ, Dragoje BM, Schumacher GF. Acrosomal proteinase and proteinase inhibitor of human spermatozoa. Science 1972; 177:702–3.

[97] Tesarík J, Drahorád J, Pěknicová J. Subcellular immunochemical localization of acrosin in human spermatozoa during the acrosome reaction and zona pellucida penetration. Fertil Steril 1988; 50:133–41.

[98] Paasch U, Heidenreich F, Pursche T, Kuhlisch E, Kettner K, Grunewald S, et al. Identification of increased amounts of eppin protein complex components in sperm cells of diabetic and obese individuals by difference gel electrophoresis. Mol Cell Proteomics 2011; 10:M110.007187.

[99] Liu J, Shen C, Fan W, Chen Y, Zhang A, Feng Y, et al. Low levels of PRSS37 protein in sperm are associated with many cases of unexplained male infertility. Acta Biochim Biophys Sin (Shanghai) 2016; 48:1058–1065.

[100] Jeulin C, Soufir JC, Weber P, Laval-Martin D, Calvayrac R. Catalase activity in human spermatozoa and seminal plasma. Gamete Res 1989; 24:185–96.

[101] Vinayagam A, Stelzl U, Foulle R, Plassmann S, Zenkner M, Timm J, et al. A directed protein interaction network for investigating intracellular signal transduction. Sci Signal 2011; 4:rs8.

[102] Westhoff D, Kamp G. Glyceraldehyde 3-phosphate dehydrogenase is bound to the fibrous sheath of mammalian spermatozoa. J Cell Sci 1997; 110 (Pt 1:1821–9.

[103] O'Bryan MK, Grima J, Mruk D, Cheng CY. Haptoglobin is a Sertoli cell product in the rat seminiferous epithelium: its purification and regulation. J Androl n.d.; 18:637–45.

[104] Yuen BTK, Bush KM, Barrilleaux BL, Cotterman R, Knoepfler PS. Histone H3.3 regulates dynamic chromatin states during spermatogenesis. Development 2014; 141:3483–94.

[105] Krejčí J, Stixová L, Pagáčová E, Legartová S, Kozubek S, Lochmanová G, et al. Post-Translational Modifications of Histones in Human Sperm. J Cell Biochem 2015; 116:2195–209.

[106] van der Heijden GW, Ramos L, Baart EB, van den Berg IM, Derijck AAHA, van der Vlag J, et al. Sperm-derived histones contribute to zygotic chromatin in humans. BMC Dev Biol 2008; 8:34.

[107] Pullar JM, Carr AC, Bozonet SM, Rosengrave P, Kettle AJ, Vissers MCM. Elevated seminal plasma myeloperoxidase is associated with a decreased sperm concentration in young men. Andrology 2017; 5:431–438.

[108] Show MD, Anway MD, Zirkin BR. An ex vivo analysis of Sertoli cell actin dynamics following gonadotropic hormone withdrawal. J Androl n.d.; 25:1013–21.

[109] Martínez-Heredia J, Estanyol JM, Ballescà JL, Oliva R. Proteomic identification of human sperm proteins. Proteomics 2006; 6:4356–69.

[110] Bonache S, Mata A, Ramos MD, Bassas L, Larriba S. Sperm gene expression profile is related to pregnancy rate after insemination and is predictive of low fecundity in normozoospermic

men. Hum Reprod 2012; 27:1556–67.

[111] Demir K, Kirsch N, Beretta CA, Erdmann G, Ingelfinger D, Moro E, et al. RAB8B is required for activity and caveolar endocytosis of LRP6. Cell Rep 2013; 4:1224–34.

[112] Khan Z, Vijayakumar S, de la Torre TV, Rotolo S, Bafico A. Analysis of endogenous LRP6 function reveals a novel feedback mechanism by which Wnt negatively regulates its receptor. Mol Cell Biol 2007; 27:7291–301.

[113] Smith GD, Wolf DP, Trautman KC, Vijayaraghavan S. Motility potential of macaque epididymal sperm: the role of protein phosphatase and glycogen synthase kinase-3 activities. J Androl n.d.; 20:47–53.

[114] Lau KF, Miller CC, Anderton BH, Shaw PC. Expression analysis of glycogen synthase kinase-3 in human tissues. J Pept Res 1999; 54:85–91.

[115] Vijayaraghavan S, Stephens DT, Trautman K, Smith GD, Khatra B, da Cruz e Silva EF, et al. Sperm motility development in the epididymis is associated with decreased glycogen synthase kinase-3 and protein phosphatase 1 activity. Biol Reprod 1996; 54:709–18.

[116] Song X, Wang S, Li L. New insights into the regulation of Axin function in canonical Wnt signaling pathway. Protein Cell 2014; 5:186–93.

[117] Stamos JL, Weis WI. The β-catenin destruction complex. Cold Spring Harb Perspect Biol 2013; 5:a007898.

[118] Pronobis MI, Rusan NM, Peifer M. A novel GSK3-regulated APC:Axin interaction regulates Wnt signaling by driving a catalytic cycle of efficient βcatenin destruction. Elife 2015; 4:e08022.

[119] Voronkov A, Krauss S. Wnt/beta-catenin signaling and small molecule inhibitors. Curr Pharm Des 2013; 19:634–64.

[120] Ahn SY, Kim NH, Lee K, Cha YH, Yang JH, Cha SY, et al. Niclosamide is a potential therapeutic for familial adenomatosis polyposis by disrupting Axin-GSK3 interaction. Oncotarget 2017; 8:31842–31855.

[121] McCarrey JR, Geyer CB, Yoshioka H. Epigenetic regulation of testis-specific gene expression. Ann N Y Acad Sci 2005; 1061:226–42.

[122] DeJong J. Basic mechanisms for the control of germ cell gene expression. Gene 2006; 366:39–50.

[123] Ghaffari Novin M, Mirfakhraie R, Nazarian H. Aberrant Wnt/β-Catenin Signaling Pathway in Testis of Azoospermic Men. Adv Pharm Bull 2015; 5:373–7.

[124] Zeng X, Tamai K, Doble B, Li S, Huang H, Habas R, et al. A dual-kinase mechanism for Wnt co-receptor phosphorylation and activation. Nature 2005; 438:873–7.

[125] Davidson G, Wu W, Shen J, Bilic J, Fenger U, Stannek P, et al. Casein kinase 1 gamma couples Wnt receptor activation to cytoplasmic signal transduction. Nature 2005; 438:867–72.

[126] Alberts B, Johnson A, Lewis J. Sperm. Molecular biology of the Cell. 4th editio. New York: Garland Science; 2002.

[127] Gur Y, Breitbart H. Mammalian sperm translate nuclear-encoded proteins by mitochondrial-type ribosomes. Genes Dev 2006; 20:411–416.

[128] de Mateo S, Castillo J, Estanyol JM, Ballescà JL, Oliva R. Proteomic characterization of the

human sperm nucleus. Proteomics 2011; 11:2714–26.

[129] Amaral A, Castillo J, Estanyol JM, Ballescà JL, Ramalho-Santos J, Oliva R. Human sperm tail proteome suggests new endogenous metabolic pathways. Mol Cell Proteomics 2013; 12:330–42.

[130] Baker MA, Naumovski N, Hetherington L, Weinberg A, Velkov T, Aitken RJ. Head and flagella subcompartmental proteomic analysis of human spermatozoa. Proteomics 2013; 13:61–74.

[131] Gur Y, Breitbart H. Protein translation in mammalian sperm. Soc Reprod Fertil Suppl 2007; 65:391–7.

[132] Jonsson PF, Cavanna T, Zicha D, Bates PA. Cluster analysis of networks generated through homology: automatic identification of important protein communities involved in cancer metastasis. BMC Bioinformatics 2006; 7:2.

[133] Yamada T, Bork P. Evolution of biomolecular networks: lessons from metabolic and protein interactions. Nat Rev Mol Cell Biol 2009; 10:791–803.

[134] Vidal M, Cusick ME, Barabási A-L. Interactome networks and human disease. Cell 2011; 144:986–98.

[135] Elliott DJ, Grellscheid SN. Alternative RNA splicing regulation in the testis. Reproduction 2006; 132:811–9.

[136] Shen C, Kuang Y, Liu J, Feng J, Chen X, Wu W, et al. Prss37 is required for male fertility in the mouse. Biol Reprod 2013; 88:123.

[137] Varmuza S, Jurisicova A, Okano K, Hudson J, Boekelheide K, Shipp EB. Spermiogenesis is impaired in mice bearing a targeted mutation in the protein phosphatase 1cgamma gene. Dev Biol 1999; 205:98–110.

[138] Schimenti KJ, Feuer SK, Griffin LB, Graham NR, Bovet CA, Hartford S, et al. AKAP9 is essential for spermatogenesis and sertoli cell maturation in mice. Genetics 2013; 194:447–57.

[139] Wang R-S, Yeh S, Tzeng C-R, Chang C. Androgen receptor roles in spermatogenesis and fertility: lessons from testicular cell-specific androgen receptor knockout mice. Endocr Rev 2009; 30:119–32.

[140] Logue JS, Whiting JL, Tunquist B, Sacks DB, Langeberg LK, Wordeman L, et al. AKAP220 protein organizes signaling elements that impact cell migration. J Biol Chem 2011; 286:39269–81.

[141] Skålhegg BS, Huang Y, Su T, Idzerda RL, McKnight GS, Burton KA. Mutation of the Calpha subunit of PKA leads to growth retardation and sperm dysfunction. Mol Endocrinol 2002; 16:630–9.

B2.7. Supplementary Material

B2.7.1. Tables

Supplementary Table B2.1. Testis expression levels of GSK3 interactome. Expression levels of all GSK3 interactors were retrieved form the human protein atlas, PaGeneBase, Expression atlas, BioGPS and UniGene were retrieved and testis expression values were normalized. Yellow: GSK3 testis interactors; Green: GSK3 sperm interactors; Orange: GSK3 database interactors.

https://www.dropbox.com/s/161dwhvy8d2ixvt/Supplementary%20Table%201%20Testis%20expression%20levels%20of%20GSK3%20interactome.xlsx?dl=0

Supplementary Table B2.2. Testis and sperm related phenotypes/diseases/annotations of GSK3 interactome. Testis and sperm related phenotypes/diseases/annotations of all GSK3 interactors were retrieved and categorized from MGI, OMIM, Phenopedia, DISEASES, DisGeNet and GeneOntology. Also, differently expression levels of protein in asthenozoospermic samples in peer reviewed papers was retrieved. Yellow: GSK3 testis interactors; Green: GSK3 sperm interactors; Orange: GSK3 database interactors.

https://www.dropbox.com/s/3qzvvi12us8ihfv/Supplementary%20Table%202%20Testis%20and%20sperm%20related%20phenotypes%3Adiseases%3Aannotations%20of%20GSK3%20interactome.xlsx?dl=0

Supplementary Table B2.3. Correlation coefficient between % of immotile sperm and GSK3 isoform expression and activation in human sperm.

Ejaculated sperm		Total GSK3α	p21GSK3α	Total GSK3β	pS9GSK3β
% of immotile sperm	Pearson Correlation	-0.910*	-0.872*	0.111	-0.458
	Sig. (2-tailed)	0.012	0.023	0.834	0.361
	N	6	6	6	6
Capacitated sperm		Total GSK3α	pS21 GSK3α	Total GSK3β	pS9 GSK3β
% of immotile sperm	Pearson Correlation	0.545	0.283	0.578	0.848*
	Sig. (2-tailed)	0.263	0.587	0.230	0.033
	N	6	6	6	6

Supplementary Table B2.4. Top 5 of GeneOntology enrichment of GSK3α testis interactome. The 5 most significant categories of biological process, molecular function and cellular component according to p-value are listed. Category, nr of protein and p-value is listed. Only results with p>0.005 were considered.

Testis GSK3α interactome enrichment		
Category	nr of proteins	p-value
Biological process		
nuclear-transcribed mRNA catabolic process, nonsense-mediated decay	7	6.06E-05
mRNA metabolic process	11	1.02E-03
nuclear-transcribed mRNA catabolic process	7	1.89E-03
mRNA catabolic process	7	2.88E-03
protein localization to membrane	8	5.47E-03
Molecular function		

Testis GSK3α interactome enrichment		
Category	nr of proteins	p-value
RNA binding	14	1.57E-02
Cellular component		
nuclear lumen	24	2.54E-04
nuclear part	25	2.89E-04
intracellular organelle part	36	3.18E-04
intracellular non-membrane-bounded organelle	24	3.92E-04
non-membrane-bounded organelle	24	3.92E-04

Supplementary Table B2.5. Top 5 of GeneOntology enrichment of GSK3α sperm interactome. The 5 most significant categories of biological process, molecular function and cellular component according to p-value are listed. Category, nr of protein and p-value is listed. Only results with p>0.005 were considered.

Sperm GSK3α interactome enrichment		
Category	nr of proteins	p-value
Biological process		
cellular amide metabolic process	8	1.27E-04
amide biosynthetic process	7	2.71E-04
protein localization to endoplasmic reticulum	5	2.76E-04
peptide metabolic process	7	5.81E-04
peptide biosynthetic process	6	3.27E-03
Molecular function		
structural constituent of ribosome	4	2.25E-02
Cellular component		
cytosolic ribosome	4	2.37E-03
ribosomal subunit	4	1.55E-02
ribosome	4	4.27E-02
cytosolic part	4	4.34E-02
extracellular matrix	6	1.96E-03

Supplementary Table B2.6. Top 5 of GeneOntology enrichment of GSK3β testis interactome. The 5 most significant categories of biological process, molecular function and cellular component according to p-value are listed. Category, nr of protein and p-value is listed. Only results with p>0.005 were considered.

Testis GSK3β interactome enrichment		
Category	nr of proteins	p-value
Biological process		
telomere maintenance via telomerase	3	4.38E-03
telomere maintenance via telomere lengthening	3	1.17E-02
RNA-dependent DNA biosynthetic process	3	2.67E-02
telomerase holoenzyme complex assembly	2	4.76E-02
Molecular function		
RNA binding	4	6.36E-04
nitric-oxide synthase regulator activity	4	3.88E-02
TPR domain binding	4	3.88E-02

Supplementary Table B2.7. Top 5 of GeneOntology enrichment of GSK3β sperm interactome. The 5 most significant categories of biological process, molecular function and cellular component according to p-value are listed. Category, nr of protein and p-value is listed. Only results with p>0.005 were considered.

Sperm GSK3β interactome enrichment		
Category	nr of proteins	p-value
Biological process		
multi-organism process	18	5.34E-07
defense response to fungus	5	1.67E-05
antimicrobial humoral response	6	3.62E-05
immune response	14	8.06E-05
response to fungus	5	9.04E-05
Molecular function		
disordered domain specific binding	3	3.56E-02
Celular component		
cytoplasmic vesicle lumen	9	6.86E-07
secretory granule lumen	9	4.48E-07
DNA packaging complex	4	5.87E-03
nucleosome	4	4.08E-03
nuclear nucleosome	3	2.12E-03

B2.7.2. Figures

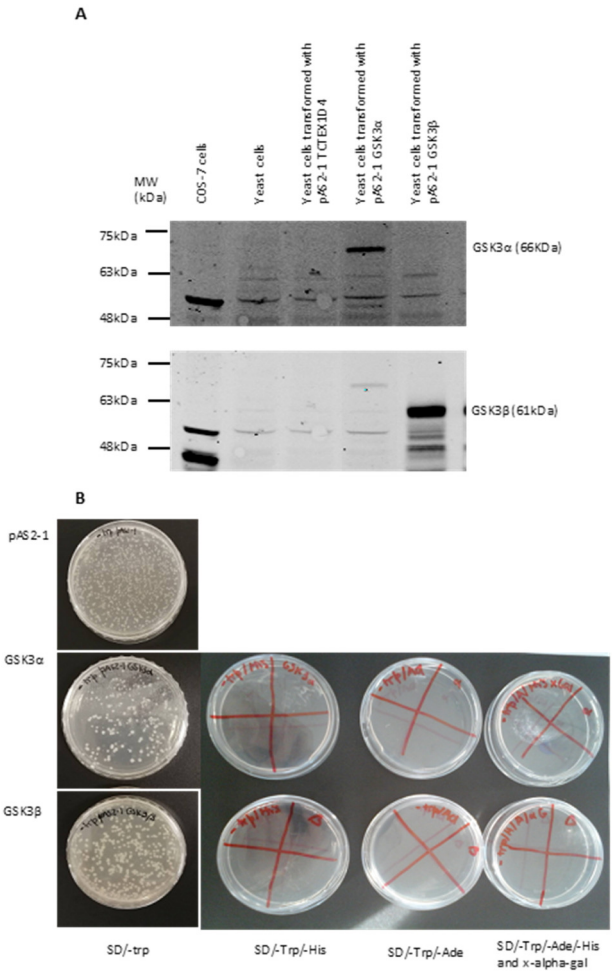

Supplementary Figure B2. 1. Expression and auto-activation of the reporter genes tests of pAS2-1-GSK3α and pAS2-1-GSK3β in AH190 yeasts. A. Yeast protein extracts previously transformed with pAS2-1-GSK3α or pAS2-1-GSK3β were probed with an anti-GSK3α antibody (Cell Signaling ref: #9338, 1:1000) and an anti-GSK3β antibody (Cell Signaling ref: #9315, 1:1000). The calculated molecular weight of hybrid protein is presented. Blots were cropped **B**. Yeast transformed with pAS2-1-GSK3α or pAS2-1-GSK3β were plated in different levels of stringency mediums.

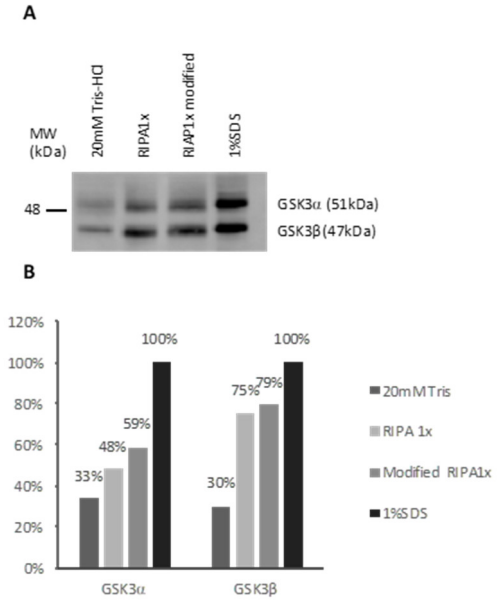

Supplementary Figure B2.2. Solubilizing effect of different lysis buffers for GSK3α and GSK3β. A. 1% SDS is very effective on solubilizing GSK3. For GSK3α, 1XRIPA and 1XRIPA modified solubilized approximately half of the protein and 20mM Tris-HCl only 30%, when compared with 1%SDS. For GSK3β, 1xRIPA and 1XRIPA modified solubilized around 70% of GSK3β and 20mM of Tris-HCl only 30%, when compared with 1% SDS. GSK3α and GSK3β were detected using a anti-GSK3α/β (Invitrogen, ref: 44-610, 1:2000). **B**. GSK3α was immunodetected using a anti-GSK3α (Cell Signaling ref: #9338, 1:1000) and GSK3β was immunodetected using a anti-GSK3β (Cell Signaling ref: #9315, 1:1000). Experience done once.

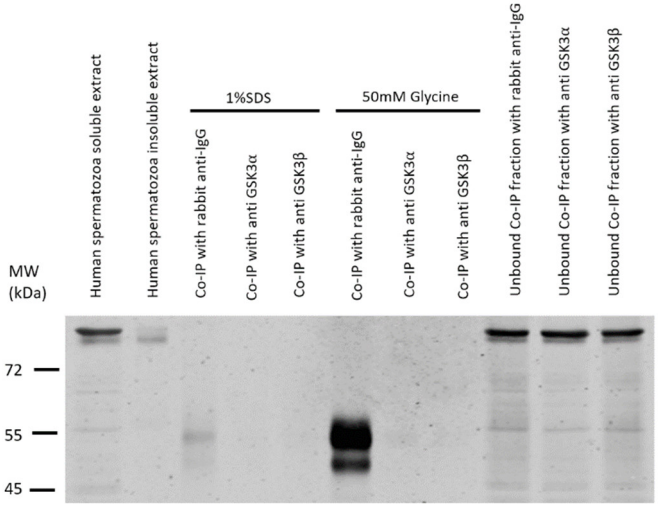

Supplementary Figure B2.3. Co-Immunoprecipitation of GSK3 from normospermic human sperm sample (previous page). Prior to GSK3 immunodetection, APP presence was evaluated by probing with 6E10 antibody. Although the reason is unknown, upon incubation with the 6E10 antibody (Sigma-Aldrich, ref: A-1474), two unspecific bands appear on the negative control eluted with 50mM of glycine.

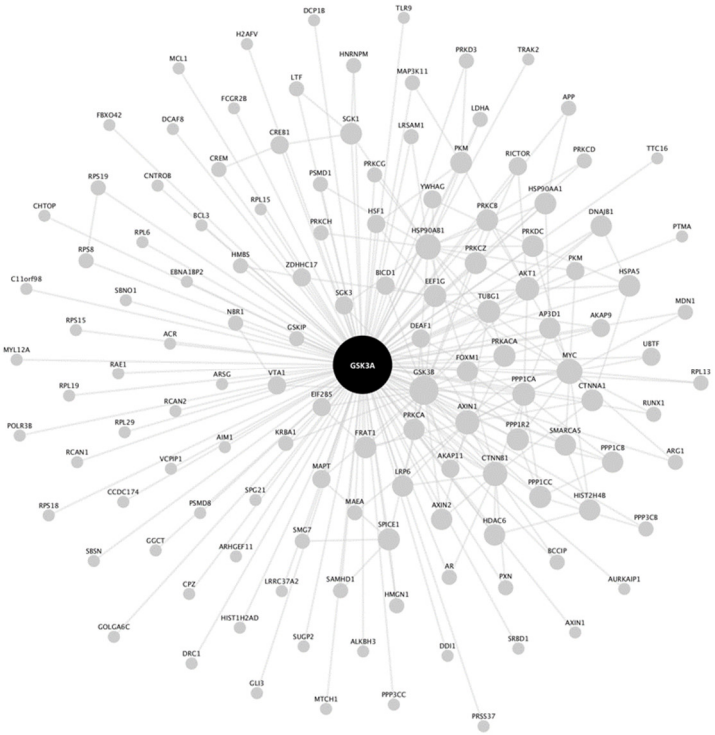

Supplementary Figure B2.4. The GSK3α interactome network. GSK3α-centered protein-protein interactome network. All GSK3α interactors (testis, sperm and databased) were used to build the network. Node size: degree (number of neighbors of a protein).

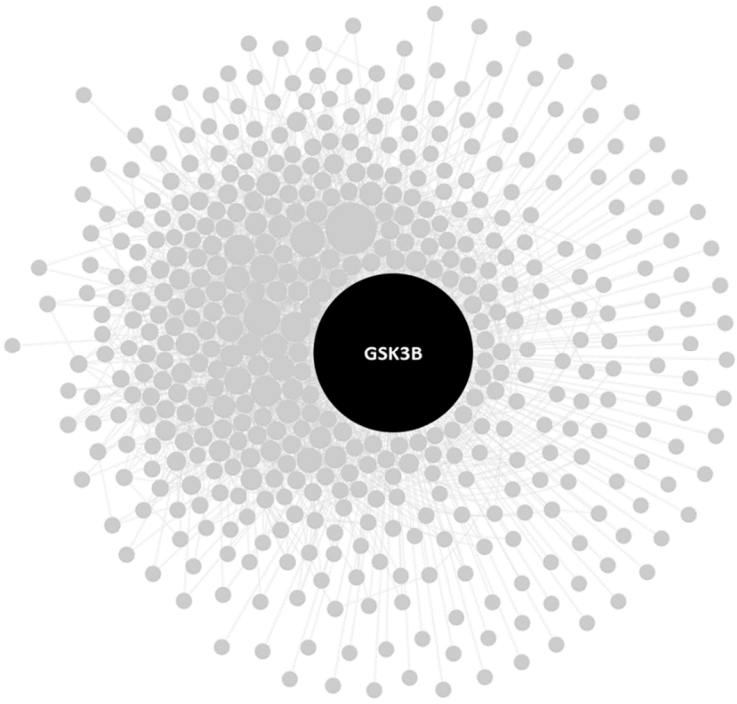

Supplementary Figure B2.5. The GSK3β interactome network (previous page). GSK3β-centered protein-protein interactome network. All GSK3β interactors (testis, sperm and databased) were used to build the network. Due to the density of the network, the name of the proteins was not possible to present Node size: degree (number of neighbors of a protein).

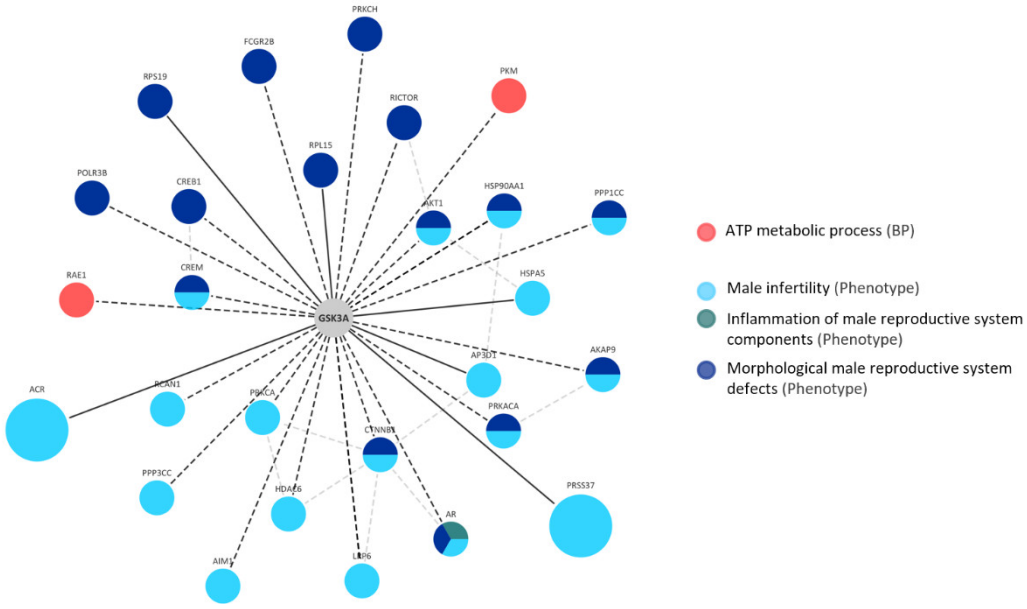

Supplementary Figure B2.6. The GSK3α general male infertility network. GSK3α-centered subnetwork for male infertility annotations extracted from GSK3α interactome network. GSK3α interactors associated with male infertility annotations were used to build the network. Solid lines: testis or sperm GSK3α interactions; Dashed lines: Databased retrieved GSK3α interactions. Node size: according to testis expression. Node colors: represent male infertility related phenotypes, biological processes (BP).

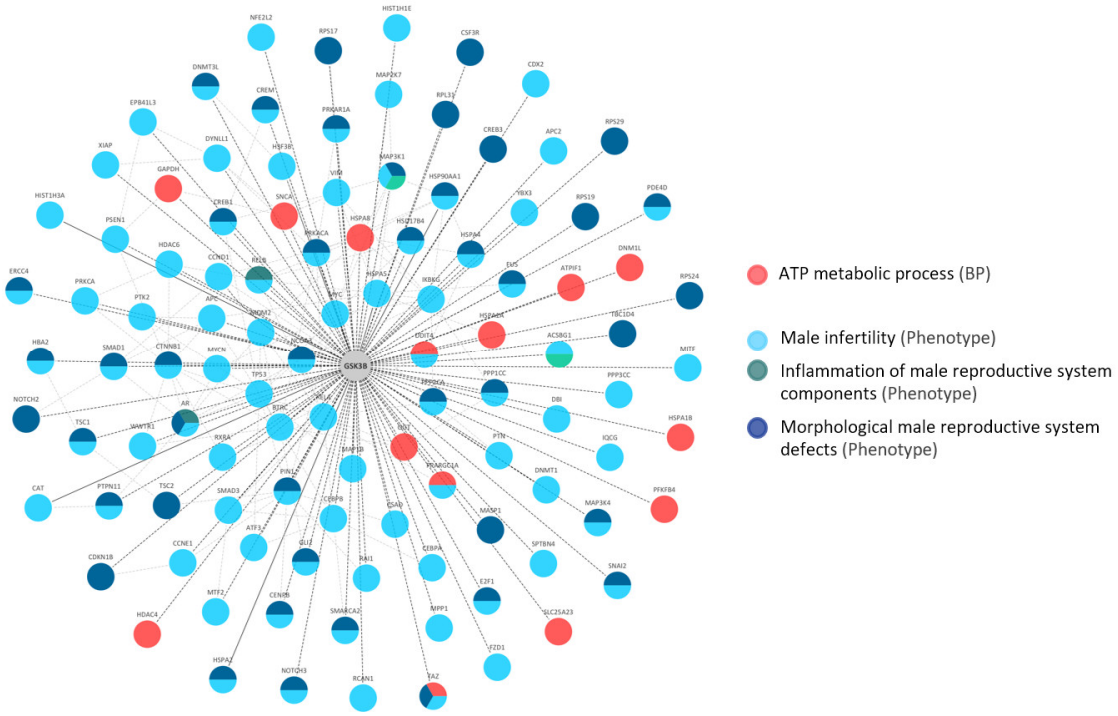

Supplementary Figure B2.7. The GSK3β general male infertility network (previous page). GSK3β-centered subnetwork for male infertility annotations extracted from GSK3β interactome network. GSK3β interactors associated with male infertility annotations were used to build the network. Solid lines: testis or sperm GSK3β interactions; Dashed lines: Databased retrieved GSK3β interactions. Node size: according to testis expression. Node colors: represent male infertility related phenotypes, biological processes (BP)

C. General Discussion

C1. Main conclusions and future perspectives

The signaling events that culminate in sperm motility acquisition and maintenance have been studied for decades [1]. Yet, many questions are still unanswered. The main goal of this thesis was to deepen the knowledge on the signaling events involved in human sperm motility by focusing on the characterization and modulation of the signaling pathway GSK3/PPP1R2/PPP1 in human sperm. Ultimately, the data generated by this work can be further applied to the development of a new group of reversible male contraceptives based sperm motility modulation.

To achieve this goal, we first developed a molecular biology tool that is capable of specifically interfere with protein-protein interactions (PPIs) in mammalian sperm (Section B1.). Although this approach has been previously applied in another cell type [2], in mammalian sperm this work is one of the first reports [3] . We chose to target phosphoprotein phosphatase 1 catalytic subunit gamma 2 (PPP1CC2) interactions in human sperm, since former work showed that the PPP1CC2 activity is associated with sperm motility control [4,5] and inhibition of PPP1 activity in sperm throughout the epididymis transit is partially responsible for highly motile sperm. Our previous work showed that PPP1 regulatory subunit 2 (PPP1R2), a PPP1 inhibitor, is involved in regulating PPP1CC2 activity in human sperm [6]. Therefore, blocking motility-related PPP1CC2 interactions, such as PPP1CC2/PPP1R2, will prevent motility acquisition. In order to disrupt PPP1CC2/PPP1R2 interaction, we undertook a PPIs disruption peptide approach based on the PPP1CC2/PPP1R2 interaction interface. With increased affinity towards PPP1CC/PPP1R2 interactions, the disruptive peptide competes and displaces PPP1RR2 from PPP1CC2, rendering active PPP1CC2 and consequently immotile mammalian sperm. To insure sperm intracellular delivery, the peptide was coupled with a cell penetrating peptide (CPP) originating a bioportide. We designed, synthetized and evaluated the effect of the disruptive PPP1CC2/PPP1R2 peptide on sperm motility. We successfully modulated PPP1CC2/PPP1R2 complex and restored PPP1CC2 activity, *in vitro*. When applied to mammalian sperm, the disruptive peptide was delivered to sperm cells and reduced sperm motility without affecting sperm viability. These results demonstrated that it is possible to target protein-protein interactions and modulate sperm complexes involved in motility using rationally-designed bioportides. We also demonstrated that the development of new type of male contraceptive based on inhibiting sperm motility is now achievable.

The disruptive peptide approach reported in this work can be applied in other key processes for reproduction. Although sperm motility acquisition is an ideal target for male contraceptive since it is a post-spermatogenesis process and hormone independent, using protein-protein interactions

disruptive peptides to interfere with sperm acrosome reaction and/or sperm-oocyte interaction can also be explored to prevent oocyte fertilization. Inhibiting sperm motility can be useful not only as a reversible male contraceptive, but also as preservative technique in assisted reproductive techniques. Sperm motility maintenance requires a high-energy turnover. Consequently, sperm energy resources are consumed and high levels of reactive oxidative species are produced [7]. Blocking sperm motility, reversibly, can help preserve the quality of sperm samples prior to, for example sperm sample storage.

Although the PPP1CC2/PPP1R2 interaction is involved in sperm motility acquisition, the fact that is not restricted to sperm, particularly due to a ubiquitous expression of PPP1R2, is an obstacle to achieve sperm-specific phenotypes. To overcome this problem, we aimed to identify testis/sperm-specific interactors of glycogen synthase kinase 3 (GSK3), a modulator of PPP1R2/PPP1 interaction in human somatic and sperm cells and a key protein in sperm motility acquisition. In sperm, PPP1R2 phosphorylation by GSK3 results in detachment of PPP1R2 from PPP1, rendering the latter active [8]. With the goal of unravel key GSK3 interactions for sperm motility, in section B2 we identified and characterized the GSK3 testis and sperm interactome. First, we showed that human sperm motility appears to be correlated specifically with GSK3α expression and activity. Then, we constructed a GSK3α-centered motility network that revealed 26 direct interactors involved in sperm motility annotations, and from those one highly expressed in testis/sperm, the PRSS37 (probable inactive serine protease 37). Besides being related with sperm motility, PRSS37 has been associated to a successful acrosome reaction [9]. Developing a male contraceptive by targeting GSK3α/PRSS37 interaction would culminate in both sperm motility and acrosome reaction disruption. An in depth PRSS37 characterization in human sperm is necessary to confirm if GSK3α/PRSS37 interaction is a viable pharmacological target. Given the reported relevance of GSK3 PPIs in sperm motility, we hypothesized that interfering with such interactions may affect motility acquisition and represent a suitable target for male contraceptive strategy. A similar strategy is currently being pursued for PPP1CC2 sperm motility related interactions [10] In figure C1.1 is an overview of the aims, results accomplished in this work as well as future perspectives.

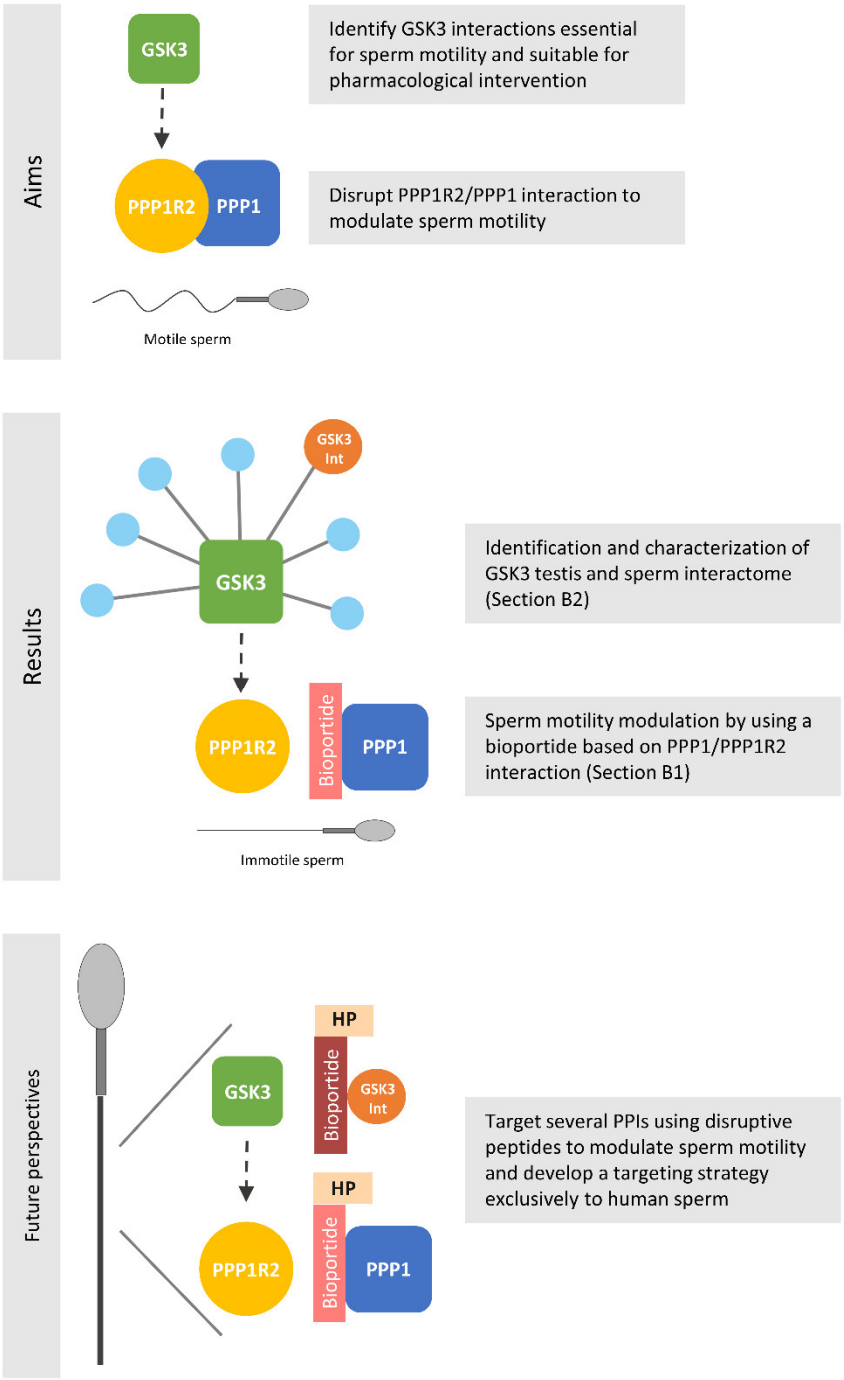

Figure C1.1. Overview of the aims, results accomplished in this work and future perspectives. Orange circle: GSK3 testis/sperm specific interactor; HP, homing peptide.

We demonstrated that disruptive bioportides based on sperm protein-protein interactions can modulate sperm motility. Molecular modelling and dynamic studies will be used to determine the interaction interfaces between bioportides and their target in order to identify and refine

bioportides with higher stability, affinity, specificity, activity and uptake to human sperm. A multi interface targeting approach will be considered to achieve a more efficient result. The most promising bioportides will be further selected for synthesis and *in vitro* and *in vivo* studies in normospermic human sperm samples. Future efforts will focus on delivering bioportides exclusively to fully mature sperm cells using a specific tissue/cells targeting system. Please note that targeting fully mature sperm requires transposing the blood epididymal barrier. A homing peptides strategy can be used to exclusively deliver bioportides to the epididymal epithelium and sperm cells.

The association between GSK3 activity and sperm motility has been described extensively [5]. Yet, we reported for the first time an isoform-specific association between GSK3α and sperm motility in human samples. A population profile concerning GSK3α activity in heterogeneous sperm samples will allow to further validate the correlation between GSK3α and human sperm motility and indisputably confirm GSK3α as suitable target for sperm motility modulation. Fully characterization of GSK3 isoforms in human sperm is required. Approaches such as inhibitory compounds and subcellular localization in morphological and motility distinct sperm samples must be undertaken. Although no testis/sperm-specific protein-protein complex involved exclusively in sperm motility was identified, the knowledge acquired in this work represents the starting point to identify potential male contraceptive targets. We believe that GSK3α motility function relies on unique interactors of this isoform in human sperm. Future work will center on identification of exclusively GSK3α interactors by a proteomic and *in silico* approach. Characterization of GSK3α and GSK3β human sperm interactome in normospermic and asthenozoospermic samples will allow to pin-point GSK3α interactions key for sperm motility. Additionally, integrating the data in publicly available databases and literature concerning testis/sperm-specific and motility-related proteins will allow to construct a sperm motility protein-protein network and, consequently, identify interactions optimal for pharmacological intervention.

C2. References

[1] Freitas MJ, Vijayaraghavan S, Fardilha M. Signaling mechanisms in mammalian sperm motility. Biol Reprod 2017; 96:2–12.

[2] Petta I, Lievens S, Libert C, Tavernier J, De Bosscher K. Modulation of Protein-Protein Interactions for the Development of Novel Therapeutics. Mol Ther 2016; 24:707–18.

[3] Silva JV. Sperm proteins as targets for contraception and fertility biomarkers. Universidade de Aveiro, 2016.

[4] Smith GD, Wolf DP, Trautman KC, da Cruz e Silva EF, Greengard P, Vijayaraghavan S. Primate sperm contain protein phosphatase 1, a biochemical mediator of motility. Biol Reprod 1996; 54:719–27.

[5] Vijayaraghavan S, Stephens DT, Trautman K, Smith GD, Khatra B, da Cruz e Silva EF, et al. Sperm motility development in the epididymis is associated with decreased glycogen synthase kinase-3 and protein phosphatase 1 activity. Biol Reprod 1996; 54:709–18.

[6] Korrodi-Gregório L, Ferreira M, Vintém AP, Wu W, Muller T, Marcus K, et al. Identification and characterization of two distinct PPP1R2 isoforms in human spermatozoa. BMC Cell Biol 2013; 14:15.

[7] Miki K. Energy metabolism and sperm function. Soc Reprod Fertil Suppl 2007; 65:309–25.

[8] Wang QM, Park IK, Fiol CJ, Roach PJ, DePaoli-Roach AA. Isoform differences in substrate recognition by glycogen synthase kinases 3 alpha and 3 beta in the phosphorylation of phosphatase inhibitor 2. Biochemistry 1994; 33:143–7.

[9] Liu J, Shen C, Fan W, Chen Y, Zhang A, Feng Y, et al. Low levels of PRSS37 protein in sperm are associated with many cases of unexplained male infertility. Acta Biochim Biophys Sin (Shanghai) 2016; 48:1058–1065.

[10] Silva JV, Yoon S, De Bock P-J, Goltsev A V, Gevaert K, Mendes JFF, et al. Construction and analysis of a human testis/sperm-enriched interaction network: Unraveling the PPP1CC2 interactome. Biochim Biophys Acta 2017; 1861:375–385.